STUDY OF SPONTANEOUS BOLD FLUCTUATION IN ANIMAL AND HUMAN BRAINS

A DISSERTATION
SUBMITTED TO THE FACULTY OF THE GRADUATE SCHOOL
OF THE UNIVERSITY OF MINNESOTA
BY

XIAO LIU

IN PARTIAL FULFILLMENT OF THE REQUIREMENTS
FOR THE DEGREE OF
DOCTOR OF PHILOSOPHY

Advisor: WEI CHEN

September 2010

ACKNOWLEDGEMENTS

First and foremost, I would like to express my most sincere and deepest gratitude to my advisor and mentor, Dr. Wei Chen, who directed me to this fascinating research with enormous support and resources throughout the program. I also wish to express my deep appreciation to my committee members, Dr. Kamil Ugurbil, Dr. Bin He, Dr. Tay Netoff, and Dr. Jame Holte, for the time they spent and the advices they gave. In particular, I would like to thank Dr. Kamil Ugurbil for being the chair of my committee and the reviewer of my dissertation.

I am also grateful to Dr. Xiao-Hong Zhu for her continuous helps on discussions and technical issues on many aspects of this dissertation, and to Dr. Yi Zhang for his excellent assistance in animal surgical preparation. Many thanks go to Dr. Nanyin Zhang, my former colleague and also good friend, for his support and help, especially when I first came to MR research field. I also want to thank all of my other colleagues at the Center for Magnetic Resonance Research (CMRR) at the University of Minnesota, particularly to Dr. Ute Geerke, Dr. Uzay Emir, Dr. Essa Yacoub, and Dr. Wanzhan Liu for their extensive and patient helps during the past several years.

Last but not least, I like to thank my wife, Mrs. Liying Luo, for her love, endless support, and sustained encouragement. I thank my parents, my sister, and my brother in law for their understanding my choice of pursuing this Ph.D degree and their caring for me.

It is impossible for me to finish this dissertation without any of these people.

ABSTRACT

Spontaneous blood-oxygen-level-dependent (BOLD) signals acquired at the resting state have recently been found to fluctuate coherently within many anatomically-connected and functionally-specific brain networks, and it may reflect an orderly organization of ongoing brain activity. Understanding this phenomenon may help us not only to understand some fundamental mechanisms of brain functions but also to find its applications in clinical field. However, the mechanisms underlying this phenomenon remains elusive, and even its neural origin is still controversial. This dissertation aimed to understand spontaneous BOLD fluctuation from its neurophysiological basis, its modulation under different brain states, and its role in brain functions. With five projects performed both on animals and humans, we have found that i) spontaneous BOLD fluctuation under deep burst-suppression anesthesia originates from underlying spontaneous neural activity, ii) spontaneous BOLD fluctuation is sensitive to changes in anesthesia depth, reflecting reorganization of ongoing brain activity at different consciousness level, iii) the resting-state visual network is spatially reorganized into activated and non-activated coherent network under continuous stimulation, and iv) the correlation strength within individuals' resting-state network can affect their evoked response to identical stimulations. These findings clearly support the functional significance of spontaneous BOLD fluctuation widely observed in animals and humans brain and provide new insights into its underlying mechanisms.

TABLE OF CONTENTS

LIST OF TABLES

LIST OF FIGURES

Chapter 1

INTRODUCTION

Over the past 40 years, the development of magnetic resonance imaging (MRI) has played an essential role in the revolution in medical imaging field. MRI has many advantages, for example, its non-invasive and non-radiative natures; moreover, it can provide a variety of contrasts for different research and clinical purposes. The discovery of blood oxygenation level-dependent (BOLD) contrast 20 years ago made it possible to image neural activity changes using MRI and thus opened a new area for MRI research called functional magnetic resonance imaging (fMRI) (Bandettini et al., 1992, Kwong et al., 1992, Ogawa et al., 1990, Ogawa et al., 1992). After two decades of development and research, fMRI has become one of the most popular neuroimaging techniques used in many neuroscience and psychology studies to investigate the brain functions, dysfunction and neural mechanisms.

Instead of directly measuring the neural activity, the fMRI BOLD signal detects secondary hemodynamic responses induced by changes in neural activity. For this reason, a typical fMRI study usually needs to include at least two different conditions: a control versus one with external stimulation or task performance. Then, by examining the BOLD contrast under different conditions, one can identify and map the brain regions functionally associated with corresponding stimulation or tasks.

A typical control condition adopted by most fMRI studies is called the resting state, during which subjects were asked to refrain from any cognitive, language, or motor tasks as much as possible but not to fall asleep. The fMRI BOLD signal acquired under the resting state usually demonstrates strong low-frequency fluctuation, especially in the gray matter. Such slow fluctuation was hypothesized at early time to be attributed partially from physiological noise, which is distinct from high-frequency thermal noise (Jezzard et al., 1993, Weisskoff et al., 1993). However, a milestone study on this low-frequency noise opened a new research area in neuroimaging field.

In 1995, Biswal et al. found that spatiotemporal correlations of resting-state BOLD signals implies a spatial pattern covering the human motor system similar to the fMRI activation pattern of evoked brain activity when performing bilateral finger-tapping task, as illustrated in Figure 1.1 (Biswal et al., 1995). The similarity led to the hypothesis that resting-state BOLD fluctuation results from spontaneous brain activity and their correlations reflect functional connectivity between different brain regions. Since then, a series of resting-state fMRI studies have reported similar spontaneous and correlated BOLD fluctuation within a variety of brain systems, for example, the visual, auditory,

language, default mode and attention systems (Cordes et al., 2000, Fox et al., 2006a, Greicius et al., 2003, Hampson et al., 2002, Lowe et al., 1998), which were then called resting-state networks.

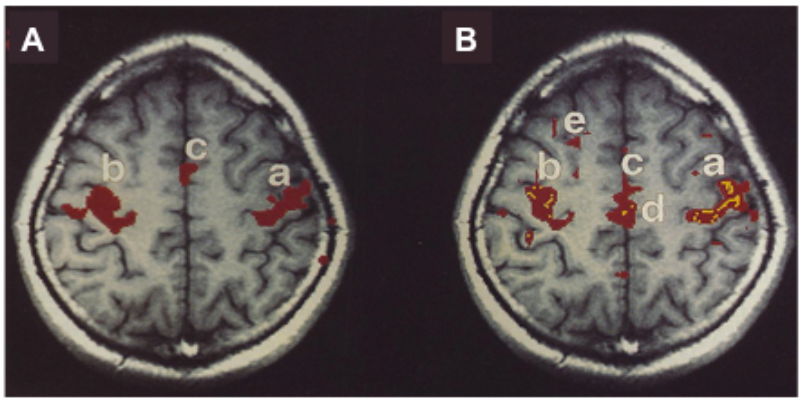

Figure 1.1 A comparison between functional activation map (A) and spontaneous BOLD correlation map (B). Functional activation map (A) indicates brain regions showing evoked response to bilateral finger task while spontaneous BOLD correlation map (B) represents an organized pattern of spontaneous brain activity. Here red stands for positive correlation, while yellow is negative. The figure is adapted from the reference (Biswal et al., 1995).

During the past 15 years, especially after 2004, the number of studies on spontaneous BOLD fluctuation has been increasing exponentially, as shown in Figure 1.2 based on MEDLINE searching results. There are at least two major reasons why spontaneous BOLD fluctuation attracted so much attention from neuroimaging and neuroscience communities. First, understanding spontaneous BOLD fluctuation may help us answer some important questions in system neuroscience. For example, why is the majority of brain energy consumed by spontaneous brain activity (Raichle, 2006, Raichle and Mintun, 2006)? The organized pattern and its associated brain network implied by spontaneous BOLD fluctuation may indicate the essential role of spontaneous neural

activity for brain's working and functioning. Second, spontaneous BOLD fluctuation may potentially provide a powerful signal source for investigating abnormal brain connectivity associated with many psychiatric diseases and mental disorders. For example, the correlation of spontaneous BOLD signals in default mode network (DMN) has been recently found to be significantly different among three groups of subjects: schizophrenia patients, their relatives, and healthy subjects (Whitfield-Gabrieli et al., 2009).

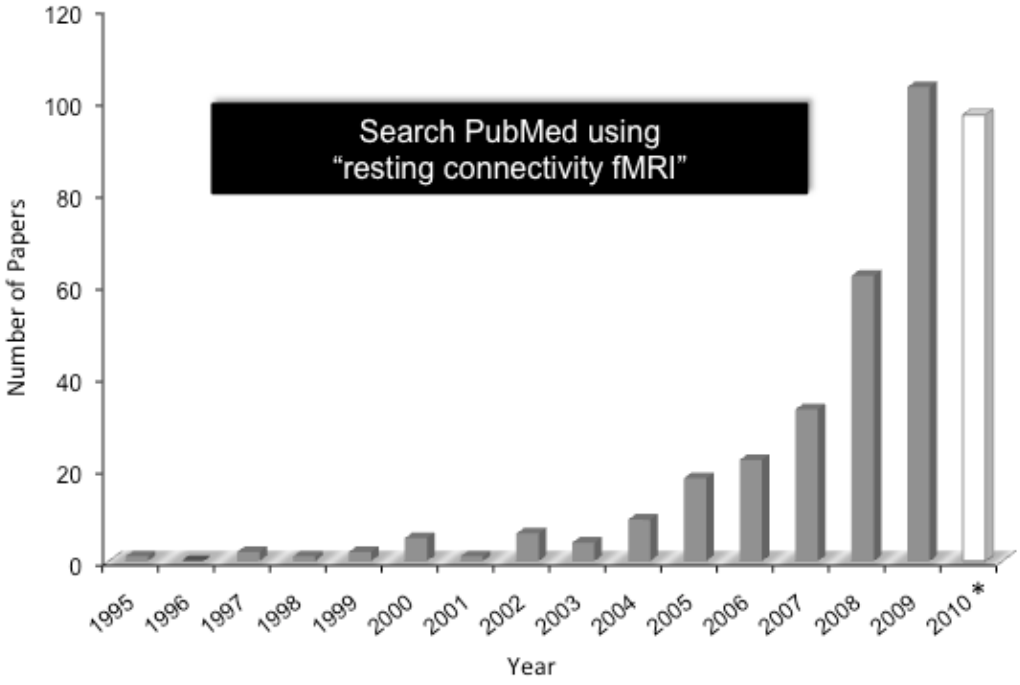

Figure 1.2 Exponential increase in studies on spontaneous BOLD fluctuation (resting-state connectivity). The column chart shows the searching result on the PubMed website using the key words "resting connectivity fMRI". *: Up to June, 2010

These anticipations have been confirmed by many interesting results on many aspects. For example, spontaneous BOLD fluctuation was also observed under deep and unconscious anesthesia, suggesting that it reflects an intrinsic organization rather than

just mentally unconstrained fluctuation of brain activity (Vincent et al., 2007). Moreover, the level of spontaneous BOLD signal prior to stimulation/task was found to be correlated with subsequent behavioral responses of subjects (Boly et al., 2007, Fox et al., 2007, Hesselmann et al., 2008b), suggesting an important role of spontaneous brain activity in determining the brain's evoked response. However, despite the dramatic growth in interest as well as the number of related studies, the research on spontaneous BOLD fluctuation is still at a very early stage and its underlying mechanisms remained unclear. Many unsettled or controversial questions need to be answered or clarified.

The purpose of my dissertation is to address several unresolved and crucial issues about spontaneous BOLD fluctuation and thus to improve our understanding of its underlying mechanisms. Specifically, I aimed to address four general questions: 1) Does spontaneous BOLD fluctuation under deep anesthesia originate from underlying neural activity? 2) How does the anesthesia (consciousness) level affect spontaneous BOLD fluctuation and functional connectivity? 3) How does the external stimulation affect spontaneous BOLD fluctuation? 4) Can the status of spontaneous BOLD fluctuation affect the evoked BOLD response? In the past 4 years, I have carried out 5 projects, on both animals and humans, to help understand those questions and the major results and findings are described and summarized in this thesis.

The organization of this thesis is as follows.

Chapter 2 briefly introduces principles of MRI and fMRI, as well as other techniques used in my thesis projects. I will also review the current stage of research on spontaneous BOLD fluctuation and the detailed organization of my thesis work.

Chapter 3 introduces a project on rat model aiming to understand neural origin of spontaneous BOLD fluctuation under deep anesthesia showing burst-suppression electroencephalography (EEG) patterns.

Chapter 4 demonstrates how spontaneous BOLD fluctuation in rat brain changed when the anesthesia level was reduced to a much lighter level, and discusses the functional significance of this phenomenon related to the specificity of connectivity.

Chapter 5 describes how the spatiotemporal correlations of spontaneous BOLD fluctuation would be modulated under continuous stimulation, resulting distinct resting and activated brain networks. This project was performed on awake human subjects.

Chapter 6 shows the distinct influences of the short and continuous stimulation on spontaneous BOLD fluctuation and provides a possible explanation for the discrepancy between network "superposition" and "reorganization" theories.

Chapter 7 describes how the status of individuals' spontaneous BOLD fluctuation could affect their evoked response to identical stimulation, suggesting a strong interaction between spontaneous and evoked brain activities.

Chapter 8 summarizes the major findings of this thesis and also gives the directions for our future research.

Chapter 2

BACKGROUND

In this chapter, I will introduce the basic theories and principles of MRI and fMRI. Moreover, the current research on spontaneous BOLD fluctuation will also be reviewed in details, and the motivation of my thesis work and its contributions on this field will be discussed. At the end of this chapter, I will also give a short introduction of several other techniques used in my thesis work.

2.1 Magnetic Resonance Imaging

2.1.1 The Principles of Nuclear Magnetic Resonance (NMR)

MRI is based on the physics of nuclear magnetic resonance (NMR), which is a quantum mechanics phenomenon discovered in 1940's by Rabi, Bloch, and Purcell (Rabi

et al., 1938, Bloch et al., 1946, Purcell et al., 1946) and has a long history of use in obtaining chemical and physical information about molecules.

According the theory of quantum mechanics, all nucleons, including protons and neutrons, have an intrinsic quantum property called spin, which comes in multiples of ½ can be positive or negative. The spins of paired protons/neutrons can be cancelled with each other; therefore the overall spin of a given nucleus is determined by the number of protons and neutrons it possesses. Only the isotopes that contain an odd number of protons and/or neutrons, for example, ^{1}H, ^{13}C, ^{17}O, ^{19}F, and ^{31}P, have a net nonzero spin known as the nuclear spin.

A nucleus with net spin (the nuclear spin) is associated with an intrinsic magnetic moment. If they are placed in a static magnetic field ($\boldsymbol{B_0}$), the associated magnetic moments tend to align themselves either parallel (the low energy state) or anti-parallel (the high energy state) to the direction of the magnetic field. However, the distribution of nuclear spins in this two direction is not completely equal, and a slightly larger number of nuclei align their magnetic moments in the parallel direction, resulting in a net magnetization ($\boldsymbol{M_0}$), called *equilibrium magnetization*, along the direction of the magnetic field (conventionally defined as *z*-direction).

The movement of individual nuclear spins is more complicated than simply aligning along with the magnetic field; they actually precess around the direction of the main magnetic field at a frequency depending on both the field strength and the type of nuclei:

$$\omega = \gamma \cdot B_0 \tag{2.1}$$

where γ is called gyromagnetic ratio, which is a constant for the same nucleus. For example, the γ for the proton is 42.58 MHz/T. B_0 is the strength of magnetic field, and the precession frequency ω is called resonance frequency or the "Larmor frequency". However, the precessions of spins are of random phase orientation, and their components transverse to the magnetic field are therefore cancelled out. For this reason, the net magnetization $\boldsymbol{M_0}$ at a macroscopic level is in the direction of the magnetic field and has no transverse components.

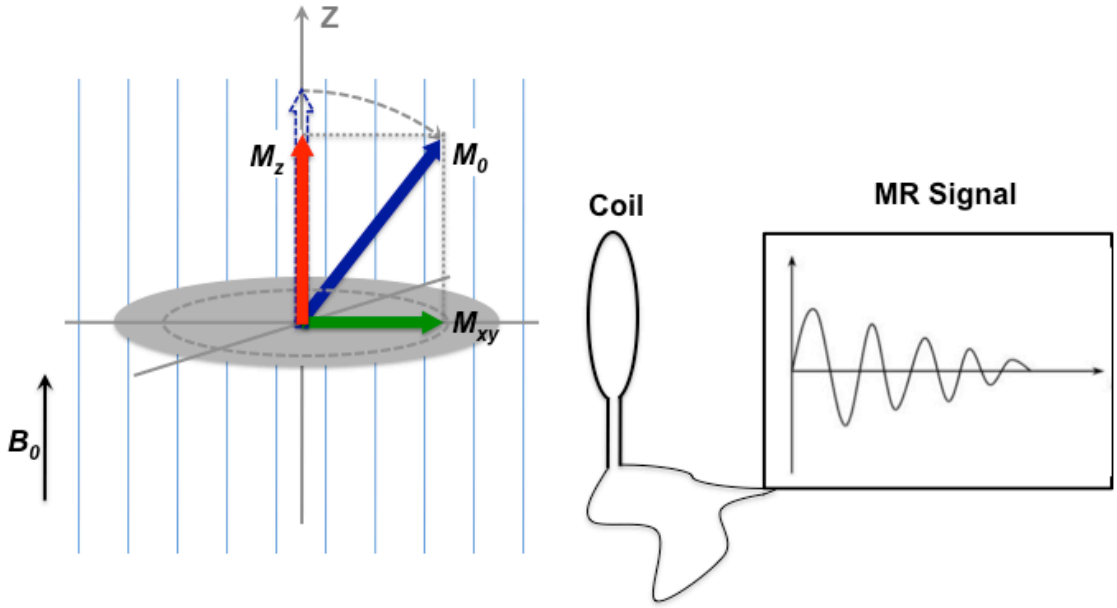

Figure 2.1 Illustration of the MR signal generation

The above described how the nuclear spins behave in a static magnetic field. The net magnetization $\boldsymbol{M_0}$ under this equilibrium condition cannot generate any MR signals. After building up the equilibrium magnetization, an electromagnetic pulse at the resonance frequency (usually in radio frequency range and therefore called RF excitation pulse) is needed to perturb the alignment of nuclear spins and thus, at the macroscopic

level, tip the net magnetization $\boldsymbol{M_0}$ away from its original direction (the direction of the static magnetic field). After the excitation pulse but with the presence of the static magnetic field, the newly formed magnetization component in the transverse plane ($\boldsymbol{M_{xy}}$ in the *x*-*y* plane) will precess around the *z*-axis at the Larmor frequency given in Equation (2.1). The precession generates a time varying magnetic flux that can be detected by a radiofrequency (RF) receive coil placed closely. MR signal is essentially the induced electrical current in the receive coil and proportional to the magnitude of precessing magnetization in the transverse plane, as illustrated in Figure 2.1.

After the RF pulse is turned off, the magnetization will return to its equilibrium state according two different relaxation processes. The longitudinal component ($\boldsymbol{M_z}$) along the main static field will recover exponentially to $\boldsymbol{M_0}$ with a time constant T_1, while the transverse component $\boldsymbol{M_{xy}}$ will decay exponentially to zero with a time constant T_2^*. The decay relaxation of the transverse component is usually much faster and involves two mechanisms: one is due to spin-spin interaction that can be characterized with a time constant T_2; and the other is caused by the inhomogeneity of the main static field. Utilizing the difference of these parameters in different tissues can develop a variety of image contrasts for MRI.

2.1.2 The Mathematical Description of NMR

In 1946, Bloch formulated a series of equations to mathematically describe the motion of a macroscopic magnetization $\boldsymbol{M}$ in a magnetic field $\boldsymbol{B}$ (Bloch et al., 1946). These equations are called Bloch equations.

In a laboratory (stationary) frame of reference, the Bloch equations are:

$$\frac{dM_z(t)}{dt} = \gamma[M_x(t)B_y(t) - M_y(t)B_x(t)] - \frac{M_z(t) - M_0}{T_1}$$

$$\frac{dM_x(t)}{dt} = \gamma[M_y(t)B_z(t) - M_z(t)B_y(t)] - \frac{M_x(t)}{T_2}$$

$$\frac{dM_y(t)}{dt} = \gamma[M_z(t)B_x(t) - M_x(t)B_z(t)] - \frac{M_y(t)}{T_2} \qquad (2.2)$$

These equations can be simplified into a vector formation by letting $\boldsymbol{M} = [M_x(t), M_y(t), M_z(t)]$ and $\boldsymbol{B} = [B_x(t), B_y(t), B_z(t)]$:

$$\frac{d\boldsymbol{M}}{dt} = \boldsymbol{M} \times \gamma\boldsymbol{B} - \frac{M_x\hat{\boldsymbol{x}} + M_y\hat{\boldsymbol{y}}}{T_2} - \frac{(M_z - M_0)\hat{\boldsymbol{z}}}{T_1} \qquad (2.3)$$

where the first term at the right side of Equation (2.3) describes the precession of magnetization in the magnetic field, because the direction of vector $d\boldsymbol{M}/dt$ is always orientated perpendicular to the plan of $\boldsymbol{M}$ and $\boldsymbol{B}$ (the cross product $\boldsymbol{M}\times\gamma\boldsymbol{B}$ is again a vector perpendicular to both $\boldsymbol{M}$ and $\boldsymbol{B}$). The latter two terms describe the two relaxation processes when the magnetization is out of its equilibrium state.

The laboratory reference is, however, not the best coordinate system to describe the motion of the magnetization, because its component in transverse plane will always precess at the Larmor frequency. It is therefore more convenient to use a "rotating frame" of reference, whose transverse plane is rotating around the *z*-axis at a frequency Ω. The unit vectors for the rotating reference are ($\hat{\boldsymbol{x}}', \hat{\boldsymbol{y}}', \hat{z}$), because its *z*-axis is overlapped with that of the laboratory reference. Now, the Bloch equations in the rotating frame become:

$$\frac{dM_z(t)}{dt} = \gamma[M_{x'}(t)B_{y'}(t) - M_{y'}(t)B_{x'}(t)] - \frac{M_z(t) - M_0}{T_1}$$

$$\frac{dM_{x'}(t)}{dt} = \gamma[M_{y'}(t)B_z(t) - M_z(t)B_{y'}(t)] - \Omega M_{y'}(t) - \frac{M_{x'}(t)}{T_2}$$

$$\frac{dM_{y'}(t)}{dt} = \gamma[M_z(t)B_{x'}(t) - M_{x'}(t)B_z(t)] + \Omega M_{x'} - \frac{M_{y'}(t)}{T_2} \tag{2.4}$$

When the frequency Ω of the rotating frame is equal to the Larmor frequency γB_z and a RF pulse is applied to create a RF filed $\boldsymbol{B_1}$, which is at rest in the rotating frame and parallel to $\hat{\boldsymbol{x}}'$, the above equation can be simplified to:

$$\frac{dM_z(t)}{dt} = -\gamma M_{y'}(t)B_1(t) - \frac{M_z(t) - M_0}{T_1}$$

$$\frac{dM_{x'}(t)}{dt} = -\frac{M_{x'}(t)}{T_2}$$

$$\frac{dM_{y'}(t)}{dt} = \gamma M_z(t)B_1(t) - \frac{M_{y'}(t)}{T_2} \tag{2.5}$$

Given a typical short RF pulse with a duration of $\tau_{rf} << T_1$ or T_2, which is the usual case for most MRI experiments, the solution for Equation (2.5) is

$$M_z(t) = M_0 - M_0 \cdot e^{-t/T_1}[1 - \cos(\gamma B_1 \tau_{rf})]$$

$$M_{x'}(t) = 0$$

$$M_{y'}(t) = M_0 \cdot e^{-t/T_2} \cdot \sin(\gamma B_1 \tau_{rf}) \tag{2.6}$$

The motion of magnetization under other combinations of static magnetic field and different RF field can be derived in a similar way by solving the Bloch equations.

2.1.3 From NMR to MRI

There was actually a big time gap between the discovery of NMR and its application in imaging. During this period of the gap, the NMR was mainly used as a spectroscopic technique to determine the structure of complex chemical compounds. However, a typical NMR experiment only provides the information about the types of nuclei in a sample but not the spatial distribution of a certain nucleus. To obtain an image, the spatial information has to be encoded into NMR signals.

Spatial localization of MRI is based on Equation (2.1) given in the previous section. According to the equation, the precession frequency (Larmor frequency) of a nuclear spin is determined not only by its type but also by the magnetic field strength it experiences. Therefore, by applying a spatially varied magnetic field, the nuclear spin in different spatial location will experience different field strength and thus have different precession frequencies. Magnetic resonance is then spatially differentiated.

Although the first 2D MRI image was created based on a back projection reconstruction method, which is conventionally used by computerized tomography (CT) (Lauterbur, 1973); a more popular reconstruction method for the modern MRI is to combine *k*-space acquisition and Fourier transform, which was proposed by Kumar et al. (Kumar et al., 1975).

The acquisition of a typical 2D MRI image starts with the slice selection step. Remember that the NMR signal comes from the precession of magnetization after a RF excitation pulse; the slice selection is to selectively excite a specific slice or slab in the space by controlling the RF pulse and magnetic field. First, a linearly varying magnetic

field called a gradient field, which is generated by gradient coils in the scanner, is added to the main static field in the direction perpendicular to the desired slice (the direction of the gradient but not of the magnetic field), for example, *z*-direction. Then, the magnetic field strength experienced by nuclear spins depends on their locations in the *z*-direction:

$$B(z) = B_0 + G_z \cdot z \tag{2.7}$$

where G_z is the strength of the gradient. Now, a RF pulse with a central frequency $\omega_0 = \gamma B_0$ and bandwidth BW will only effectively excite a slice centered at $z = 0$ with a thickness of $BW / \gamma G_z$.

After the slice selection, the spatial localization in the slice (*x*-*y* plane in our example) is accomplished by a 2D encoding: frequency encoding in the readout direction (for example, *x*-direction) and phase encoding in the direction orthogonal to it (*y*-direction).

During the data acquisition, a linear gradient field is turned on along *x*-axis and then the precession frequency of the local magnetization varies along this direction. The acquired MR signal is a sum of signals from all these local magnetizations. Using a Fourier transform, the contribution from different magnetizations could be decoded. However, this 1D encoding and decoding can only resolve a projection of the image along the *x*-axis. To obtain a 2D image, an additional phase encoding is needed. The principle of the phase encoding is quite similar to that of the frequency encoding but with a very different implementation. Prior to each frequency encoding step, the gradient field in phase encoding direction (*y*-axis in this example) is turned on for a very short time, during which the local magnetizations precess in different frequencies and thus produce a

linearly phase difference along this direction. The phase difference can be accumulated across multiple phase encoding steps to contain different information for each step. In other words, the phase encoding is similar to breaking down the frequency encoding into different pieces, while the frequency encoding is the continuous phase encoding.

Conventionally, a parameter $\boldsymbol{k}$ is used to describe the integration of gradient over time, which is defined as:

$$\boldsymbol{k} = \gamma \int_0^t \boldsymbol{G}(\tau) d\tau \tag{2.8}$$

and MR signals with the frequency and phase encoding can be expressed as a function of $\boldsymbol{k}$. The MR signal acquisition is then regarded as a sampling of this *k*-space. Using a 2D Fourier transform, the *k*-space data can be transformed to the real space and a MRI image is reconstructed.

2.2 Functional Magnetic Resonance Imaging

2.2.1 Introduction to fMRI BOLD Contrast

It has been known, as early as 1890, that the neural activity can affect the regional blood-supply in the brain and induce a series of vascular and hemodynamic responses in the local brain region (Roy and Sherrington, 1890). However, it is until the early of 1990s that MR technique began to be used to detect those hemodynamic responses associated with the neural activity. MRI can provide a variety of contrasts to image different hemodynamic parameters, for example, cerebral blood flow (CBF) and cerebral blood

volume (CBV), but the most common and widely used technique is still blood oxygenation level-dependent (BOLD) contrast.

The BOLD contrast was first observed and named by Ogawa et al. in 1990 (Ogawa et al., 1990). They observed many dark lines representing blood vessels under the conditions with reduced blood oxygenation level and proposed that this contrast may be used for mapping the regional neural activity change. Two years later, three groups independently demonstrated the feasibility of using BOLD contrast to map neurophysiologic changes in response to visual stimulation (Kwong et al., 1992, Ogawa et al., 1992) and motor tasks (Bandettini et al., 1992).

From a MR perspective, the BOLD contrast is based on the magnetic susceptibility property of hemoglobin: it is paramagnetic when dissociated with oxygen (deoxyhemoglobin) but diamagnetic when oxygenated (oxyhemoglobin) (Pauling and Coryell, 1936). The paramagnetic property of deoxyhemoglobin can cause a susceptibility difference between the blood and the surrounding brain tissues. This difference can produce a local magnetic field inhomogeneity, causing more rapid phase dispersion and thus decay of the MR signal. Therefore, changes in blood oxygenation level, i.e., the concentration of deoxyhemoglobin, can change the decay parameters T_2^*/T_2 of MR signals, which can then be detected by gradient/spin-echo or other MR imaging techniques. The most commonly used MRI technique for fMRI is the echo-planar imaging (EPI), which can collect MR signals for an entire image slice at one time following the RF excitation pulse and provide sufficient temporal resolution for imaging

hemodynamic response induced by neural activity. The generation of the BOLD contrast is demonstrated in Figure 2.2.

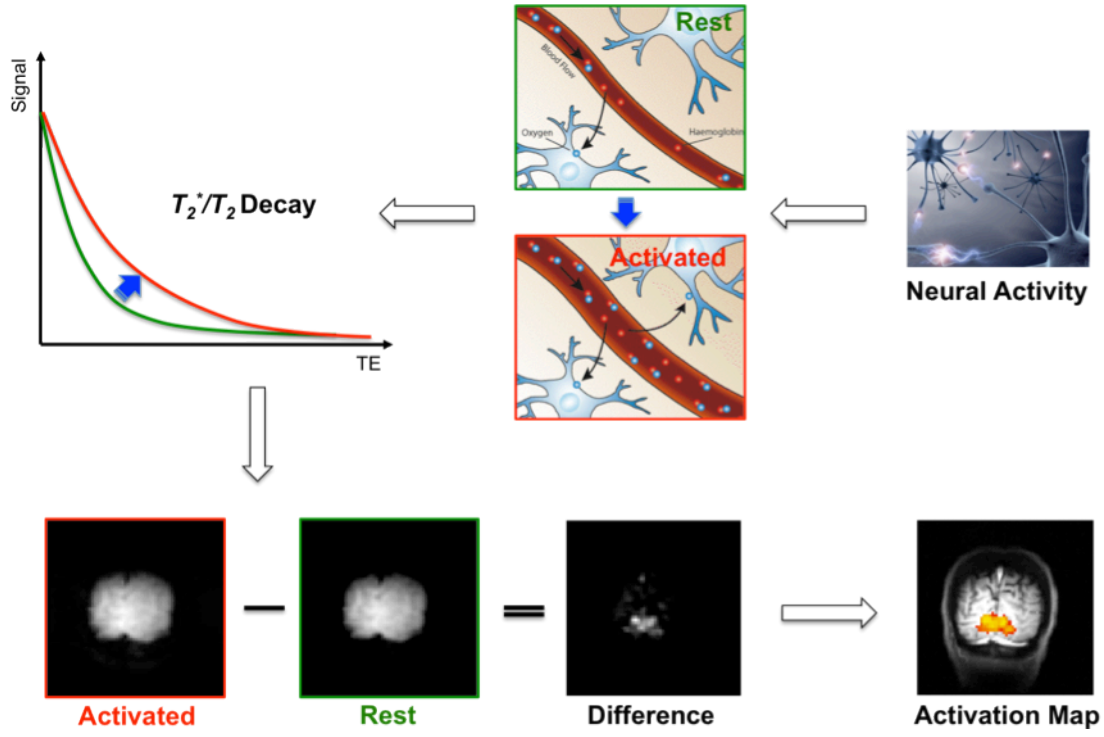

Figure 2.2 Mechanism of fMRI BOLD contrast

From a physiological perspective, the BOLD contrast originates from unbalanced increases of regional blood flow and oxygen metabolism following neural activity. At rest the brain energy is mainly provided through the oxidation of glucose to carbon dioxides and water, and the ratio of oxygen consumption to glucose consumption is about 5:1, which is close to the ratio for complete oxidative metabolism of glucose 6:1. However, neurons do not have their own reservation for glucose and oxygen. Following local neural activity, the regional CBF suddenly increase to provide more glucose and oxygen to the activated brain site. However, even though the increase in local glucose

consumption can match the increase of regional CBF, the increase in oxygen consumption is much less (Fox and Raichle, 1986, Fox et al., 1988). This is probably because the local metabolism of glucose switches from the complete oxidation to less effective but more rapid aerobic glycolysis (non-oxidative metabolism) (Raichle and Mintun, 2006). The mismatch between supply of CBF and demand on oxygen leads to a shift in relative concentration of oxyhemoglobin to deoxyhemoglobin and thus blood oxygenation level in local activated brain region, which is ready to be detected by T_2/T_2^*-weighted MRI techniques as described in the last paragraph.

2.2.2 Neural Correlates of BOLD

Understanding the precise relationship between neural signals and BOLD is very crucial to interpretation of results of many fMRI studies using BOLD contrast, and it is therefore a very active research topic. The major debate on this issue is whether the BOLD signal originates from neuronal synaptic (input) or spiking (output) activity.

Early studies combining results from fMRI experiment on human and electrophysiology recording on primate have found a close relationship between BOLD signal and neural spiking activity in V1 and V5 areas (Heeger et al., 2000, Rees et al., 2000). Later, a study on monkeys with simultaneous measurements of fMRI BOLD and electrophysiology signals confirmed this finding by showing a strong correlation (r^2 = 0.45) between neural spike rate and BOLD; but more importantly, this study also reported an even higher correlation (r^2 = 0.52) between local field potentials (LFPs) and BOLD (Logothetis et al., 2001). In contrast, a more recent study, in which electrophysiology and fMRI BOLD signals were separately recorded from the auditory

cortex of patients and healthy subjects when they were watching the same video, obtained an opposite result that BOLD has a better correlation with neuronal firing rate than with LFPs (Mukamel et al., 2005). Nevertheless, the discrepancy is not so surprising because LFPs are expected to be highly correlated with local average firing rate under most circumstances due to the small-world organization of the brain, i.e., majority of local short connections with a few long-range wiring. Based on only a small difference in correlations, it is really hard to give a correct answer for the true neural correlates of BOLD.

Even though there is still no final conclusion, evidence has been increasing to support that the BOLD contrast likely originates from synaptic activity rather than spiking activity (Arthurs and Boniface, 2002, Hoogenboom et al., 2006, Niessing et al., 2005, Raichle and Mintun, 2006, Caesar et al., 2003, Mathiesen et al., 1998). Among them, special attention should be given to a series of studies on the rat cerebella, in which regional CBF signals can be dramatically dissociated from the neuronal spiking activity but not from the LFPs (Caesar et al., 2003, Mathiesen et al., 1998). These findings are also in agreement with the fact that hemodynamic response following neural activity is driven by metabolic demand on glucose, which is tightly linked to synaptic activity (Schwartz et al., 1979, Shulman and Rothman, 1998, Sibson et al., 1998).

2.3 Spontaneous BOLD Fluctuation (Resting-state Connectivity)

2.3.1 Initial Observations

The temporal variation of BOLD signals acquired under the steady-state brain condition without any stimulation or tasks have been noticed right after it was applied to functional studies on humans, and it was initially regarded as physiological and/or MRI system noises caused, for instance, by respiration and heart pulsation (Jezzard et al., 1993, Weisskoff et al., 1993). The early study with the analysis of power spectrum (Weisskoff et al., 1993) found the slow fluctuation (< 0.5 Hz) of spontaneous BOLD signals is much stronger in gray matter than in white matter. By extending such analysis from time to space domain, Biswal et al. (Biswal et al., 1995) found that correlations of low-frequence (< 0.1 Hz) spontaneous BOLD fluctuation are much stronger within a functionally specific brain region responsible for motor function than between this region and other brain regions. To follow the term previously used for correlation analysis on positron emission tomography (PET) data (Friston et al., 1993), they named this phenomenon as "functional connectivity" in the resting state, which they believed to reflect the underlying neurophysiological fluctuation. In contrast, to avoid the loose definition of "resting state", some researchers would more like to describe this phenomenon as spontaneous BOLD fluctuations (Fox and Raichle, 2007).

Such spontaneous and correlated BOLD signal fluctuation is not limited to the motor system of the brain. Similar phenomena were soon observed not only in other low-level sensory systems, such as visual (Lowe et al., 1998) and auditory (Cordes et al.,

2000) regions, but also in high-level networks, including language (Hampson et al., 2002), dorsal attention network (DAN) (Fox et al., 2006a) and DMN (Fransson, 2005). It is not limited to cortical regions either, and the functional connectivity was also observed between the cortex and subcortical regions (Zhang et al., 2008). These consistent observations led to the hypothesis that spontaneous BOLD fluctuation may reflect underlying spontaneous brain activity and imply a variety of resting-state networks that have significant functional meanings. However, the early studies mainly focused on identification of the resting-state networks implied by spontaneous BOLD fluctuation rather than understanding its underlying mechanisms.

2.3.2 Methodology

Many methods have been used for identifying patterns hidden behind spontaneous BOLD fluctuation. The most common strategy is the correlation analysis based on a reference region (or seed). The implementation of this method is as following. First, a spatially specific reference brain region of interest is defined and the BOLD signal time course is then extracted from this region, as well as from every voxel of the brain. Secondly, the correlation, usually Pearson's correlation, is calculated between the reference region and each voxel to create a correlation map, which can also be further transformed to other parametric map, such as *Z* map if necessary (Fox et al., 2005). This approach is easy to be implemented and interpreted, and the correlation map represents the functional connectivity between each voxel and the reference region.

Compared to the hypothesis-driven correlation mapping, spatial independent component analysis (ICA) is a data-driven algorithm. ICA is a statistical method to

decompose multivariate signals into multiple components (sources) with maximized statistical independence. In contrast to correlation mapping, ICA does not require a priori-defined reference region and can extract multiple components (resting-state networks) simultaneously. However, it is not a complete objective method. Results of this analysis are highly dependent on the number of components that needs to be defined subjectively before the decomposition process. Moreover, not all of extracted components are neuronal origin, and a significant proportion of them result from other sources, for example, motion artifacts or physiologic noise. Identification of meaningful components usually involves comparing them with certain know component templates.

There are other methods used for extracting information from spontaneous BOLD fluctuation, for example, principle component analysis (PCA) (Zhong et al., 2009), hierarchical clustering (Cordes et al., 2002, Salvador et al., 2005), graph theory (Achard et al., 2006, Honey et al., 2009), but they are not used as common as correlation mapping and ICA.

2.3.3 Modulation of Spontaneous BOLD Fluctuation under Brain Activation

Although spontaneous BOLD signals are acquired under conditions without stimulations/tasks, it is also very important to understand how spontaneous BOLD fluctuation modulates under other brain conditions, which can help us understand its underlying mechanism and significance for brain functions.

It has been found that spontaneous BOLD fluctuation and task-evoked BOLD response can be linearly superimposed onto each other (Fox et al., 2006b). In that study, BOLD signals were acquired in an event-related paradigm with a right-handed button-

press task. After subtracting the BOLD time courses of the right motor cortex (not activated by the task) from those of the left motor cortex (activated by the task), the trial-to-trial variability was reduced by about 40%. It was therefore hypothesized that spontaneous brain activity reflected by spontaneous BOLD signals can be superimposed onto task-evoked brain activity (Fox et al., 2007, Fox et al., 2006b).

The spatiotemporal correlation of BOLD signals has also been examined under continuous stimulations/tasks by different studies, and the results are controversial. Most of these studies reported increased correlation between BOLD signals acquired with continuous stimulations/tasks. It was first reported by Lowe et al. that a resting-state network related to memory increased its functional connectivity (the correlation strength of BOLD signals) when subjects were performing spatial working memory task (Lowe et al., 2000). Similar increases in BOLD correlations were also observed within the language system during continuous listening task (Hampson et al., 2002) and within parahippocampal areas (PHPA) during a continuous episodic memory (Xu et al., 2006). Not all of studies on this topic obtained similar results. For example, it has been found that most of subjects showed a slight but consistent reduction, even though not statistically significant, in BOLD correlation within the motor cortex while tapping their fingers sequentially (Morgan and Price, 2004).

The discrepancy between these studies could be explained at least by two possible reasons. First, different brain systems, in particular high-level cognitive versus low-level sensory systems, could show distinct responses to continuous stimulations/tasks. Second, the high-level tasks employed by some studies have a relatively slow pace, and

fluctuations in subjects' engagement may potentially contribute to low-frequency BOLD components and thus increase BOLD correlations.

2.3.4 Spontaneous BOLD Fluctuation under Brain Conditions without Consciousness

There had been an argument that spontaneous BOLD fluctuation in the resting state merely reflects unconstrained but consciously mental activity fluctuation (Morcom and Fletcher, 2007). But studies on spontaneous BOLD fluctuation under unconscious brain conditions are not likely to support this hypothesis.

A common unconscious condition is induced by anesthesia, but there is still no agreement on how spontaneous BOLD fluctuation would modulate under anesthesia condition. A study on non-human primates has shown that even under deep anesthesia characterized by burst-suppression EEG spontaneous BOLD signals still preserved stronger correlations within occulomotor, sensorimotor, and visual systems, as well as a network analogous to human DMN (Vincent et al., 2007). This result is very important because it suggests that spontaneous BOLD fluctuation reflects an intrinsic organization of the brain rather than just the fluctuation of mental activity. Even though other studies confirmed the existence of spontaneous BOLD fluctuation under anesthesia and sedation, they obtained, however, quite controversial results in term of the specific influence of anesthesia on spontaneous BOLD fluctuation. Some of these studies reported a decreased BOLD correlation under anesthesia (Peltier et al., 2005, Martuzzi et al., 2010), while the others had completely opposite observations (Kiviniemi et al., 2005, Kiviniemi et al., 2000, Greicius et al., 2008). The discrepancy is not very surprising because these studies

were performed on different species with different types and dosages of anesthetic agents and BOLD signals were acquired from different brain regions.

Spontaneous BOLD fluctuation was also preserved during sleep (Fukunaga et al., 2006, Horovitz et al., 2008, Horovitz et al., 2009) and under the vegetative state (Boly et al., 2009) though with certain modulations. Spontaneous BOLD fluctuation within the visual cortex and DMN shows larger magnitude but preserve its spatiotemporal correlation patterns during light sleep (Fukunaga et al., 2006, Horovitz et al., 2008). When subjects went to the deep sleep stage, the medial prefrontal/ anterior cingulate cortex (MPFC/ACC), the frontal components of the DMN, were dissociated from the DMN by showing reduced functional connectivity; whereas the other posterior components of the DMN, including the posterior cingulate cortex (PCC), bilateral inferior parietal cortices (IPC) and angular gyri (AG), showed increased correlations with each other (Horovitz et al., 2009). Such changes in the DMN were hypothesized to be related to changes in consciousness level. It was also found that spontaneous BOLD fluctuation in a vegetative patient showed similar spatiotemporal correlations in cortical regions, but the cortico-thalamic BOLD functional connectivity is absent.

2.3.5 Spontaneous BOLD Fluctuation in Patients

One of major driving forces for the research on spontaneous BOLD fluctuation is its potential applications in clinical field, for example, the diagnosis of brain diseases and mental disorders associated with abnormal brain connectivity. For this reason, the modulation of spontaneous BOLD fluctuation (resting-state functional connectivity) in

various brain diseases is a very active research area. Significant differences have been reported between healthy subjects and patients with a variety of brain diseases.

The corpus callosum is the most important hub connecting two brain hemispheres. Its dysfunction is expected to cause changes in brain's functional connectivity. Quigley et al. confirmed this with a study on three patients with agenesis of the corpus callosum (Quigley et al., 2003). The study found that inter-hemisphere correlations between spontaneous BOLD signals acquired from the patients were significantly lower than those from healthy subjects, even though tasks can still successfully evoke BOLD responses in both hemispheres of the patients. The striking reduction in functional connectivity was also witnessed in a 6-year-old child before and after complete section of the corpus callosum for the treatment of intractable epilepsy (Johnston et al., 2008).

Different from the patients with dysfunctional corpus callosum, schizophrenia patients generally demonstrate stronger correlation over different brain regions when compared with healthy subjects (Jafri et al., 2008, Salvador et al., 2007, Whitfield-Gabrieli et al., 2009). Such change was not only observed between patients and healthy subjects but also between the healthy subjects and nonpsychotic first-degree relatives of the patients. Moreover, in the same study the functional connectivity within the DMN was also found to correlate with the degree of psychopathological symptoms (Whitfield-Gabrieli et al., 2009). Liu et al. characterized the modulation of functional connectivity in schizophrenia from another perspective, and they found that the small-world network property was disrupted in schizophrenia with reduced clustering coefficients, i.e., the reduced local connectivity (Liu et al., 2008). Surprisingly, they also reported decreased

connectivity between different brain regions, which is, however, probably due to the use of partial correlation method in their study.

Patients with AD and mild cognitive impairment (MCI) also exhibit modulated spontaneous BOLD fluctuation when compared with healthy subjects. Decreased functional connectivity has been observed between left and right hippocampus (Li et al., 2002) as well as between hippocampus and DMN (Sorg et al., 2007, Wang et al., 2006, Zhang et al., 2009), suggesting important roles of the hippocampus and DMN in AD and MCI. Similar to the approach used for schizophrenia patients, the small-world network property of resting-state functional connectivity was also examined in AD patients, and the clustering coefficients for AD patients are significantly lower than those of normal control, indicating a disrupted local connectivity in AD (Supekar et al., 2008).

Altered functional connectivity has also been found in a number of other brain diseases and mental disorder, for example, autism (Cherkassky et al., 2006, Monk et al., 2009), depression (Anand et al., 2005, Greicius et al., 2007), multiple sclerosis (Lowe et al., 2002), epilepsy (Bettus et al., 2009, Waites et al., 2006), posttraumatic stress disorder (Bluhm et al., 2009), attention-deficit hyperactivity disorder (ADHD) (Tian et al., 2006), etc., with specific modulation. All these studies demonstrated the feasibility of using spontaneous BOLD signals to understand the pathological mechanisms of brain diseases, to distinguish patients from healthy subjects, and even to evaluate the severity of diseases or potentially monitor treatment.

2.3.6 Influence of Spontaneous BOLD Fluctuation on Brain's Responses

During the past several decades, the theory in system neuroscience regarding how the brain works has been shifting from the classical one viewing brain as a passive and stimulus-driven system (Aloimonos and Rosenfeld, 1991, Hubel and Wiesel, 1965) to the new view that the brain is a perpetually active, adaptive and self-organized system (Beer, 2000, Engel et al., 2001, Varela et al., 2001). According to the new theory, spontaneous activity is very essential for brain functions and cannot be just random noise. The organized patterns hidden behind spontaneous BOLD fluctuation may reflect the underlying organization of spontaneous brain activity and provide a good support for this notion.

Moreover, the new theory also tells us that the brain's response to external perturbations (stimulations/tasks) may depend on the spontaneous brain activity. Evidence has been found to support this notion. A typical scalp-EEG study found that the event-related potential (ERP) induced by a visual stimulus is highly dependent on alpha oscillation prior to the stimulus (Makeig et al., 2002). Similar relationship has also been found between spontaneous brain activity and behavioral responses. For example, the perception of sensory stimuli near the threshold of detection could be biased by both amplitude (Linkenkaer-Hansen et al., 2004) and phase (Palva et al., 2005) of pre-stimulus oscillations in the somatosensory and parietal regions.

Since spontaneous BOLD fluctuation was hypothesized to reflect spontaneous bran activity, it may affect evoked brain response as well. A series of fMRI studies confirmed this by showing a relationship between subjects' spontaneous BOLD signals

and their behaviors. It has been found that the amplitude of BOLD signal precedes the onset of stimulation is able to predict subjects' performance in a motion discrimination task (Sapir et al., 2005). Similarly, subjects' detection of threshold-intensity sensory stimuli has been shown to correlate with preceding levels of BOLD signals in medial thalamus and lateral frontoparietal network positively and with those in DMN negatively (Boly et al., 2007). More interestingly, Hesselmann et al. demonstrated that how the pre-stimulus BOLD signal level in the fusiform face area could bias subjects' perception of an ambiguous picture (known as Rubin's vase-faces picture), which can be perceived as either a vase or two faces (Hesselmann et al., 2008a). These studies gave very good illustrations how spontaneous activity can influence evoked brain responses. From another perspective, they also support the hypothesis that spontaneous BOLD fluctuation reflects the underlying spontaneous brain activity.

2.3.7 Neural Correlates of Spontaneous BOLD Fluctuation

Understanding neurophysiologic basis of spontaneous BOLD fluctuation is essential for revealing its underlying mechanisms. As discussed previously, more and more evidence indicated that fMRI BOLD signals are very likely to result from neuronal synaptic activity. It is therefore not so surprising when the relation was found between spontaneous BOLD fluctuation and LFPs.

By analyzing electrophysiology data recorded from multiple electrodes in the visual cortex of monkeys, Leopold et al. demonstrated that band-limited (BLP) of local field potential (LFP) signals shows very slow (< 0.1 Hz) but highly correlated fluctuation over different brain regions, which is very similar to spontaneous BOLD fluctuation. It

therefore suggested that the BLP of LFPs may make a significant contribution to spontaneous BOLD fluctuation (Leopold et al., 2003). Their hypothesis obtained supports from three independent studies with simultaneous EEG/fMRI recording on human subjects (Feige et al., 2005, Goldman et al., 2002, Moosmann et al., 2003). Even though with some subtle differences in their results and methods, all of these studies found a strong negative correlation between power fluctuation of alpha-band activity (8−12 Hz) and spontaneous BOLD signals from the occipital lobe. However, the findings of these studies were limited by the low spatial resolution of scalp-EEG and its insensitivity to high-frequency LFP band. From this perspective, the animal study with intracranial recording could provide more information about the relationship between brain electrical activity and spontaneous BOLD signals.

A study on rats with alpha-chloralose anesthesia found strong correlations of spontaneous BOLD signals within the bilateral primary somatosensory cortex (S1FL). Through a separate electrophysiological recording experiment, this study also demonstrated that the power modulation of delta-band LFPs in the bilateral S1FL regions showed a similar dependency on anesthesia levels as spontaneous BOLD fluctuation. These results indicate a close relationship between spontaneous BOLD fluctuation in anesthetized rats and delta-band brain activity. In comparison, another animal study with simultaneous measurements of fMRI BOLD and electrophysiological signals from the V1 of primates provided more direct evidence for the neuronal basis of spontaneous BOLD fluctuation. It was found in this study that spontaneous BOLD signals were correlated with gamma-band LFP, multi-unit activity (MUA), and neuronal firing rate (Shmuel and

Leopold, 2008). Nonetheless, the result of this study was challenged by Logothetis et al. with reanalysis of the same data. They claimed that the data was not measured in the "real" resting state but under the condition with physiologically detectable flicker induced by the visual stimulator (Logothetis et al., 2009). This debate needs to be solved in the future.

Unlike task-evoked BOLD responses, spontaneous BOLD fluctuation is likely to have a much more complicated neurophysiologic basis that may depend on both brain status and specific brain regions studied. Although the big progress has been made towards understanding this issue, many questions remains to be answered in the future.

2.3.8 Motivation and Contribution of My Thesis Work

As reviewed in this section, the research on spontaneous BOLD fluctuation has already made very rapid progress during the past several years, especially after 2004. Nevertheless, it is still at a very early stage and many unsettled or controversial questions remain to be answered or clarified. This dissertation presents 5 projects we have done during the past 4 years in order to answer several important questions about spontaneous BOLD fluctuation.

It has been discussed previously in this dissertation that the preservation of spontaneous BOLD fluctuation in deep anesthetized animals is a very important finding, suggesting it may reflect the brain's intrinsic organization. However, the underlying neural correlates of spontaneous BOLD fluctuation under such condition remained unknown. The first project we have done was trying to understand the neurophysiologic basis of spontaneous hemodynamic fluctuation under deep anesthesia with burst-

suppression EEG pattern. We found a tight coupling between spontaneous EEG and CBF signals simultaneously recorded from the bilateral S1FL regions of isoflurane-anesthetized rats. At the same time, spontaneous BOLD signals separately acquired under the same conditions demonstrated very similar temporal characteristics as CBF, indicating a close relationship between them. The overall result provides very strong evidence for the neural origin of spontaneous BOLD fluctuation under burst-suppression anesthesia and the physiological basis of resting-state fMRI. This project is summarized and presented in Chapter 3.

Our first project has also shown that spatiotemporal correlations of spontaneous BOLD signals under the deep anesthesia indicate a widely-distributed coherent network, which is different from specific resting-state networks observed in conscious human subjects. The different consciousness levels could be an explanation for the discrepancy. To test this hypothesis, we investigated spontaneous BOLD fluctuation under a wide range of anesthesia depths in our second project. A dramatic modulation was observed between different anesthesia levels: the coherent networks implied by spontaneous BOLD fluctuation became much more specific under the light anesthesia. The change may reflect a reorganization of spontaneous brain activity under different conditions, and supports a recent theory about consciousness and brain connectivity. The results of this project also suggests the network specificity is another important aspect for quantification of spontaneous BOLD fluctuation. The details about this project can be found in Chapter 4.

The other three projects on humans aimed to understand the interaction between endogenous spontaneous BOLD fluctuation and external perturbations (stimulation/task). The third project was aiming to understand how the resting-state networks implied by spontaneous BOLD fluctuation would change under continuous stimulation. The finding is that the resting-state visual network is dissociated into two distinct networks covering the activated and non-activated regions of the visual system, respectively, suggesting a spatial reorganization of neural networks under continuous stimulation. Chapter 5 presents the work of this project.

The reorganization of resting-state networks under continuous stimulation is, however, conflicting with the previous finding in human somatosensory system that spontaneous activity reflected by spontaneous BOLD fluctuation can be superimposed onto task-evoked brain activity. In order to further understand reasons causing the discrepancy, the fourth project was carried out to investigate the superimposition of spontaneous BOLD signal and evoked BOLD response in the visual cortex under the condition with short visual stimuli. The results confirmed the superimposition of spontaneous and evoked BOLD signals under short stimulation, but an explanation based on basic BOLD mechanism was given with the results in Chapter 6.

Besides the influence of external stimulation on spontaneous BOLD fluctuation, in turn we are also interested in how spontaneous BOLD fluctuation could affect evoked brain response to stimulation. To this end, the fifth project was performed to examine the relationship between individuals' spontaneous BOLD fluctuation and their evoked BOLD responses to identical stimuli. We found a strong relation between the correlation strength

of spontaneous BOLD fluctuation and the amplitude of evoked BOLD response at the group level. The finding indicates the important role of spontaneous BOLD fluctuation in brain function; moreover, it could also be used to reduce the large inter-subject variation in evoked BOLD responses commonly observed in conventional fMRI studies. Chapter 7 gives a summary of this project.

2.4 Other Modalities Used in This Dissertation

2.4.1 Electroencephalography

Electroencephalography (EEG), a technique for recording brain electrical activity, is widely used in clinical and psychological laboratories. According to location of electrodes, EEG can be divided into scalp-EEG or intracranial-EEG.

The scalp-EEG is noninvasive and thus can be safely used on healthy humans, however its spatial resolution is very limited and increasing the number of electrodes can only partially solve this problem. A map of the brain's electrical activities can be reconstructed by integrating the information from many electrodes located in different scalp sites. The mapping technique is essentially same as the one that seismologists use to predict the earthquakes. However, the source localization technique, or called "inverse problem" solving, faces many challenges in locating the neural field generators, even for the special case, like epilepsy. One of main reasons is the limited information provided by surface recording. The signal picked up by a single scalp-EEG electrode is thought to be a smoothed version of LFPs under a scalp surface on the order of ~10 cm^2. Moreover,

the signal comes mainly from the superficial layers of the cortex, since contribution from the deeper layer drops very fast.

In contrast, the intracranial-EEG either using subdural grids or strips of electrodes placed directly on the surface of the cortex (also known as Electrocorticography, ECoG) or using multi-lead depth electrodes can monitor the locally generated extracellular field potentials and provide much better spatial localization. In addition, it is free from many artifacts associated with scalp-EEG. Nevertheless, intracranial-EEG is invasive and mainly used on neurosurgical patients or animals, and its spatial coverage is often limited by the number of electrodes used.

However, compared to neuroimaging techniques based on hemodynamic and metabolic response, EEG techniques can provide much higher temporal resolution and directly measure neural activity.

EEG mainly reflects synchronized synaptic activity caused by post-synaptic potentials (PSP) of cortical neuron. Low impedance and positioning of EEG electrodes only allow measuring synchronized neural activity of a large population of neurons, therefore EEG signals can be regarded as spatially averaged LFPs, which originate from relatively slow currents in the brain tissue. The major slow current is PSP, including excitatory post-synaptic potentials (EPSP) and inhibitory post-synaptic potentials (IPSP). By contrast, EEG has little contribution from neuronal spiking activity caused by action potentials due to their short duration and associated bidirectional currents, which can be cancelled out when averaged over space.

2.4.2 Laser Doppler Flowmetry

Laser Doppler flowmetry (LDF) is a technique of continuously measuring microcirculatory blood flow. It is based on the Doppler shift phenomenon: the frequency change that light undergoes when reflected by moving objects. The principle of LDF is as following: when a tissue sample is illuminated with monochromatic laser light, red blood cells (RBCs) in the tissue can reflect the laser light and make it undergo a Doppler shift. The back-scattered light contains both unshifted and Doppler-shifted components, and the magnitude and frequency distribution of the latter depend on the number and velocity of moving RBCs within the tissue sample. By analyzing the frequency distribution of the backscattered light, the relative blood perfusion (or cerebral blood flow) can be estimated.

The first LDF experiment for blood flow measurement in a retinal vessel model in rabbit was performed in 1972 (Riva et al., 1972). After that, this technique was developed quickly. In the early 1980s the fiber-optic based laser Doppler perfusion monitoring (LDPM) technique was introduced, which allows for instant perfusion measurements in a small sampling volume.

LDF can only provide a relative but not the absolute quantification of blood perfusion, which is one of its major limitations. However, it has many advantages such as its reliability, high sensitivity, and high temporal resolution. For these reasons, it is now widely used in clinical and research fields.

Chapter 3

NEURAL ORIGIN OF SPONTANEOUS HEMODYNAMIC FLUCTUATIONS IN RATS UNDER BURST-SUPPRESSION ANESTHESIA CONDITION

This is a manuscript that has been published in Cerebral Cortex.

3.1 Introduction

Recent findings from resting-state functional MRI (fMRI) studies have increased the interest in imaging and studying spontaneous brain activity under a resting state in the absence of brain stimulation or task performance. These studies indicate that the blood-oxygenation-level-dependent (BOLD) (Ogawa et al., 1990, Ogawa et al., 1992, Kwong et al., 1992, Bandettini et al., 1992) signals acquired by fMRI in a resting brain are characterized by slow (< 0.1 Hz) and coherent fluctuations within a variety of specific brain networks related to, for example, the motor, visual, auditory, thalamus,

hippocampus, language and default mode systems (Biswal et al., 1995, Lowe et al., 1998, Cordes et al., 2000, Stein et al., 2000, Hampson et al., 2002, Greicius et al., 2003, Fox and Raichle, 2007, Fair et al., 2008). The spatiotemporal correlations of spontaneous BOLD fluctuations have been hypothesized to reflect the "functional connectivity" (Biswal et al., 1995) between the different brain regions and imply many resting-state functional networks (Mantini et al., 2007, Fox and Raichle, 2007).

Despite their great potential and importance, the neurophysiology underlying coherent BOLD fluctuations in a resting brain is not fully understood; in particular, it is still not clear whether they have a neural origin, vascular origin, or both (Lund, 2001). Even though most evidence suggests a possible neural origin, there is still debate over whether the resting-state BOLD signals simply reflect the fluctuations of unconstrained and consciously directed mental activity or coherent networks with significant functional meaning (Morcom and Fletcher, 2007). This argument was partially resolved when the resting-state fMRI research was recently extended from conscious human subjects to anesthetized, unconscious non-human primates. Based on the correlations of spontaneous BOLD signals acquired from isoflurane-anesthetized primates, four distinct spontaneous coherent networks were identified, even under deep anesthesia (using 1.25% isoflurane) showing burst-suppression electroencephalogram (EEG) activity (Vincent et al., 2007), which is a clinical indicator of unconsciousness. This finding suggests that spontaneous BOLD fluctuations and coherent networks implied by the spatiotemporal BOLD correlations persist even in an unconscious brain without normal perceptions and behaviors. It was therefore hypothesized that coherent BOLD fluctuations may represent

a fundamental and intrinsic property of functional brain organization (Vincent et al., 2007). It is, therefore, of great importance to understand the neurophysiological basis of spontaneous hemodynamic fluctuations under the unconscious brain state induced by deep anesthesia. The present study aimed to quantitatively investigate the neurovascular coupling relation between spontaneous hemodynamic fluctuations and neuronal activity in the rat brain under deep anesthesia characterized by burst-suppression EEG activity; and thus to understand the underlying mechanisms of spontaneous hemodynamic fluctuations in the brain in an unconscious state.

This study consisted of two experiments. In the first experiment, spontaneous cerebral blood flow (CBF) signals were measured simultaneously with epidural EEG signals from the bilateral somatosensory cortices of rats with isoflurane-induced burst-suppression anesthesia. The neurovascular coupling was examined and quantified using the temporal correlation between the CBF and EEG signals. In the second experiment, fMRI was used to image spontaneous BOLD signals from another group of rats under the same anesthesia conditions as used for the simultaneous EEG–CBF measurements. Spatiotemporal correlations of BOLD fluctuations were then examined and used to generate correlation maps. For both experiments, data acquisition was repeated under three isoflurane levels of ~1.8%, ~2% and ~2.2% (defined as ISO 1.8, ISO 2.0 and ISO 2.2 anesthesia conditions in this study), and the correlation strength and fluctuation magnitude of spontaneous BOLD/CBF signals were quantified for each anesthesia level. By quantitatively comparing the temporal and spatial characteristics of hemodynamic

signals (CBF and BOLD) and their dependence on anesthesia level, we linked the results of both experiments and drew conclusions.

3.2 Materials and Methods

3.2.1 Simultaneous EEG–CBF Experiments

Six male Sprague-Dawley rats (289–389 g body weight) were anesthetized with ~2% isoflurane in a mixture of O2 and N2O gases with a 2:3 volume ratio. The femoral artery and vein were catheterized for physiological monitoring and/or blood gas sampling. The animal respiratory rate and volume were controlled mechanically using a ventilation machine. During the experiments, the mean arterial pressure (MAP), inspired/expired O_2, CO_2, N_2O, body temperature and heart rate were continuously monitored and recorded. The MAP and heart rate results are summarized in Table 3.1, and no substantial changes were found in any of the three anesthesia conditions. Arterial blood gas was sampled every 1–2 hours and all parameters (pO_2, pCO_2, pH, and plasma glucose level) were maintained within normal physiological limits.

Table 3.1 Mean Arterial Pressure and Heart Rate under Varied Anesthesia Levels

Anesthesia Conditions	*Mean Arterial Pressure (Mean±SD)*	*Heart Rate (Mean±SD)*
ISO 1.8 (n=16)	98.2±8.3	359±21
ISO 2.0 (n=16)	97.6±6.8	360±23
ISO 2.2 (n=13)	93.0±10.5	358±24

One EEG electrode was grounded on the animal's nose, and the other two EEG electrodes were inserted symmetrically, through two small holes in the skull, into the S1FL regions of the rat somatosensory cortex (~1.5 mm deep from the surface of the skull, ~1.5 mm posterior to the bregma, and ~3 mm lateral to the brain midline) in the two hemispheres. The EEG signals were sampled at 1 kHz using commercially available EEG equipment (GRASS TELEFACTOR, RI) and then filtered with a band-pass filter (0.1–30 Hz). A dual-channel Laser Doppler flowmetry (LDF) instrument (OxyLab LDF/OxyFlo, Oxford Optronix, UK) was used to measure regional relative CBF changes simultaneously with the EEG measurement. Two LDF probes were inserted into the somatosensory cortices slightly under the EEG electrodes through the same skull holes. The CBF signals were acquired at a sampling rate of 10 Hz. The simultaneous CBF/EEG recordings were performed under three anesthesia conditions using 1.8%, 2.0% and 2.2% isoflurane, respectively; and after the rats were sacrificed with a bolus injection of KCl solution. Animal surgical procedures and experimental protocols were approved by the Institutional Animal Care and Use Committee of the University of Minnesota.

3.2.2 MRI Experiments

Ten male Sprague-Dawley rats (288–381 g body weight) were used for MRI experiments. The animal preparations were identical to those for the simultaneous EEG–CBF recording experiments. The head position of the rat was fixed by a home-built head-holder with a mouth-bar and ear-bars for minimizing head motion. All MRI studies were performed on a 9.4T horizontal magnet (Magnex Scientific, UK) interfaced with a Varian INOVA console (Varian Inc., Palo Alto, CA) using a proton radiofrequency (RF) surface

coil. First, the multi-slice T_1-weighted anatomical images were acquired from different orientations to identify the rat somatosensory cortex and select appropriate image slice positions for acquiring fMRI data. Secondly, the gradient-echo echo-planar image (GE-EPI) (Mansfield, 1977) was used to acquire five consecutive coronal fMRI slices (field of view = 3.2 × 3.2 cm^2; repetition time (TR)/echo time (TE) = 612/16.5 ms; 64 × 64 image matrix size; 1 mm slice thickness) covering the rat somatosensory cortex (-4.3–0.7 mm from the bregma) by referring to the stereotaxic rat brain atlas (Paxinos and Watson, 1998). All fMRI BOLD signals were acquired when the rats were in complete darkness. The fMRI measurements were conducted for three rats under the ISO 1.8 and ISO 2.0 conditions; for three different rats under the ISO 1.8, ISO 2.0, and ISO 2.2 conditions; and for the remaining four rats under the ISO 1.8, ISO 2.0 and ISO 2.2 conditions, as well as approximately 5 minutes after being sacrificed.

The fMRI acquisition was repeated two to five times under each condition, and each run included 500 GE-EPI volumes (~ 306 seconds).

3.2.3 Data Processing

The simultaneously recorded EEG and CBF time courses were first divided into 300-second segments, and the segment duration was close to the total imaging time of one fMRI run. The EEG data were down-sampled to 100 Hz by averaging every ten data points to retain the signal-to-noise ratio (SNR). The amplitude of EEG signals was extracted by Hilbert transform and then convolved with a hemodynamic response function (HRF), which was determined in anesthetized rats in a previous study (Martin et al., 2006), to generate the EEG-predicted CBF time courses that were further down-

sampled to 10 Hz to match the temporal resolution of the experimentally measured CBF time courses.

The experimentally measured CBF signals were band-pass filtered (0.005–0.1 Hz) in the Fourier domain to remove the baseline drift and high-frequency noise.

For each fMRI run, all GE-EPI images were first spatially filtered with a Gaussian kernel (FWHM = ~1 mm) to increase SNR, and the first 20 image volumes were discarded to avoid transient BOLD signals at the initial image acquisition stage. The time course of each image pixel was normalized by its mean, and then band-pass filtered (0.005–0.1 Hz) to remove the DC component, linear drift, and high-frequency noise. The standard deviations of BOLD time courses were then calculated to generate a standard deviation (SD) map for each fMRI run. A 2-pixel × 2-pixel region located in the right S1FL region was selected as the reference region, which was close to the locations of the EEG electrodes and LDF probes in the EEG–CBF measurements. The BOLD time courses of all image pixels were then cross-correlated (Pearson's correlation) with the reference time course extracted from the S1FL reference region to generate a correlation coefficient (CC) map for each fMRI run. In addition, two regions of interest (ROIs) were selected from the cortical regions, mainly covering the left and right S1FL according to the anatomical images, for statistical analysis.

3.2.4 Statistics

To quantify the strength of neurovascular (EEG–CBF) coupling, the temporal correlation coefficients between the EEG-predicted CBF and the experimentally

measured CBF time courses were calculated as a function of temporal lags for each segment.

To quantify the inter-hemisphere correlation of the spontaneous CBF signals, correlation coefficients between the CBF signals measured from two brain hemispheres for each segment were calculated. To quantify the inter-hemisphere correlation of the spontaneous BOLD signals, the correlation coefficients of each CC map were averaged within the left S1FL ROI (contralateral to the S1FL reference region) to give an average correlation coefficient for each fMRI run.

To quantify the fluctuation magnitude of spontaneous CBF signals, the standard deviation of the normalized CBF signals was calculated for each segment. The standard deviation was also calculated for EEG-predicted CBF signals (arbitrary units), and then normalized by the value observed under the ISO 1.8 anesthesia condition. To quantify the fluctuation magnitude of spontaneous BOLD signals, the SD maps of each fMRI run were averaged within the two S1FL ROIs defined previously.

To test whether the baseline levels of CBF and fMRI signals change at different anesthesia depths, the mean CBF and fMRI signals (averaged within the S1FL ROIs) were calculated for each segment (or run) acquired under the three anesthesia conditions; the results were then normalized by that of the ISO 1.8 anesthesia condition.

Finally, a linear mixed model taking the rats as the random variable and the isoflurane anesthesia level as the fixed variable was used to summarize the statistics from all rats and give the statistical inference. The statistical analyses were performed in R

(Team, 2008) using the "nlme" package (Pinheiro et al., 2009). A p value of ≤ 0.01 was considered to be statistically significant.

3.3 Results

3.3.1 Temporal Correlations between Spontaneous EEG and CBF Changes

Figure 3.1 shows the EEG and CBF time courses measured in the bilateral S1FL regions from a representative rat under the three anesthesia conditions. The EEG signals measured under the ISO 1.8 and ISO 2.0 conditions exhibited a typical burst-suppression EEG pattern: quasi-periodical bursts of high-voltage slow wave (mainly < 15 Hz) separated by suppression periods of a low-voltage flat EEG pattern lasting from a few seconds to a few minutes (Stern and Engel, 2005, Kroeger and Amzica, 2007). Interestingly, the distinct EEG "bursts" were always followed by corresponding triangular-shaped "bumps" in the CBF time courses simultaneously recorded in the same S1FL region. This observation is consistent with an early study (Golanov et al., 1994), qualitatively suggesting a close neurovascular coupling between the spontaneous EEG and CBF signal changes. When the anesthesia level was increased from ISO 1.8 (Figure 3.1A) to ISO 2.0 (Figure 3.1B), the appearance frequency of the spontaneous EEG bursts was largely reduced; and the number of CBF bumps also decreased accordingly. Once anesthesia reached the deepest level of ISO 2.2, the EEG burst activity almost disappeared and only single spikes were occasionally observed; correspondingly, the

CBF fluctuations were almost flat (Figure 3.1C). The relation between the isoflurane concentration and the appearance frequency of EEG bursts is shown in Figure 3.S1.

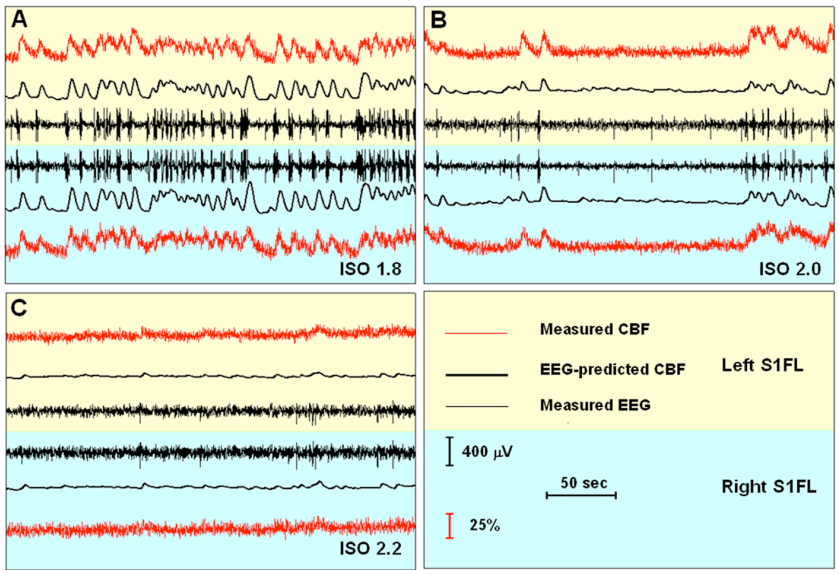

Figure 3.1 Spontaneous EEG and CBF signals simultaneously recorded from bilateral S1FL regions of a representative rat under varied anesthesia depths: (A) ISO 1.8: 1.8% isoflurane; (B) ISO 2.0: 2.0% isoflurane; and (C) ISO 2.2: 2.2% isoflurane. Each "burst" in the EEG time courses (thin black traces) was always followed by a triangular-shaped "bump" in the simultaneously recorded CBF signals (thin red traces, unfiltered). The EEG-predicted CBF time course (thick black traces), which is the convolution of the EEG amplitude and a hemodynamic response function, was very similar to the measured CBF time course. Moreover, both the temporal EEG and CBF changes were highly synchronized between the left (light yellow background) and right (light blue background) hemispheric S1FL. The appearance frequency of spontaneous EEG "bursts" and CBF "bumps" decreased as anesthesia became deeper, and they almost disappeared under the deepest ISO 2.2 anesthesia condition.

The EEG-predicted CBF time courses (thick black traces in Figure 3.1) were highly correlated to the experimentally measured CBF time courses (red traces in Figure 3.1) under the different anesthesia conditions; and their correlation coefficients are plotted in Figure 3.2 as a function of temporal lags. The EEG–CBF coupling was very

strong under the ISO 1.8 and ISO 2.0 anesthesia conditions with correlation coefficients of 0.61 ± 0.19 and 0.66 ± 0.17 (mean ± SD) at the zero lag, respectively. In contrast, the correlation was significantly reduced to 0.28 ± 0.22 under the ISO 2.2 condition and disappeared (0.04 ± 0.09, not statistically different from zero) when EEG activity became completely silent after the animal was sacrificed. These results indicate that a tight EEG–CBF correlation exists in the deeply-anesthetized (but not dead) rat brain.

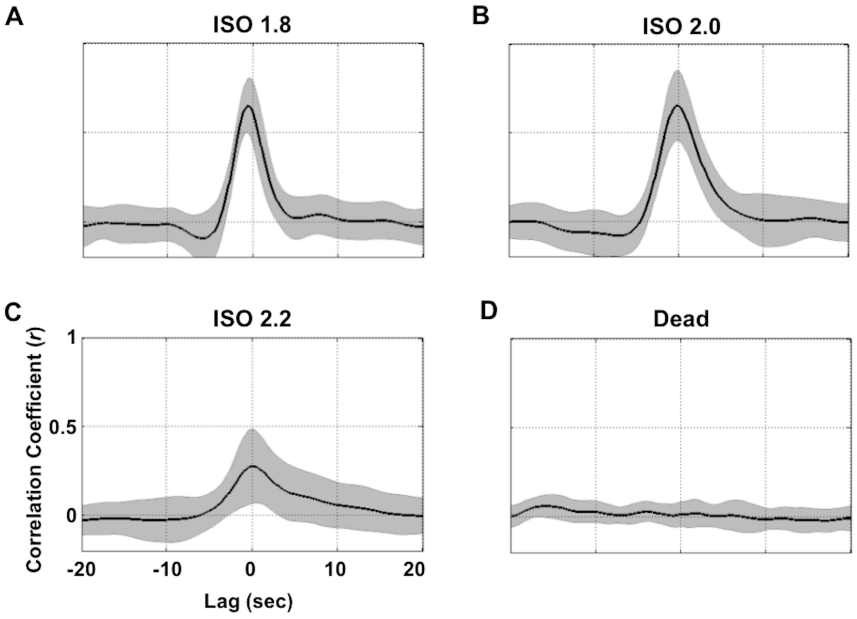

Figure 3.2 Correlation coefficients between the EEG-predicated and measured CBF signals as a function of temporal lags under different conditions. The black curves present cross-correlation functions averaged over different segments from six rats, and the gray shadows represent regions within two standard deviations. Correlations were strong under (A) the ISO 1.8 and (B) 2.0 anesthesia conditions, reduced significantly under (C) the ISO 2.2 anesthesia condition, and finally approached zero (D) after the rats were sacrificed.

Besides the tight correlation between the EEG and CBF signals acquired from the same S1FL cortical region, both EEG and CBF signals themselves were also found to be

strikingly synchronized across the two brain hemispheres, in particular, under the ISO 1.8 and ISO 2.0 conditions (Figures 3.1A and 3.1B). Such strong inter-hemisphere correlations suggest that both spontaneous neuronal activity and coupled CBF fluctuations are highly synchronized within somatosensory cortices under these two deeply-anesthetized, unconscious conditions.

3.3.2 Spatiotemporal Correlations of Spontaneous BOLD Fluctuations

Compared with the CBF signals recorded using the dual-channel LDF system, the fMRI BOLD signals have a larger coverage and can provide more information about the spatial distribution of spontaneous hemodynamic fluctuations. To obtain such information, correlation maps were generated by correlating spontaneous BOLD signals of all image pixels with that of a reference region (the blue cross in Figure 3.3) located in the right S1FL (Paxinos and Watson, 1998). The correlation maps from a representative rat (Rat 8) are shown in the left panel of Figure 3.3. Under the ISO 1.8 and ISO 2.0 conditions, the spontaneous BOLD fluctuations showed strong correlation over the majority of the cortical regions covered by the five acquired fMRI slices, which mainly included the brain regions of M1, M2, S1HL, S1FL, S1DZ, S1BF, and S2 (Paxinos and Watson, 1998) associated with sensorimotor functions. In contrast, the correlations of spontaneous BOLD signals were much weaker at the ISO 2.2 anesthesia level. After the rats were sacrificed but with the air ventilation still running, only the reference region appeared in the correlation maps due to auto-correlation, and its correlation with other brain regions completely disappeared as illustrated in Figure 3.3 and Figure 3.4. These

results suggest that the physiological noise from periodic respiration had a negligible effect on the BOLD time courses measured in a live rat brain in this study.

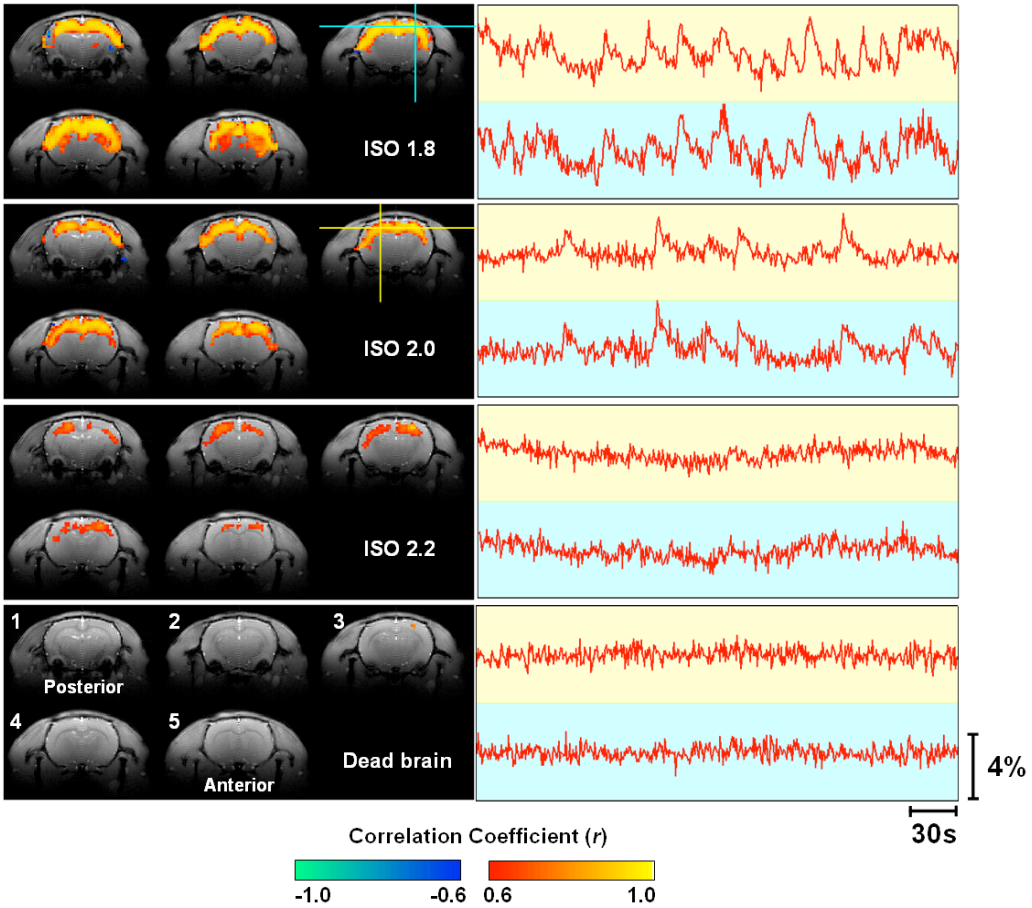

Figure 3.3 BOLD correlation maps and time courses measured under three anesthesia conditions from a representative rat brain (Rat 8). The reference region for the correlation maps was located at the right S1FL region. The five coronal fMRI slices (ordered from 1 to 5) were located -3.8, -2.8, -1.8, -0.8, and 0.2 mm from Bregma, respectively. The BOLD time courses were extracted from both the reference region (blue cross) and the contralateral S1FL region (yellow cross) without being filtered and plotted on backgrounds with the corresponding colors. Spontaneous "bumps" similar to those CBF bumps appeared frequently on the BOLD time courses acquired under the ISO 1.8 and ISO 2.0 anesthesia conditions. * The baseline fMRI signal acquired from the dead brain was smaller than the other three conditions (see Figure 6E).

To further understand the anesthesia-level-dependency of BOLD, for each anesthesia condition the BOLD signals were extracted from both the reference S1FL region (the blue cross in Figure 3.3) and the contralateral S1FL region (the yellow cross in Figure 3.3), and are plotted on the right side in Figure 3.3 (the right panel) next to their corresponding correlation maps. Interestingly, the BOLD signals acquired under the ISO 1.8 and ISO 2.0 conditions have triangular-shaped bumps, which highly resemble those CBF bumps observed in the first experiment (e.g., shown in Figure 3.1). The BOLD bumps have a fast rising phase and a slow declining phase; they appear less frequently as the anesthesia level deepens, and disappear under the ISO 2.2 anesthesia condition. Moreover, these bumps are highly synchronized between the bilateral S1FL regions and result in a strong BOLD correlation between those cortical regions. The correlation maps averaged over multiple fMRI runs are shown in Figure 3.4 for all ten rats to demonstrate the excellent reproducibility and reliability of the fMRI BOLD measurements across individual rats. The reproducibility and reliability were further demonstrated in detail in the Supplementary Materials (see Figures S2 and S3)

Besides the cortical regions, the subcortical regions including some thalamic nuclei and the caudate putamen (CPu) also show correlations to the reference S1FL region, especially under the ISO 1.8 anesthesia condition, although to a lesser extent compared to cortico-cortical correlation. Figure 3.5 demonstrates the correlation maps measured from a single fMRI run from two rats showing the strongest cortical–subcortical correlations. From the posterior to anterior brain position, the correlated subcortical regions move from the thalamic nuclei, mainly including the posterior

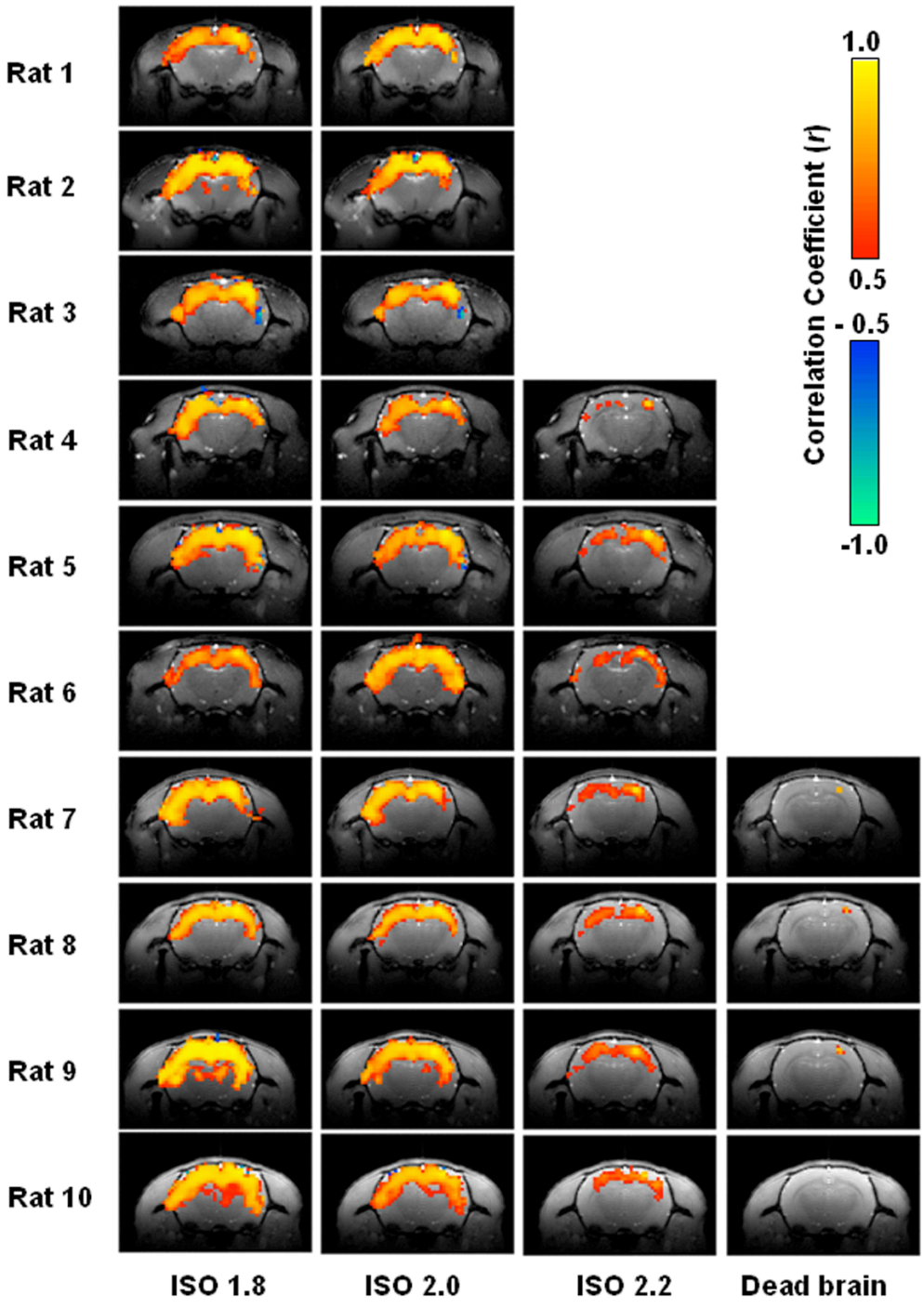

Figure 3.4 Correlation maps measured under different conditions from all individual rats studied. For each rat, the correlation maps present the results averaged from multiple fMRI runs acquired under the same condition.

thalamic nucleus (PO), ventral posterolateral thalamic nucleus (VPL), ventral posteromedial thalamic nucleus (VPM), and ventral anterior thalamic nucleus (VA) to the CPu accordingly. This observation is consistent with the anatomy of the rat brain (Paxinos and Watson, 1998). Although the strength of such cortical–subcortical correlations varied across individual rats, the spatial correlation pattern was consistent among them.

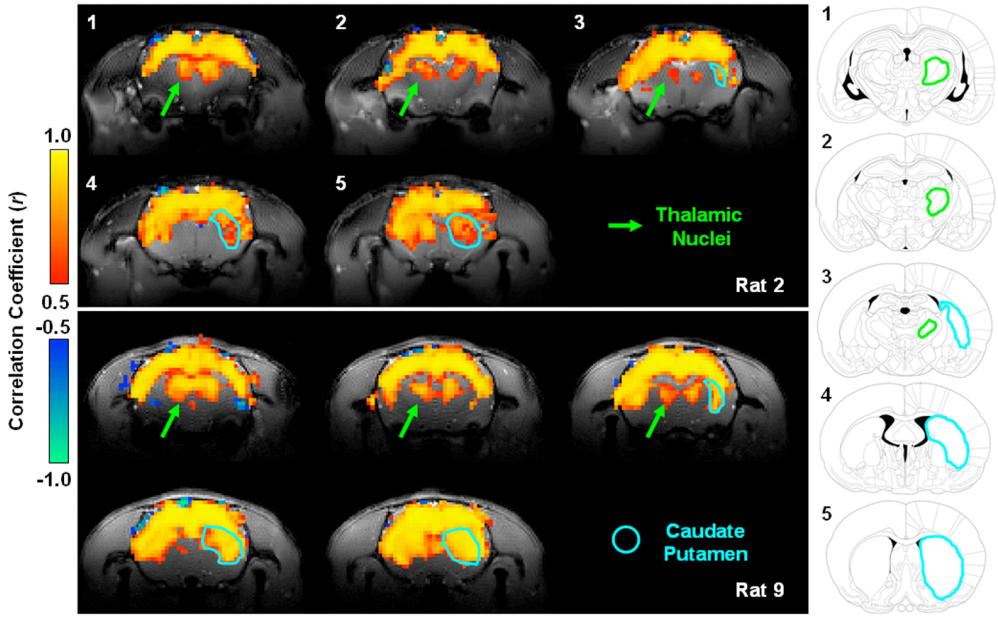

Figure 3.5 Demonstration showing the coherent BOLD fluctuations between the cortical and subcortical regions. Left panel: the correlation maps under the ISO 1.8 anesthesia condition based on single fMRI runs acquired from two rats (Rat 2 and Rat 9). The green arrows point out thalamic regions and the blue lines delineate the caudate putamen (CPu). Right column (adopted from the rat brain atlas (Paxinos and Watson, 1998)): the corresponding anatomical drawings for all fMRI slices. The regions delineated by the blue lines are belong to the CPu, and the areas outlined with green lines mainly cover several thalamic nuclei including the posterior thalamic nucleus (PO), ventral posterolateral thalamic nucleus (VPL), ventral posteromedial thalamic nucleus (VPM) and ventral anterior thalamic nucleus (VA).

3.3.3 Multimodal Comparison and Statistical Summary

To quantitatively illustrate the above observations, statistics for evaluating the coherence strength and fluctuation magnitude of spontaneous CBF and BOLD signals were calculated and are summarized according to anesthesia levels (Figure 3.6). The fluctuation magnitudes of the experimentally measured CBF, the EEG-predicted CBF (Figure 3.6A) and BOLD signal (Figure 3.6C), which were quantified by the standard deviation of normalized signals, decrease with very similar trends as the anesthesia depth increases. The similar dependences led to two excellent linear relations of fluctuation magnitudes under varied anesthesia conditions: one between the CBF and BOLD signals, and the other between the EEG-predicted CBF and BOLD signals (Figure 3.6B). These results suggest tight coupling among spontaneous BOLD, CBF, and EEG signals.

Although a significant difference in fluctuation magnitude was found between the ISO 1.8 and ISO 2.0 anesthesia conditions ($p = 2.98\times10^{-3}$ for CBF, $p = 5.37\times10^{-11}$ for EEG-predicted CBF, and $p = 4.03\times10^{-8}$ for BOLD), the coherence strength quantified by the inter-hemisphere correlation coefficient did not differ significantly (Figure 3.6D) between these two conditions ($p = 0.56$ for CBF and $p = 0.22$ for BOLD). However, it was significantly reduced under the ISO 2.2 condition ($p = 7.20\times10^{-7}$ for CBF and $p = 3.36\times10^{-18}$ for BOLD, compared to ISO 1.8), and more drastically after the animals were sacrificed ($p = 8.53\times10^{-42}$ for BOLD compared to ISO 1.8).

Again, the coherence strength of the CBF and BOLD signals showed a very similar dependence on anesthesia level (Figure 3.6D). All of these results confirm and

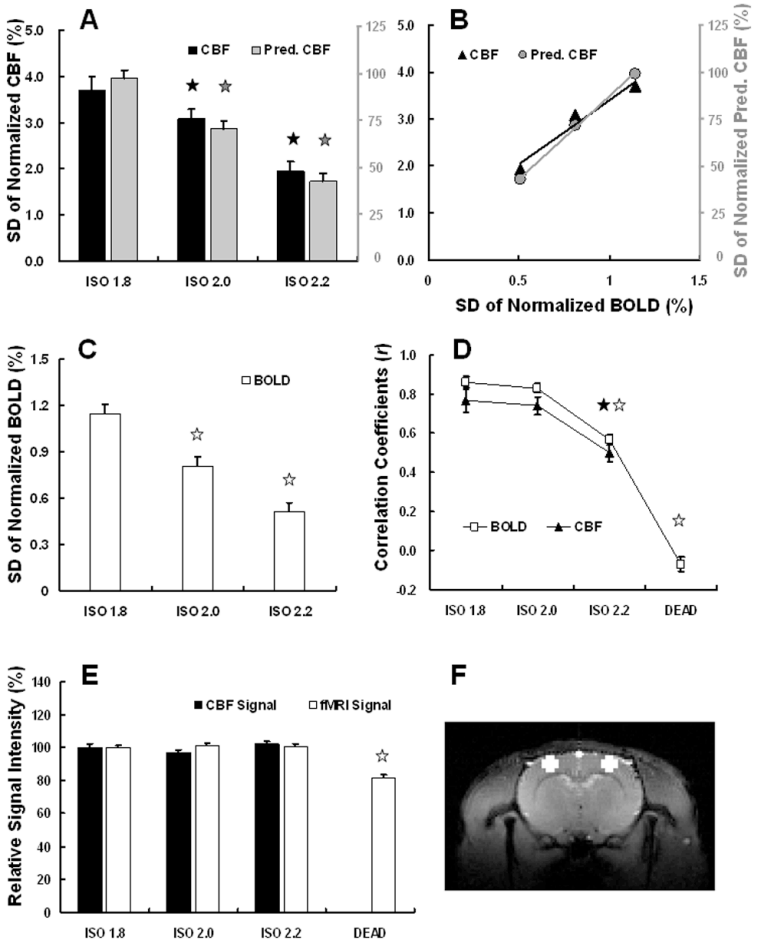

Figure 3.6 Multimodal comparisons and statistical summary of fluctuation magnitudes and coherence strength among the measured CBF, EEG-predicted CBF and BOLD signals. The standard deviations of normalized CBF (A, black), EEG-predicted CBF (A, gray), and BOLD (C) signals, which quantify the fluctuation magnitudes, decrease as the anesthesia depth increases. Such dependences show an excellent linear correlation between CBF and BOLD signals (R^2 = 0.96, B, black triangles), as well as between EEG-predicted CBF and BOLD (R^2 = 0.99, B, gray circles). The inter-hemisphere correlations, which quantify the coherence strength of spontaneous fluctuations, also show the similar dependency on the anesthesia depth for the CBF and BOLD signals (D). The baseline levels of both CBF and fMRI signals did not change significantly under the three anesthesia conditions (E). An example of ROIs used for calculating BOLD statistics (see Methods) is shown with white color (F). The error bars in this figure represent the standard error of the mean (SEM). All comparisons were made with the ISO 1.8 anesthesia condition, and the pentacles are used to mark the conditions showing a statistically significant difference ($p < 0.01$).

support the qualitative observations based on the EEG and CBF time courses and functional BOLD correlation maps shown in Figure 3.1 to Figure 3.4.

To further examine whether the anesthesia level could change the baseline level of CBF and fMRI signals (i.e., T_2*-weighted GE-EPI signals), and thus influence the quantification of CBF and BOLD fluctuation magnitudes, the mean CBF and fMRI signals obtained under all conditions were normalized by those of the ISO 1.8 condition and the results are summarized in Figure 3.6E. No statistically significant difference was found between the three anesthesia conditions (for CBF signal: $p = 0.07$ under ISO 2.0 and $p = 0.25$ under ISO 2.2; for fMRI signal: $p = 0.19$ under ISO 2.0 and $p = 0.65$ under ISO 2.2; compared to ISO 1.8 condition). After the animals were sacrificed, the baseline CBF approached zero and the baseline fMRI signal level decreased by 21.2% ($p = 1.76\times10^{-18}$), simply due to a large reduction in the brain blood oxygenation level.

3.4 Discussion

3.4.1 Neural Origin of Spontaneous Hemodynamic Fluctuations

In this study, tight neurovascular coupling was found between the co-localized EEG and CBF signals simultaneously recorded from the rat somatosensory cortex under burst-suppression anesthesia conditions. The spontaneous high-voltage bursts in EEG signals, which presumably result from the strong synchronization of neuronal activity from a large population of neurons, induce triangular-shaped CBF bumps with a few seconds of latency from the EEG bursts (Figure 3.1). Increasing the anesthesia level can

reduce the appearance frequency of EEG bursts and CBF bumps, which in turn can reduce the magnitude of spontaneous CBF fluctuations. Moreover, both the EEG bursts and CBF bumps are highly synchronized between two recording sites located in the bilateral S1FL regions in the two hemispheres.

The fMRI BOLD signals acquired under the same anesthesia conditions also show spontaneous bumps, which have a very similar shape to the CBF bumps (Figure 3.1 and Figure 3.3). The similarity between spontaneous BOLD and CBF fluctuations is also evident from their strong synchronization over the large scale of two hemispheres and their similar dependence upon anesthesia depth. Quantification and comparison of the inter-hemisphere correlation strength and fluctuation magnitude of spontaneous CBF and BOLD signals provide statistical evidence to support the tight CBF–BOLD relation in a deeply anesthetized brain (Figure 3.6). This finding is in line with the theory that BOLD contrast is usually dominated by CBF change (Ogawa et al., 1998).

The overall results of excellent EEG–CBF and CBF–BOLD correlations from the present study suggest that the spontaneous hemodynamic (CBF and BOLD) fluctuations observed under the burst-suppression anesthesia conditions are mainly induced by spontaneous high-voltage burst activity, and the synchronization of these spontaneous EEG bursts across a large population of neurons results in the strong correlation of hemodynamic fluctuations over different brain regions. This notion can probably be generalized to different species under similar burst-suppression anesthesia, for instance, isoflurane-anesthetized primates in which a number of coherent networks were identified

based on the spatiotemporal correlations of spontaneous BOLD fluctuations (Vincent et al., 2007).

Previous studies have suggested that the spontaneous low-frequency hemodynamic fluctuations may have both neural and vascular origins (Kannurpatti et al., 2008, Biswal et al., 1997, Hudetz et al., 1992). In the present study, under the ISO 1.8 and ISO 2.0 anesthesia conditions, the high-voltage EEG bursts induced large bumps in the CBF (~25% peak-to-peak change, Figure 3.1) and BOLD (~3% peak-to-peak change, Figure 3.3) signals with almost a one-to-one relation (Figures 1 and 3) and strikingly high coherence. Therefore, they are probably the major source leading to the spontaneous CBF and BOLD fluctuations observed under these conditions. However, when the anesthesia level is further increased to ISO 2.2 and EEG activity becomes much quieter (Figure 3.1C), it is not clear whether or not other sources such as the vascular component could make substantial contributions since the neurovascular coupling becomes much weaker (Figure 3.2C). This aspect deserves further investigation.

Previous animal studies (Kannurpatti et al., 2008, Hudetz et al., 1992) also showed that a significant reduction in mean arterial pressure (MAP) under certain severe conditions, such as exsanguination, can affect the autoregulation function of the vascular system and result in strong, low-frequency fluctuations of CBF (Hudetz et al., 1992) and BOLD (Kannurpatti et al., 2008) signals. To avoid this complication, all the CBF and BOLD data acquired in the present study were obtained when physiological parameters including MAP and heart rate were stable and within a normal physiological range. There were no substantial MAP or heart rate variations among the three anesthesia conditions

(Table 3.1). It is interesting to note that MAP was slightly higher under the relatively lighter anesthesia conditions (ISO 1.8 and ISO 2.0; Table 3.1) in which we observed stronger CBF/BOLD fluctuations and coherence. Therefore, the dependence of hemodynamic fluctuations on anesthesia depth found in the present study cannot be attributed to the vascular autoregulation associated with MAP variation.

3.4.2 Neural Correlates of Spontaneous Hemodynamic Fluctuations

A number of studies have demonstrated or suggested the neural correlates of spontaneous hemodynamic fluctuations in different species under various brain states. Spontaneous BOLD signals in the occipital lobe of awake human subjects were found to be negatively correlated with α-band EEG activity from the same brain region (Goldman et al., 2002, Moosmann et al., 2003, Feige et al., 2005). In addition, the power fluctuation of δ-band EEG activity was suggested to contribute significantly to the spontaneous cerebral blood volume (CBV) fluctuations in α-chloralose-anesthetized rats (Lu et al., 2007), based on the finding of the similar inter-hemisphere correlation dependence of CBV and δ-band EEG on anesthesia level. It is also interesting to note that spontaneous BOLD fluctuations in lightly anesthetized primates were found to be correlated with γ-band local field potential activity, multi-unit activity and neuronal spiking rates (Shmuel and Leopold, 2008), although this result is still under debate (Logothetis et al., 2009).

Compared to the studies reported in the literature, the neurovascular coupling observed under the burst-suppression anesthesia condition in the present study seems to be much stronger, probably due to the quasi-periodical alternation between high-voltage

EEG bursts and low-voltage EEG suppression patterns. Furthermore, the time-frequency analysis from a previous electrophysiological study (Hudetz and Imas, 2007) indicated that the relatively low-frequency band (9–12 Hz) activity dominates such spontaneous EEG bursts under burst-suppression anesthesia.

One possible explanation for the discrepancies in the way different types of spontaneous neural activities (e.g., γ-band LFP, δ-band, α-band EEG, and burst-suppression EEG activity) are correlated with spontaneous hemodynamic fluctuations (e.g., BOLD, CBF and CBV) may be attributed to the different species and brain states studied. In studies on anesthetized animals, both the depth of anesthesia and the type of anesthetic are likely to significantly affect spontaneous brain activity. On the one hand, this complexity may make it difficult to provide a generic understanding of spontaneous hemodynamic fluctuations and their neural origins. On the other hand, it also suggests that different brain states are associated with distinct spontaneous brain activities and thus different hemodynamic fluctuations, which can be readily imaged and investigated using noninvasive fMRI methods. This notion is supported by a series of recent studies, which observed spontaneous BOLD fluctuations and their organized spatial pattern (resting-brain coherent networks) across a wide range of resting-brain states from awake, sleep, lightly sedated or even vegetative human brains (Biswal et al., 1995, Greicius et al., 2008, Horovitz et al., 2008, Boly et al., 2009) to lightly and deeply anesthetized primate brains (Shmuel and Leopold, 2008, Vincent et al., 2007).

3.4.3 Spatial Characteristics of Coherent BOLD Fluctuations

The correlation maps based on the spatiotemporal correlation analysis of BOLD signals in the present study cover a large portion of the cortical regions in the scanned fMRI slices; and the relocation of the reference region within these cortical areas or the size of the reference region did not significantly change the spatial pattern of the correlation maps. Although the majority of these brain regions showing strong BOLD correlations still belong to the sensorimotor system, our results differ from those of previous studies investigating functional connectivity within the rat somatosensory system. In those studies, a more specific network mainly covering the bilateral S1FL regions was identified through spatiotemporal correlations of spontaneous CBV (or BOLD) fluctuation in rats anesthetized with α-chloralose (Lu et al., 2007) or medetomidine (Zhao et al., 2008). This discrepancy could again be due to the distinct spontaneous neural activities, as well as their different spatiotemporal correlations, induced by the different anesthetics and/or anesthesia depth.

As reported previously (Hudetz and Imas, 2007, Steriade et al., 1994, Swank, 1949), the burst-suppression activity is characterized by wide synchronization over the whole neocortex, although the strength of the bursts may not be uniform over all brain regions (Hudetz and Imas, 2007). Furthermore, structural connectivity in the brain is essential for maintaining such synchronization, since a lesion in the corpus callosum produced asymmetric (not coherent) burst-suppression patterns between two hemispheres (Lazar et al., 1999, Lambrakis et al., 1999). These electrophysiological studies are consistent with our observations based on the BOLD correlation maps, which reflect the

large-scale synchronization of underlying neural activity and reveal the "functional connectivity" in the unconscious, burst-suppression anesthesia condition.

According to a new theory about consciousness and anesthesia (Alkire et al., 2008, Hudetz, 2006), loss of consciousness could be due to two mechanisms. One is the breakdown of cortical connectivity and thus of integration; and the other is the collapse of the repertoire of cortical activity pattern and thus of information, even though the information may still be integrated globally. The strong but less-specific "connectivity" observed under burst-suppression anesthesia herein can be regarded as a valuable illustration of the second mechanism of the theory. It suggests that although the deeply anesthetized brain characterized by burst-suppression activity has already completely lost consciousness, spontaneous neural activity could still be highly synchronized over different brain regions.

Even though the BOLD correlation is widely distributed and less-specific under the burst-suppression anesthesia, the correlation maps (for example, Rat 3 in Figure 3.4) show a trend that the strongest correlation with the right S1FL reference region usually appears at the contralateral S1FL region. This observation was further confirmed by either using a higher CC threshold for displaying the correlation maps or applying the global signal regression procedure (Fox et al., 2009) to removing the global correlations of BOLD signals, and the remaining fMRI pixels with strong coherence indeed located within the S1FL regions, bilaterally. This finding may suggest that the coherence of widely distributed and synchronized burst-suppression activity is still relatively stronger between the brain regions with the most intense anatomical connections. Therefore, the

specificity of the BOLD coherent network reduced substantially under deeply anesthetized and unconscious brain state; however, it was not completely disappeared.

Our results also indicate a correlation between cortical regions and subcortical regions, including some thalamic nuclei and the CPu, although its correlation strength was relatively weaker than the cortico–cortical correlation. It is still not fully understood whether the thalamus and neocortex are functionally connected to each other under deep burst-suppression anesthesia. Earlier studies suggested that the neocortex is isolated from thalamic sensory inputs under burst-suppression anesthesia, because the firing activity of cortical neurons is correlated with the EEG burst-suppression pattern but is independent of the thalamic neuron firing pattern (Steriade et al., 1994, Topolnik et al., 2003). Moreover, undercut anesthetized neocortex can still generate burst-suppression activity (Swank, 1949, Topolnik et al., 2003). However, this view may need further investigation based on new evidence from a number of studies showing that a variety of sensory stimuli (visual, auditory, and somatosensory) were able to nonspecifically elicit global burst activity under burst-suppression anesthesia conditions (Hartikainen et al., 1995, Hudetz and Imas, 2007, Kroeger and Amzica, 2007). Our findings may provide some clues with regard to this issue, and also suggest that the fMRI technique may provide a useful neuroimaging tool for future research on this topic.

3.4.4 Technical Considerations

Since the major focus of the present study was to investigate the neurovascular couplings underlying spontaneous BOLD fluctuations, it ideally required simultaneous EEG–BOLD measurement. However, this experimental configuration still faces many

technical challenges; for example, to deal with the increased susceptibility effects that could lead to severe fMRI artifacts, especially at ultrahigh field. Therefore, two separate experiments were carefully designed and conducted in the present study to avoid these technical difficulties and complications. The rigorous multimodal comparisons and statistical analysis of the data obtained from these two experiments not only found very similar "bumps" in the BOLD and CBF signals, but also indicated almost identical dependence of their fluctuations on anesthesia depth, leading to the conclusion that tight EEG–BOLD coupling exists in the isoflurane-anesthetized rat brain.

The hemodynamic response function (HRF) applied in the present study to link the EEG and CBF signals was taken from a previous study using a rat model and urethane anesthesia (Martin et al., 2006). From the results of cross-correlation functions between the EEG-predicted CBF and measured CBF (Figure 3.2), the applied HRF seems to work slightly better under the ISO 2.0 anesthesia condition than under the ISO 1.8 anesthesia condition, whose correlation function peak appeared slightly ahead of zero lag (Figure 3.2A). This observation raises an interesting question: does the hemodynamic response function alter under different anesthesia conditions? Nevertheless, our analyses indicated that the correlation between the EEG-predicted CBF and experimentally measured CBF was less sensitive to the precise shape of the hemodynamic response function applied. For instance, the use of the HRF from awake human brain, which has a much longer BOLD peak latency and broad HRF shape compared to the rat brain HRF, did not significantly change the outcomes and conclusions. Moreover, the rat brain HRF taken from the literature was similar with the HRF de-convolved from the EEG-CBF data

obtained in the present study. Therefore, it provided a good approximation for examining the EEG–CBF coupling relation.

The raw data of spontaneous CBF and fMRI time courses measured in the present study were both in arbitrary unit; thus, they were normalized by their mean signals before the standard deviations were calculated to quantify the CBF and BOLD fluctuation magnitudes. One potential complication is that a significant change in baseline perfusion level (CBF) or baseline fMRI signal under varied anesthesia conditions or in a dead brain may affect the reference level of normalization and thus quantification of fluctuation magnitude. To address this concern, the baseline levels of CBF and fMRI signals were examined and compared under all the conditions studied herein, and no significant difference was found between the three anesthesia conditions (Figure 3.6E) except for a significant fMRI signal reduction in the dead rat brain due to a large decrease in the blood oxygenation level. This result is not surprising since the global perfusion level of rat brain increased by only ~10% when isoflurane was increased from 1.4% to 2.8%, as reported previously (Lenz et al., 1998). A much narrower range (1.8%–2.2%) of isoflurane concentration was applied in the present study; and the anesthetic and vasodilatation effects of isoflurane may compensate each other within this range such that baseline CBF and fMRI levels did not change, as shown in Figure 3.6E. Therefore, the standard deviation of normalized CBF/BOLD signals should provide a reliable, quantitative indicator reflecting the magnitude of the hemodynamic fluctuation.

3.4.5 Other Perspectives

Recent research on neuroenergetics using neuroimaging techniques has revealed that a large portion of the total brain energy is used to support the spontaneous neural activity and "housekeeping" power in the brain (Du et al., 2008, Raichle, 2006, Raichle and Mintun, 2006, Shulman et al., 2007). Also interestingly, the pre-stimulus baseline hemodynamic signals have been found to be linked to human behavioral responses and can influence task-evoked brain activity (Sapir et al., 2005, Hesselmann et al., 2008a, Fox et al., 2007, Boly et al., 2007). These findings emphasize the essential roles of spontaneous brain activity in supporting basic brain function and in understanding the working mechanism of the brain. The large hemodynamic fluctuations and their highly organized spatial coherence as observed under the unconscious brain state in the present study support these findings. Although the measured spontaneous CBF and BOLD signal changes cannot be used to directly determine the absolute baseline energy levels in the rat brain, they indeed imply a high brain energy demand for supporting the large CBF/BOLD fluctuations, which showed similar magnitudes to those evoked by brain stimulation. Since relative CBF and BOLD changes can be quantitatively linked to the change in the cerebral metabolic rate of oxygen consumption (CMRO2) by using the BOLD calibration model (Kim and Ugurbil, 1997, Davis et al., 1998), the observed tight coupling between spontaneous CBF and BOLD signal changes in this study indirectly implies a substantial CMRO2 or energy fluctuation for supporting spontaneous brain activity.

It has been documented that a loss of bilateral and symmetric burst-suppression EEG synchronization between two hemispheres is a clinical indication of brain

dysfunction (e.g., unilateral brain infarction or stroke) (Stern and Engel, 2005). The neuroimaging approaches based on either BOLD or CBF signal source should provide a sensitive tool for noninvasively imaging and diagnosing these types of brain dysfunction with superior spatial and temporal resolution.

3.5 Conclusion

Several conclusions can be drawn from the present study. There is tight neurovascular coupling between the spontaneous EEG amplitude and spontaneous hemodynamic (CBF and BOLD) fluctuations in the deeply anesthetized, unconscious brain state characterized by burst-suppression EEG activity. The coupled EEG, CBF and BOLD signals were highly synchronized in large-scale cortical regions as well as some of the subcortical nuclei associated with the sensorimotor system. The synchronization pattern of spontaneous brain activities can be mapped by fMRI based on spatiotemporal correlations of low-frequency BOLD fluctuations, resulting in "coherent networks" in the deeply-anesthetized rat brain. It was also found that the coherence strength and fluctuation amplitude of spontaneous hemodynamic signals as well as the spatial extent of the mapped "coherent networks" are sensitive to the patterns of spontaneous brain activity, which can be modulated by anesthesia depth or other interventions. The overall findings support the conclusion that the spontaneous CBF/BOLD fluctuations observed under burst-suppression anesthesia conditions are mainly of neural origin. They provide valuable insights into the neurophysiological basis for the use of BOLD- and CBF-based

fMRI methods to investigate spontaneous and synchronous brain activity under various brain states.

3.6 Supplementary Figures

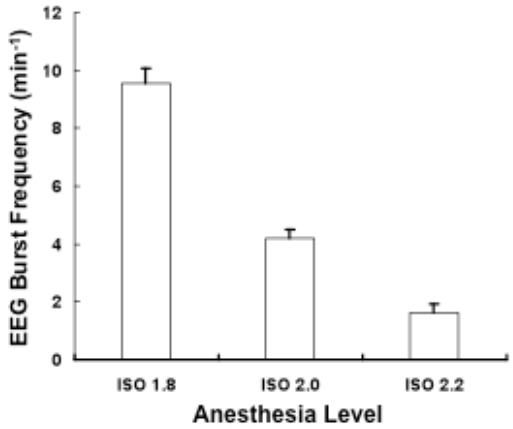

Figure 3.S1 Appearance frequency of the EEG bursts as a function of isoflurane anesthesia level. The error bars stand for the standard errors across measurement runs.

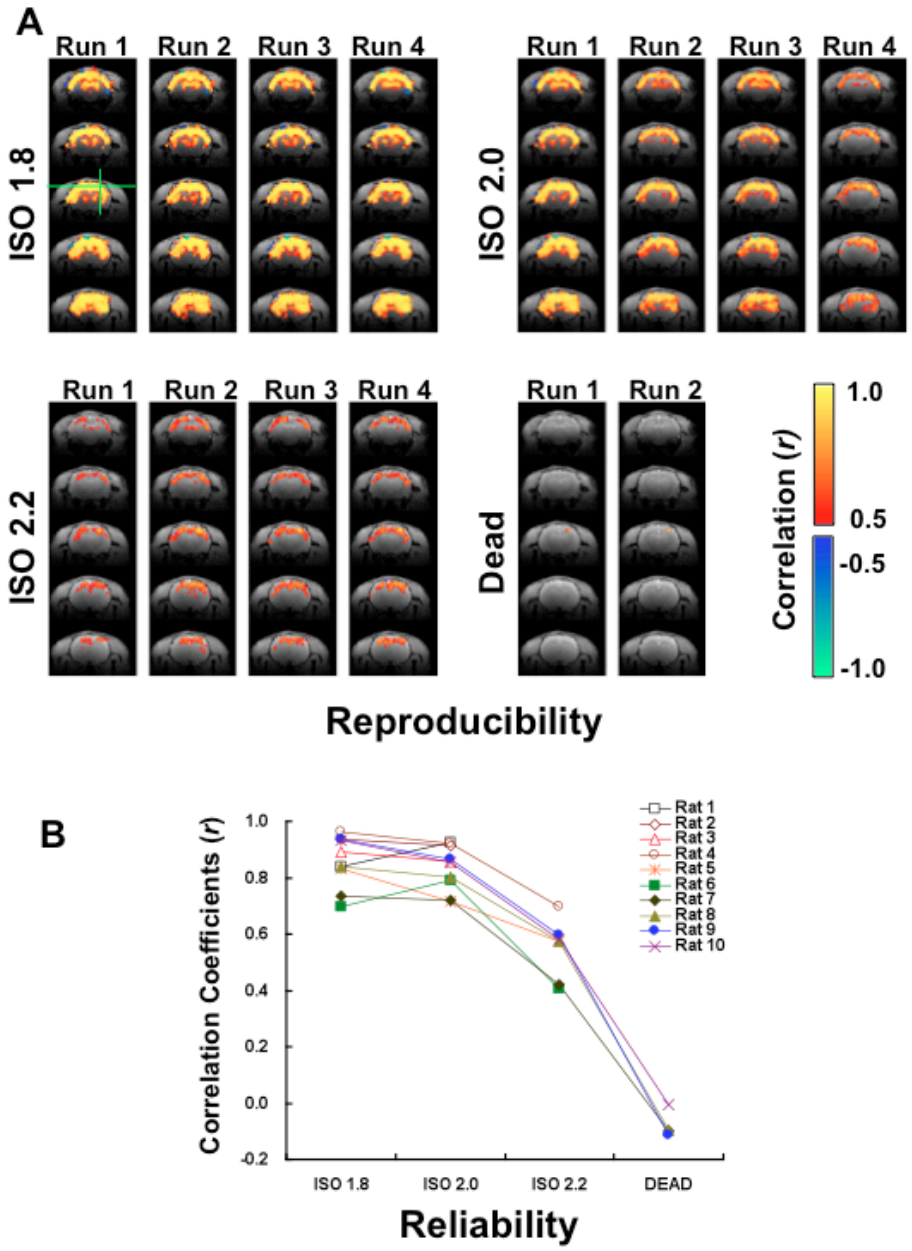

Figure 3.S2 Reproducibility and reliability of the individual fMRI experimental results. The BOLD correlation maps generated based on fourteen fMRI runs from a representative rat (Rat 9) show a consistent pattern under the same condition across multiple runs, and distinct patterns between different conditions (A). For each individual, the correlation strength (between a ROI in the left S1FL and the right S1FL reference region, see Materials and Methods in the manuscript for details) was plotted as a function of anesthesia level (B). All animals show a very similar trend, and the averaged inter-subject result and statistics have been presented in the manuscript (Figure 3.6E).

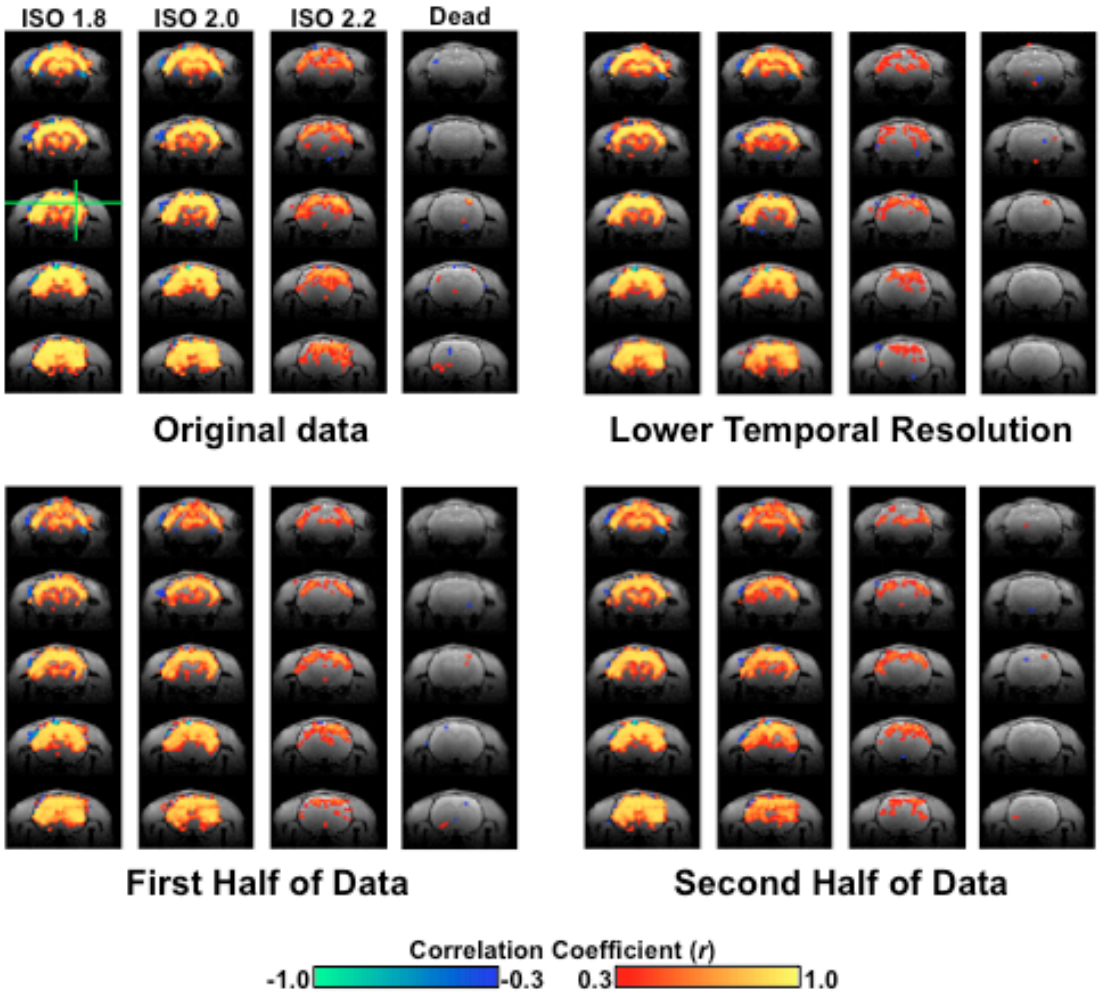

Figure 3.S3 Reproducibility of the BOLD correlation maps. The original correlation maps from a representative rat (Rat 9) are compared with those generated based on three reorganized datasets. The comparison datasets were created by temporally under-sampling the original datasets (keeping one time point every three), only using the first half of total time points (240 image volumes), and only using the second half of total time points, respectively. All correlation maps demonstrate similar trends across different conditions with only the original ones show a relatively higher correlation power due to favorable time averaging.

Chapter 4

A SPECIFIC-TO-LESS-SPECIFIC TRANSITION OF RESTING-STATE BRAIN NETWORK FROM LIGHT TO DEEP ANESTHESIA

This manuscript is ready for submission.

4.1 Introduction

Recent resting-state functional Magnetic Resonance Imaging (fMRI) studies have shown that slow (< 0.1 Hz) blood-oxygen-level-dependent (BOLD) signals recorded from the resting brain demonstrated spontaneous and coherent fluctuations within a variety of anatomically-connected and functionally-specific brain networks, for example, the visual, motor, auditory, language, and default mode systems (Biswal et al., 1995, Fox and Raichle, 2007). It has been suggested that such spontaneous BOLD fluctuations could reflect underlying spontaneous brain activity; and their temporal correlations may

reflect the “functional connectivity” (Biswal et al., 1995) and imply many “resting-state networks” (Mantini et al., 2007). These findings are of great importance, because they may potentially explain the large portion of biochemical energy "mysteriously" consumed by the resting brain for supporting the spontaneous neuronal activity (Du et al., 2008, Raichle, 2006, Raichle and Mintun, 2006, Shulman et al., 2007), and also provide new insights into some fundamental mechanisms of brain function. This notion has gained supports from a series of fMRI studies, which found that the pre-stimulus/pre-task spontaneous BOLD fluctuations can influence human subject behavioral responses to stimuli/tasks (Boly et al., 2007, Fox et al., 2007, Hesselmann et al., 2008a, Hesselmann et al., 2008b, Sapir et al., 2005).

Rather than the fluctuations of unconstrained and consciously directed mental activity, the spontaneous BOLD fluctuations and associated resting-state networks are believed to reflect a more fundamental and intrinsic organization of the resting brain; because they have been widely observed not only in awake human brains but also under the brain states with reduced level or complete loss of consciousness, for example, during sleep, under light sedation, with deep anesthesia, or even in vegetative state (Horovitz et al., 2008, Greicius et al., 2008, Boly et al., 2009, Vincent, 2007 #12, Lu et al., 2007).

A recent study has shown that even in the deeply-anesthetized, unconscious rat brain characterized by burst-suppression (BS) electroencephalogram (EEG) pattern the spontaneous BOLD correlations still imply a highly-coherent but less-specific resting-state network covering a large cortical region associated with sensorimotor functions (Liu et al., 2010). However, the strong correlation of spontaneous BOLD signal (functional

connectivity) under such a deep anesthesia condition is, to some extent, against intuition; moreover, such a less-specific pattern of the resting-state network is distinct from those observed in rats anesthetized with different doses and types of anesthetics, which cover more specific brain regions, i.e., the bilateral S1FL (primary somatosensory cortex, forelimb) regions (Lu et al., 2007, Zhao et al., 2008). These observations therefore raise an interesting question: what causes the different specificities of the resting-state networks observed in these studies, difference in anesthetics types or in anesthesia levels, i.e., consciousness levels?

A new theory has been recently proposed to link consciousness and anesthesia (Alkire et al., 2008). According to this theory, both information and integration are essential for consciousness. One of the two working mechanisms of anesthesia to induce unconsciousness is to disrupt the repertoire of cortical activity pattern, and thus the brain's capability of encoding information, even though the information may still be integrated globally. The less-specific resting-state BOLD coherent networks (or functional connectivity) observed previously (Liu et al., 2010) is, to some extent, consistent with the electrophysiology study showing a collapse of the repertoire of rat cortical activity pattern under the deep anesthesia characterized by BS EEG pattern (Alkire et al., 2008). This analogy may suggest a possible link between the specificity of resting-state network and consciousness level of the brain; and the investigation of this relationship will not only help us further understand the mechanisms of anesthesia, but also provide new insights regarding the functional significance of resting-state networks.

This work aimed to quantitatively study the relationship between the specificity of resting-state BOLD coherent network and the anesthesia depth using a rat model. To minimize the confounding effects potentially caused by different anesthetics, only isoflurane was applied in the present study; and spontaneous BOLD signals were imaged from the rat brain under three isoflurane levels of ~1.0%, ~1.5% and ~1.8% (defined as light, mild, and deep anesthesia condition, respectively, in this study). Through the spatiotemporal correlations of acquired BOLD signals, the resting-state networks, especially their specificity, were examined and compared across different conditions to test the hypotheses that the specificity of resting-state network would be modulated by the anesthesia depth and this modulation could reflect the change of underlying neural activity associated with the various level of consciousness.

4.2 Materials and Methods

4.2.1 Animal Preparation

Eight male Sprague-Dawley rats (250–339 g body weight) were initially anesthetized with ~2% isoflurane in a mixture of O2 and N2O gases with a 2:3 volume ratio. The femoral artery and vein were catheterized for physiological monitoring and/or blood gas sampling. A ventilation machine was used to mechanically control the animal respiratory rate and volume. The mean arterial pressure (MAP), inspired/expired O_2, CO_2, N_2O, body temperature and heart rate were continuously monitored and recorded during the experiment. Table 4.1 summarizes the MAP and heart rate results, only less

than 10% changes were observed across different anesthesia conditions. Arterial blood gas was sampled every 1–2 hours. The pO_2, pCO_2, pH and plasma glucose level were maintained within normal physiological limits.

Table 4.1 Mean Arterial Pressure and Heart Rate under Varied Anesthesia Levels (n=8)

Anesthesia Condition (% isoflurane)	*Mean Arterial Pressure (Mean±SD)*	*Heart Rate (Mean±SD)*
Light (1.0%)	113.6±14.2	409±46
Mild (1.5%)	109.5±9.3	401±38
Deep (1.8%)	101.8±6.1	374±20

4.2.2 MRI Experiments

All experiments were performed on a 9.4T horizontal magnet (Magnex Scientific, UK) interfaced with a Varian INOVA console (Varian Inc., Palo Alto, CA) using a proton radiofrequency (RF) surface coil. The head position of the rat was fixed by a home-built head-holder with a mouth-bar and ear-bars to minimize head motion. At the beginning of the experiment, the multi-slice T_1-weighted anatomical images were acquired from axial, sagittal, and coronal orientations to identify the rat somatosensory cortex and select appropriate image slice positions for fMRI data acquisition. Then, five consecutive coronal fMRI slices (field of view = 3.2 × 3.2 cm^2; repetition time (TR)/echo time (TE) = 612/16.5 ms; 64 × 64 image matrix size; 1 mm slice thickness) were acquired using the gradient-echo echo-planar image (GE-EPI) (Mansfield, 1977) to cover the rat somatosensory cortex (-4.3–0.7 mm from the bregma), with reference to the stereotaxic

rat brain atlas (Paxinos and Watson, 1998) and the acquired anatomical images. All fMRI BOLD signals were acquired when the rats were in darkness and all monitored physiological parameters were normal and stable.

For each rat, the fMRI measurements were repeated 3–4 runs under the light (isoflurane ~1.0%), mild (isoflurane ~1.5%), and deep (isoflurane ~1.8%) anesthesia conditions and 2 runs after the rat was sacrificed. Each fMRI run consists of 500 GE-EPI volumes (~306 seconds). Ten dummy scans were also added before each run to avoid the transient BOLD signal change during the initial acquisition period.

4.2.3 Data Analysis

All GE-EPI images were first spatially filtered with a Gaussian kernel (FWHM = ~1 mm) to increase signal to noise ratio (SNR), and motion correction was then performed on all data using the 3D registration tool (3dvolreg) of AFNI (Cox, 1996). The first 20 image volumes of each run were discarded to further eliminate the transient BOLD signal recorded during the initial GE-EPI acquisition period. The BOLD signal time course of each image pixel was normalized by its mean, and then band-pass filtered (0.003–0.5 Hz) to remove the DC component, very slow drift, and high-frequency noise.

Three 2-pixel × 2-pixel regions located in the left and right S1FL (primary somatosensory cortex, forelimb: -1.8 mm from the bregma and ~2.5 mm from the brain midline), and the right S1BF (primary somatosensory cortex, barrel field; -1.8 mm from the bregma and ~5 mm from the brain midline) regions were selected as the reference regions. For each fMRI run, the BOLD time courses of all image pixels were then cross-

correlated (Pearson's correlation) with those extracted from the reference regions to generate three correlation coefficient (CC) maps.

A region of interest (ROI) was selected based on the anatomical images to cover cortical regions in the left brain hemisphere. For each correlation map, the CC values within the defined ROI were projected (by averaging) onto a line orthogonal to the brain midline to obtain a profile, that describes how the correlation to the reference regions changes along this line.

4.2.4 Global Signal Regression

To test how the removal of global signal fluctuations can affect the outcomes of correlation analysis (i.e., correlation maps), in addition to the data processing strategy described above we also processed the same fMRI data using a second strategy, in which the global mean signal (averaged within the defined ROI) was removed by sample linear regression from the BOLD time courses of all GE-EPI image pixels during pre-processing stage.

All data were analyzed using MATLAB7.5 (MathWorks, Natick, MA).

4.3 Results

4.3.1 Specificity of Coherent Network Changes as Anesthesia Level Varies

Figure 4.1 shows BOLD correlation maps and the corresponding reference BOLD time courses from a representative rat (Rat 3). It illustrates how the spatiotemporal

correlations of spontaneous BOLD signals and associated resting-state BOLD coherent networks change under various anesthesia conditions. Under the deep anesthesia with 1.8% isoflurane, spontaneous BOLD signals show very strong temporal correlations over most cortical and some sub-cortical regions covered by the fMRI slices; and the spatial pattern of the correlation maps is insensitive to the location of the reference regions (see the upper part of the right panel in Figure 4.1). This observation suggests that a highly-

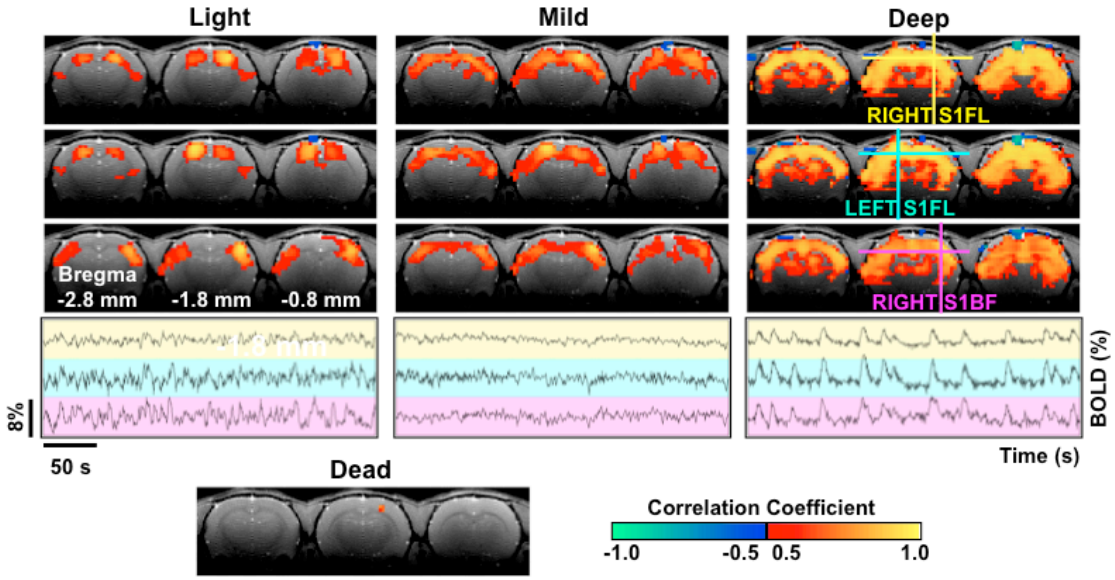

Figure 4.1 BOLD correlation maps and corresponding reference time courses from a representative rat. Top three rows display BOLD correlation maps with respect to the bilateral S1FL (yellow and blue cross) and the right S1BF (magenta cross) regions, respectively, under the light (left panel), mild (middle panel), and deep (right panel) anesthesia conditions; while the BOLD time courses from these reference regions are plotted on a background with corresponding color at the bottom row. The BOLD signals demonstrate distinct fluctuation patterns at different anesthesia level, and the specificity of their correlation maps decreases as the anesthesia increase from light to deep. A correlation map with respect to the right S1FL obtained after the rat being sacrificed (lower left panel) only shows the reference region, indicating a diminished BOLD correlation at this condition.

coherent but less-specific network covering a wide range of brain regions exists in the deeply-anesthetized rat brain. The strong BOLD correlations under this condition could be easily understood through the BOLD time courses extracted from the reference regions, i.e., the left and right S1FL, and the right S1BF regions (Figure 4.1, the lower part of the right panel). These BOLD time courses display large, spontaneous triangular-shaped bumps, which are highly synchronized over the three reference regions.

In contrast, the patterns of both correlation maps and BOLD time courses become significantly different under the light anesthesia condition with 1% isoflurane. The reference BOLD time courses show a distinct fluctuation pattern: the stereotypic bumps disappear even though fluctuation magnitude is still considerably large (Figure 4.1, the lower part of the left panel). The correlations between the BOLD time courses are no longer easily judged by visualization under the light anesthesia, but could be examined through the correlation maps (Figure 4.1, the upper part of the left panel). The correlation maps with respect to the left and right S1FL regions overlap each other and cover very similar brain regions, i.e., the bilateral S1FL and S2 regions; while the correlation map with respect to the right S1BF region mainly covers the bilateral S1BF regions. These observations suggest that the large, less-specific coherent network under the deep anesthesia condition has been dissociated into smaller and more specific networks covering much localized brain regions under the light anesthesia.

In terms of the specificity of correlation maps, the mild anesthesia condition with 1.5% isoflurane sits between the light and deep anesthesia conditions (Figure 4.1, the upper part of the middle panel); however, the magnitude of spontaneous BOLD

fluctuations (Figure 4.1, the lower part of the middle panel) is the smallest among three anesthesia conditions.

A correlation map based on the BOLD signals acquired after the animal was sacrificed (the air ventilation still running) is also shown in Figure 4.1, and only the reference region appears in the map due to autocorrelation. This result suggests that the physiological noise from periodic respiration had a negligible effect on the BOLD correlations observed in the live rat brain in this study.

To better quantify the observations described above, the values of the correlation maps within a ROI covering the left-hemisphere cortical regions were projected (by averaging) onto a line orthogonal to the brain midline, and the obtained profiles from all eight rats were then averaged according to anesthesia levels and the results are shown in Figure 4.2. The average profile shows strong but relatively uniform correlation coefficients (CCs) over different cortical regions under the deep anesthesia condition (the blue curve). In contrast, it displays well-defined and narrow peaks at the position symmetric to the reference region at the light anesthesia (the red curve). The average profile at the mild anesthesia (the green curve) again appears intermediate to those of the other two anesthesia conditions.

For the correlation maps with respect to the right S1FL region, the distribution of correlation coefficients within the ROI is also estimated through histograms (Figure 4.3) for all the rats. Under the deep anesthesia, most of image pixels have very strong correlations (high CC value) with the reference regions and therefore result in the very left-skewed histogram (blue color); while the histogram for the light anesthesia condition

(red color) is much closer to a normal distribution with a much smaller mean. The histogram of the mild anesthesia condition (green color) sits between those of the other two conditions. This observation is consistent across different rats. All of these results suggest that the specificity of spatiotemporal correlations of spontaneous BOLD fluctuations significantly changes under different anesthesia levels.

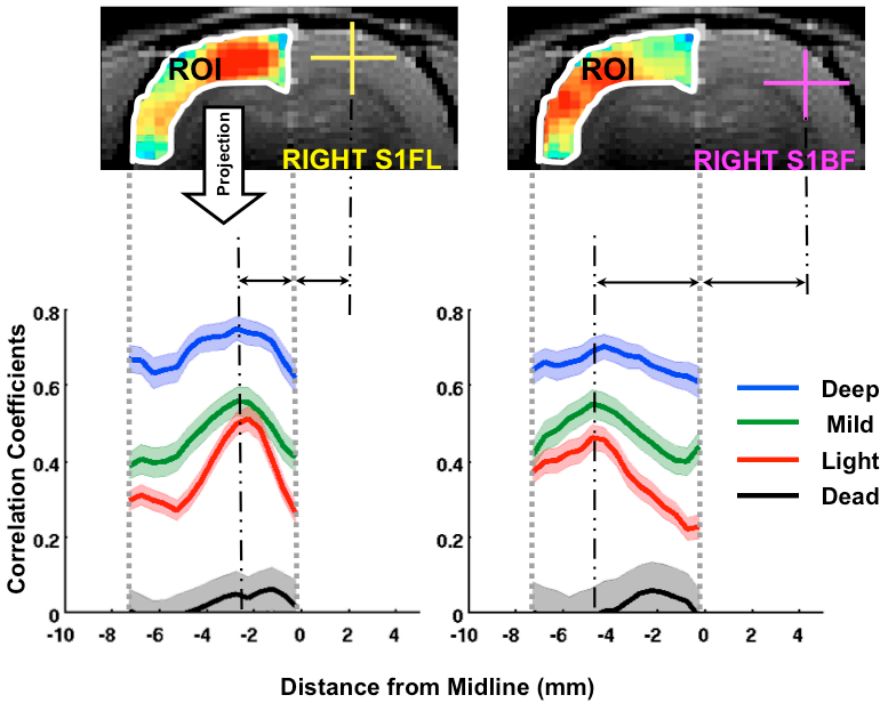

Figure 4.2 Projection of BOLD correlation maps on a line orthogonal to the brain midline. Within a ROI covering the left-hemisphere cortical regions, the BOLD correlation maps with respect to the S1FL (left) and S1BF (right) regions from all the rats (n=8) was projected onto a line orthogonal to the brain midline by averaging in vertical. The projection profiles show distinct, sharp peaks at the locations symmetric to the reference regions under the light anesthesia (red, n = 28 runs), but relatively uniform at the deep anesthesia (blue, n = 31 runs), with the profiles for the mild anesthesia (green, n = 26 runs) sitting between them. After the animals were sacrificed, the profiles (black, n = 16 runs) approach the zero line. Shadows regions are within two standard errors.

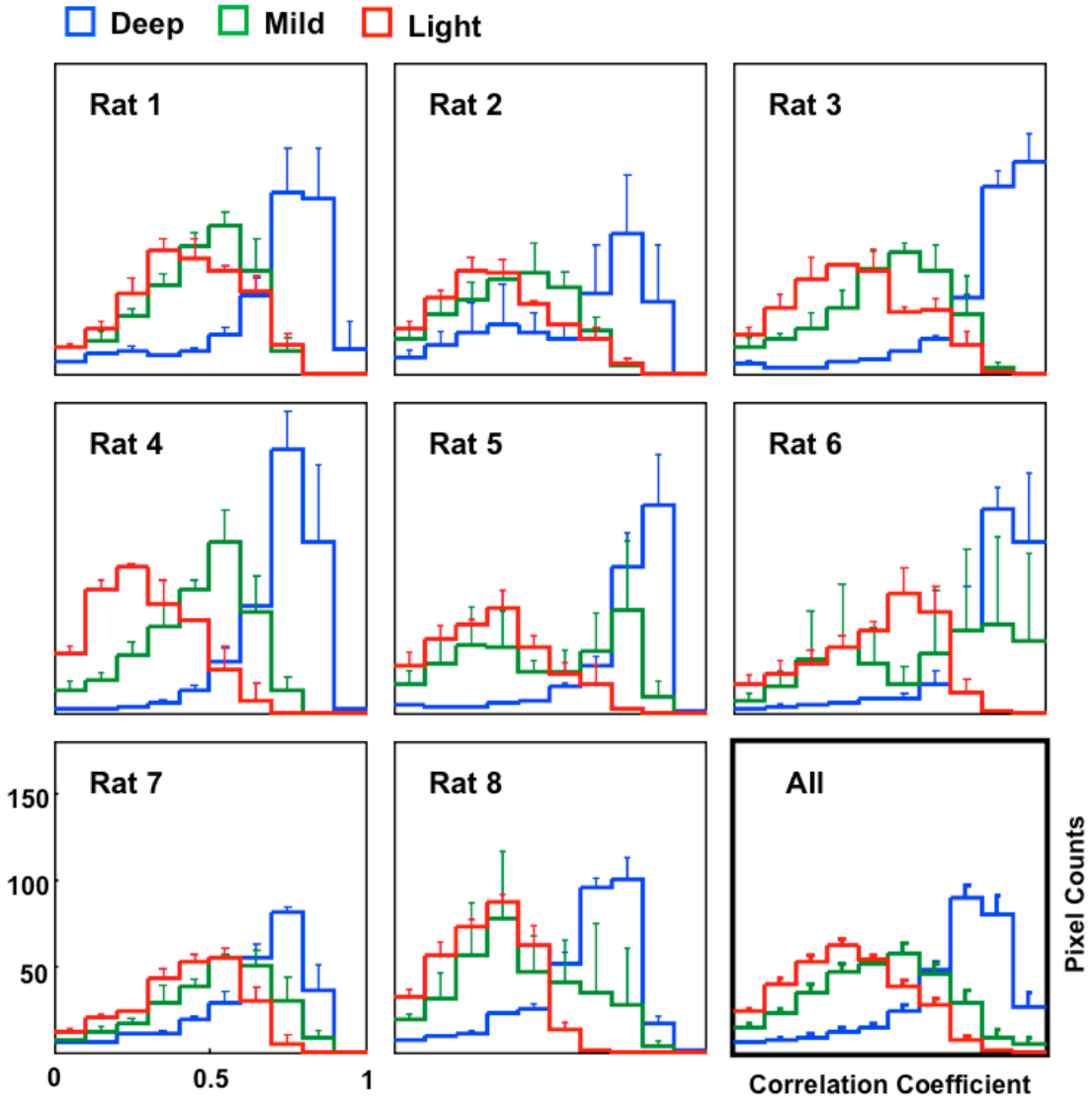

Figure 4.3 Histograms showing the positive CC distribution of correlation maps with a ROI covering the left-hemisphere cortical regions (see Figure 4.2). The left-skewed distribution under the deep anesthesia (blue) is consistent with the strong, but less-specific correlation pattern. In contrast, the CC distribution at the light anesthesia (red) is closer to a normal distribution, and that under the mild anesthesia (green) sits between those of the other two conditions. The above observation is consistent across individuals. Only few pixels showed negative CC values in the correlation maps and they are therefore not shown in the histograms. The error bars stand for the standard errors across runs.

4.3.2 Global Signal Regression

Removing global signal fluctuation by linear regression is a common and useful step used in many resting-state functional connectivity fMRI (fcMRI) studies to pre-process data before performing correlation analysis (Fox et al., 2009). This approach was also applied to processing the same fMRI dataset in the present study, in parallel, to examine the impact of global signal regression on the resting-state correlation maps. Generally speaking, the global signal regression has a subtle influence on the correlation maps under the light anesthesia condition, but can significantly affect those obtained with deep anesthesia.

Figure 4.4 compares the correlation maps from two representative rats under the deep anesthesia condition created based on the fMRI data pre-processed with and without the global signal regression. With the global signal regression, the strong global BOLD correlation over large cortical regions is dramatically reduced, and specific patterns appear in the correlation maps covering much localized and well-defined brain regions, for example, the bilateral S1FL regions (Figure 4.4, the bottom row).

At the same time, by gradually raising the CC threshold for displaying the correlation maps obtained without the global signal regression, we can show the specific pattern (Figure 4.4, the middle row) similar to those obtained with the global signal regression (Figure 4.4, the bottom row). Therefore, the effect of the global signal regression is approximately equivalent to removing the CC range accounting for global correlation (for example, CC < 0.6 for the deep anesthesia) and then expanding the remaining CC range.

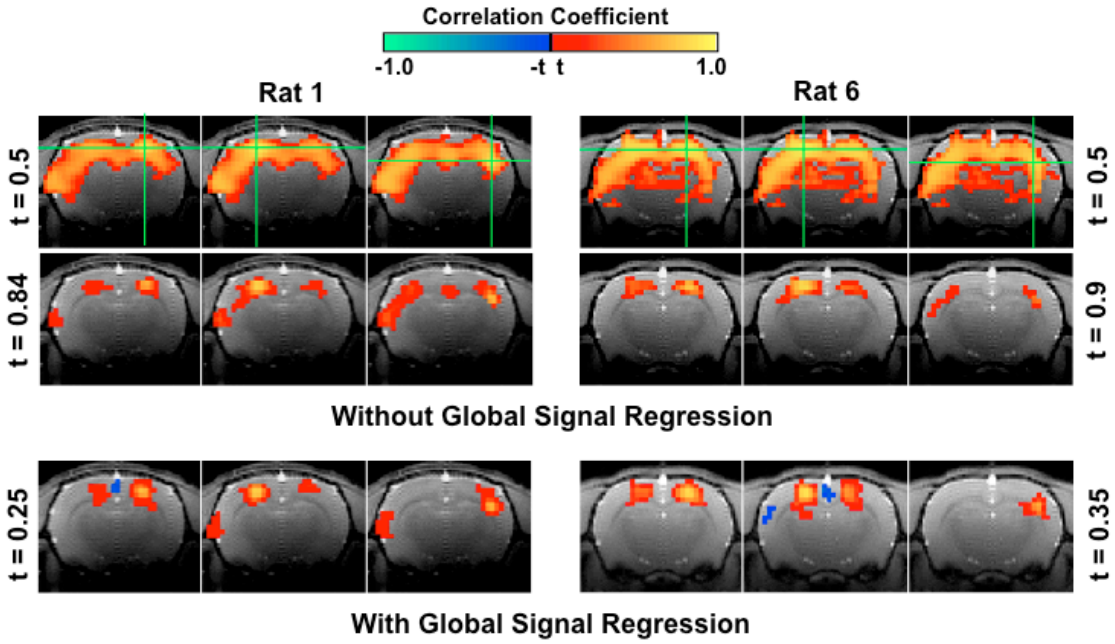

Figure 4.4 Deep anesthesia correlation maps from two representative rats generated with and without global signal regression. The correlation maps under the deep anesthesia (the top row) become much more specific after the global signal fluctuation was removed by regression (the bottom row). Such specific patterns, however, can also be obtained by adjusting the CC threshold (t) to a much higher value (the middle row). The finding suggests a "less-specific" but not completely "non-specific" correlation pattern for the spontaneous BOLD signals under the deep anesthesia.

On the other hand, this comparison also suggests that the correlation maps (or the coherent networks) under deep anesthesia are "less-specific" but not completely "non-specific", since the brain regions with most intensive anatomical connections, such as the bilateral S1FL regions, still hold the strongest BOLD correlations (or functional connectivity). This notion is also evident by the correlation profiles of the deep anesthesia showing CC peaks, though less sharp, symmetric to their reference regions (Figure 4.2, the blue curve). `

4.4 Discussion and Conclusion

In this study, by analyzing the spatiotemporal correlations of spontaneous BOLD fluctuations in the anesthetized rat brain, we found that the specific resting-state coherent networks covering different sub-regions of the rat sensorimotor system gradually merged into a highly-coherent but less-specific network covering almost the entire brain cortical region when the anesthesia depth changes from light to deep. This finding may suggest a reorganization of ongoing brain activity pattern across different consciousness levels, which can be robustly imaged by fMRI.

4.4.1 Spontaneous BOLD Fluctuations under Different Anesthesia Conditions

Spatiotemporal correlations of spontaneous BOLD signals acquired under the light anesthesia indicated specific coherent networks covering distinct sub-regions of the rat sensorimotor system, for example, the bilateral S1FL versus S1BF regions. This is consistent with the pattern of the resting-state network observed in medetomidine-sedated rats (Zhao et al., 2008). Moreover, such somatotopic organization of resting-state functional connectivity is also in agreement with those observed in the primary motor cortex of awake human subjects (van den Heuvel and Hulshoff Pol, 2009). Collectively, these results suggest that the specificity may be one of important characteristics of the resting-state networks under awake and lightly-anesthetized brain states. The mapped specific networks using fMRI reflect the underlying neuroanatomical connectivity associated with specific brain functionalities.

Compared to the light anesthesia, the spontaneous BOLD signals measured under the deep anesthesia condition show a completely different temporal fluctuation pattern: the large, stereotypic triangular-shaped BOLD bumps appear intermittently and spontaneously. The synchronization of these bumps results in strong and widely-distributed correlation of BOLD signals over large cortical regions. These observations are consistent with the results from our previous resting-state fcMRI study on the deeply-anesthetized rat with a high isoflurane concentration of ≥ 1.8% (Liu et al., 2010). More importantly, the previous study has also shown that the anesthesia level of ~1.8% isoflurane is deep enough to produce the BS EEG pattern in the rat brain, which consists of alternating spontaneous high-voltage EEG bursts and suppressed near-flat EEG periods (Kroeger and Amzica, 2007, Stern and Engel, 2005); and the triangular-shaped BOLD bumps are actually induced by such high-voltage EEG bursts. Therefore, the spontaneous BOLD signals under the deep anesthesia condition reflect the ongoing brain activity and their temporal correlations truly reveal the dynamic connectivity (or neural synchronization) between different brain regions under this completely unconscious condition. It is also important to note that the BOLD coherent network under deep anesthesia is spatially "less-specific", but not completely "non-specific". The bilateral S1FL regions still have strongest synchronization that is clearly evident in the results of correlation maps as demonstrated in Figure 4.4.

As a transition stage, the mild anesthesia condition, however, shows the smallest magnitude of spontaneous BOLD fluctuations. In rats, isoflurane can induce the BS EEG pattern at concentrations of 1.4–1.8% (Hudetz and Imas, 2007), and the appearance

frequency of spontaneous EEG bursts is known to decrease as isoflurane concentration increases within this range. At the mild anesthesia level (~1.5% isoflurane), the EEG bursts probably occur so frequently as to result in substantial overlapping between adjacent BOLD bumps; therefore, a relatively "flat" BOLD time course without obvious bumps was observed (Figure 4.1, the lower part of the middle panel). Interestingly, even though the BOLD time courses are relatively flat without distinct bumps, their correlations are still very strong and exhibit an expected transition pattern between the light and deep anesthesia levels.

4.4.2 Specificity of Resting-state Coherent Network versus Consciousness State

According to a new theory about consciousness and anesthesia (Alkire et al., 2008, Hudetz, 2006), there are two possible working mechanisms about how anesthesia affects brain function and consciousness. One is to break down cortical connectivity and thus the brain's ability of integration; and the other is to disrupt the repertoire of cortical activity pattern and thus the brain's capacity for encoding information, even though information may still be integrated globally. An essential evidence for supporting the second mechanism comes from rat studies. In deeply-anesthetized rats showing BS EEG activity, a visual stimulation evoked global and highly synchronized field potential responses in many brain regions including the occipital, parietal, and frontal lobes, which are much beyond the visual system; in contrast, the same stimulation on awake rat brain only elicited the neuronal responses confined within the visual cortex inside the occipital lobe (Hudetz and Imas, 2007). The lack of regional specificity is also true for non-

anesthetic unconsciousness. The application of the transcranial magnetic stimulation (TMS) over the sensorimotor cortex of awake human subjects produced a specific, sequential pattern of brain activation; in contrast, the identical stimulation applied during the deep non-rapid eye movement (NREM) sleep elicited a global, stereotypic brain response spreading widely from the TMS stimulation site to most of other cortical regions (Massimini et al., 2007).

The finding of the present study supports the second mechanism of the consciousness and anesthesia theory from a different perspective. Under the unconsciousness induced by deep anesthesia, not only did BOLD signals show a stereotypic fluctuation pattern, the multiple discriminable resting-state networks (spatial patterns implied by BOLD correlations) observed under the light anesthesia also shrank to one widely-distributed and less-specific network with strong BOLD correlation. Our study provides an important illustration (from the perspective of neuroimaging) that the repertoire of cortical activity pattern (the multiple specific resting-state coherent networks) collapses even though the global integration (functional connectivity) sill exists. In contrast to other evidence, the specific-to-less-specific transition of the resting-state networks observed in the present study reflects a reorganization of intrinsic, ongoing brain activity instead of evoked brain activity.

The specificity of resting-state networks also alters during brain development. A previous resting-state fcMRI study found that the development of two resting-state control networks (the cinguloopercular and frontoparietal networks) (Dosenbach et al., 2007) from child to adult may involve two brain processes: segregation (i.e., reduction of

short-range functional connectivity) and integration (i.e., enhancement of long-range functional connectivity) (Fair et al., 2007). In other words, the specificity of these two networks increases from children's to adult's brains. The change of functional connectivity specificity during the brain development is more likely due to reconfiguration of structural connectivity, which is different from those caused by anesthetics herein. But both of them suggest that the functional segregation of brain regions and neural networks is critical for brain working and functioning, and it could be quantitatively investigated through the specificity of resting-state functional connectivity.

Changes in resting-state network specificity have also been witnessed in patients with schizophrenia. It has been found that their spontaneous BOLD fluctuation generally shows stronger correlations than healthy subjects (Jafri et al., 2008, Salvador et al., 2007, Whitfield-Gabrieli et al., 2009). Moreover, the small-world properties of their resting-state networks also altered with decreased clustering coefficients (reduced local connectivity) and longer absolute path length compared with healthy controls (Liu et al., 2008), indicating a change of specificity.

Increased neuronal synchrony has also been observed in cats anesthetized with anesthetics other than isoflurane (Contreras and Steriade, 1997). It was found under the anesthesia condition showing sleep-like slow wave EEG pattern, additional doses of urethane, ketamine-xylazine, or N2O could largely increase temporal correlations between cortical and thalamocortical neurons with corresponding changes in EEG pattern. Moreover, this highly synchronized activity transcends the borders limiting the

functioning of the waking brain, and unites neurons located distantly and belonging to different brain systems into large neuronal assemblies.

4.4.3 Global Signal Regression

Global signals regression is a common practice in most resting-state fcMRI studies (Fox et al., 2009). One merit of this approach is to remove or at least reduce globally correlated noise introduced by instability of data acquisition or non-neural physiological sources (e.g., respiration and heart pulsation). Moreover, since the main purpose of most resting-state fcMRI studies is to identify specific correlation patterns of spontaneous BOLD fluctuations, the removal of the global signal fluctuations from either non-neural or neural origins should help to achieve this goal by largely enhancing the specificity of resting-state networks.

Nevertheless, the global signal regression was not included in our main stream of data analysis for the following two reasons. First, the large, global BOLD fluctuation observed under the deep BS anesthesia has already been proven to originate from the underlying spontaneous neural activity and to reflect the functional connectivity of the brain (Liu et al., 2010); it therefore provides vital information for understanding the resting-state neural network. Such a tight neuro-BOLD coupling is also evident by the completely diminished BOLD correlations after animal being sacrificed (see an example shown in Figure 4.1), suggesting that the global, non-neural noise has a negligible effect on our correlation analysis. Secondly, the main focus of the present study aims to understand the impact of anesthesia level on the specificity of resting-state networks, and this goal can not be achieved if the global signal regression is applied to removing global,

non-specific BOLD correlation component and thus increasing the specificity of resting-state networks under all the conditions to a similar level.

4.4.4 Influence of Anesthesia on Resting-state Networks

To understand the relationship between the brain's functional connectivity and its consciousness level, a number of studied have been done to examine how anesthesia or sedation would affect the resting-state functional connectivity, but the results are conflicted.

Some studies reported a decrease of functional connectivity as anesthesia level increases (Peltier et al., 2005, Martuzzi et al., 2010, Liu et al., 2009), while others showed opposite results (Kiviniemi et al., 2005, Kiviniemi et al., 2000, Greicius et al., 2008). There was also the third opinion that anesthesia, even at a very deep level, has a negligible effect on resting-state networks (Vincent et al., 2007, Peltier et al., 2005). These discrepancies could be explained by many reasons, including the differences in species studied, the types and dosages of anesthetic agents used, and the resting-state networks investigated. Nevertheless, we want to emphasize that different strategies used for fMRI data analysis, for example, whether to remove global signal fluctuation, may also lead to different outcomes, as discussed above.

A previous resting-state fcMRI study of isoflurane-anesthetized monkeys (Vincent et al., 2007) had similar experimental set-up as the present study: it used the same anesthetic agent and had both light versus deep (with the BS activity) anesthesia conditions. This study concluded that no significant modulation of resting-state networks was caused by changing anesthesia level; meanwhile, it was also mentioned in its

supplementary material that BOLD signals measured at light anesthesia were associated with more system-specific correlations. This early observation does not conflict with our conclusion when considering that of the global signal regression was used in the previous study but not in the present study.

4.4.5 Resting-state Networks May Predict Evoked Activation Pattern

Forepaw stimulation on rats anesthetized with ~1.2% isoflurane has been shown previously to be able to robustly evoke BOLD responses specifically in the S1FL regions (Liu et al., 2004, Sommers et al., 2009, Masamoto et al., 2007); correspondingly, the specific resting-state coherent network covering the bilateral S1FL regions was observed at the similar anesthesia level in the present study. Although we did not find similar fMRI studies performed under the deep BS anesthesia condition, a number of electrophysiology studies showed that a variety of sensory (visual, auditory, and somatosensory) stimuli can nonspecifically evoke global brain activity in rat (Hudetz and Imas, 2007), cat (Kroeger and Amzica, 2007), and human (Hartikainen et al., 1995) under deep anesthesia characterized by the BS EEG pattern. This is, to some extent, consistent with the less-specific resting-state network observed at the deep anesthesia in the present study.

This comparison suggests that the organization of ongoing brain activity may have a significant influence on the activation pattern of evoked brain activity, and the resting-state networks may play an essential role in determining the brain's responses to external stimulation. This notion has actually gained supports from a series of recent studies, which found that the level of ongoing brain activity reflected by spontaneous BOLD signals can influence subjects' subsequent behavioral responses to external

stimulation (Boly et al., 2007, Fox et al., 2007, Hesselmann et al., 2008a, Hesselmann et al., 2008b, Sapir et al., 2005)

Based on these results, we hypothesize that a parallel relationship may exist between the organization pattern of ongoing brain activity under resting state and the activation pattern of evoked brain activity during brain stimulation or task performance.

4.4.6 Other Perspectives

It is clear that not only the temporal correlation strength (CC value) but also the spatial specificity is essential for the interpretation and understanding of resting-state coherent networks and their impact on brain functions. This is particularly important for mapping the dynamic change of neural network under various brain conditions covering from conscious to non-conscious state, because the judgment based solely on BOLD coherence strength within a resting-state network of interest may sometimes be misleading.

Another relevant and vital question is how to quantify the specificity of resting-state BOLD coherent network? A simple approach suggested herein is to compare the difference in correlation strength within a network of interest before and after the use of global signal regression. By doing so, one can estimate how much the global neural synchronization accounts for the total BOLD correlation within the network, and this estimation can provide a qualitative index reflecting the network specificity. However, one should be cautious that this approach could fail in the case that the global BOLD correlation is mainly caused by non-neural noise rather than synchronized neural activity.

Chapter 5

DISTINCTION IN COHERENT NEURAL NETWORK BETWEEN RESTING AND ACTIVATED BRAINS

This chapter, together with the next chapter, is being prepared as a manuscript.

5.1 Introduction

During the last two decades synchronized neural activity has become an important topic in the neuroscience research field because it plays a variety of functional roles in large-scale integration, cell assembly binding, neuronal plasticity and temporal coding (Buzsaki and Draguhn, 2004, Fries et al., 2007, Varela et al., 2001). The major approach to investigate the synchronized neural activity and associated neural network is to analyze the temporal correlations of electrophysiological signals collected from multiple neurons (or neuron groups) in different brain regions. However, electrophysiological recording techniques have limitations in studying the large populations of neurons covering the

entire network of interest, and their invasive nature also limits their application in healthy humans.

Comparatively, the functional magnetic resonance imaging (fMRI) technique based on the blood oxygenation level dependent (BOLD) contrast (Ogawa et al., 1990, Ogawa et al., 1992, Bandettini et al., 1992, Kwong et al., 1992) is able to noninvasively detect and image neural activity change by measuring the secondary hemodynamic/metabolic responses; and has advantages in its comprised large spatial coverage and high spatial resolution. Temporal correlation analysis has also been used on the fMRI BOLD signals evoked by brain stimulation or task performance to infer the "functional connectivity" and "effective connectivity" (Friston, 1994, Horwitz, 2003) among activated brain regions.

More recently, it was found that spontaneous BOLD signals acquired under the resting state without any stimulation and/or task performance are characterized by slow (< 0.1 Hz) and coherent fluctuation within anatomically interconnected and functionally specific brain systems; e.g., the motor, visual, auditory, thalamus, hippocampus, language and default mode systems (Biswal et al., 1995, Lowe et al., 1998, Cordes et al., 2000, Stein et al., 2000, Hampson et al., 2002, Greicius et al., 2003, Vincent et al., 2007). These findings suggest that the resting brain is not silent but rather highly active in an organized manner; and the spatiotemporal correlations of spontaneous BOLD signals could reflect the underlying functional connectivity under the resting state (Biswal et al., 1995) and are useful for mapping a large number of "resting-state" coherent networks. Nevertheless, it

is still elusive whether and how these resting-state networks would be modulated when the brain is activated by sensory stimulation and/or task performance.

Several studies have examined how the temporal correlation (i.e., BOLD coherence strength) within a resting-state coherent network changes during task performance or stimulation. However, uncertainty remains (Fox and Raichle, 2007) because of the contradictory results. One possible reason for the discrepancy lies in the different tasks employed by those studies. The highly cognitive tasks, like the spatial working memory and the language task, used in some studies (Xu et al., 2006, Lowe et al., 2000, Hampson et al., 2002, Morgan and Price, 2004) may induce a slow and task-related BOLD fluctuation component within the activated networks and, thus, result in a significantly enhanced BOLD coherence strength. While others using tasks without such a slow component (Morgan and Price, 2004) did not observe any increase of coherence. Moreover, all of these early studies aimed to infer the neuronal interaction strength through the coherence strength of BOLD fluctuations under stimulation; therefore they focused only on the temporal correlations of BOLD signals within the defined region of interest in the activated brain regions without considering the spatial modulation of the resting-state coherent networks, which might be more essential for understanding the relationship between the "resting-state" and "activated" coherent networks within the same sensory system.

The present study aims to investigate the temporal and spatial modulation of coherent neural networks in the human visual system under continuous brain activation condition with desired visual stimuli. Our working hypothesis is that the resting-state

coherent network can be dynamically reorganized upon stimulation, and such reorganization is stimulus-specific. To exclude the possible stimulus-evoked slow BOLD components, two sustained, continuous visual stimuli were used in this study: i) the continuous hemi-field visual stimulus; and ii) the continuous full-field visual stimulus with 8-Hz reversal, radial red-black checkerboards. The fMRI BOLD signals were collected from the occipital lobe of healthy subjects when the stimuli were presented continuously, as well as under the resting state with the subjects' eyes closed. The coherent networks were mapped through the spatiotemporal correlation analysis of the acquired fMRI datasets. Conclusions were drawn through quantitative comparisons among the coherent network maps obtained under the three conditions, and between these coherent network maps and the conventional fMRI activation maps obtained by presenting the same hemi- or full-field visual stimuli using the block-design paradigm.

5.2 Materials and Methods

5.2.1 Subjects and Visual Stimuli

Ten human subjects (five females and five males, 21−54 years old) participated in this study with written informed consent proved by the Institutional Review Board of the University of Minnesota. All of them were healthy and without history of neurological or psychiatric diseases. One subject (male) participated twice, so there were eleven sets of data in total. One of the datasets suffering serious head motion was discarded; therefore, ten datasets from nine subjects were used for the final data analysis and drawing

conclusions. The hemi-field (100 degree sector on the right side of visual field) and full-field visual stimuli used in this study were both 8-Hz reversal, radial red-black checkerboards with a white cross-mark at the center for visual fixation.

5.2.2 MRI Data Acquisition

All MRI experiments were performed on a 4T/90 cm bore magnet (Oxford, UK) interfaced with the Varian INOVA console (Varian Inc., Palo Alto, CA). A single-loop radiofrequency surface coil (10 cm in diameter) was applied to detect the brain MRI signal mainly attributed to the occipital lobe. At the beginning of the experiments anatomical images in transversal, sagittal, and coronal orientations were acquired with T1-weighted TurboFLASH MRI method (Haase, 1990). The acquisition parameters used for the anatomical images were: field of view (FOV) = 20×20 cm^2; repetition time (TR) = 3 s; 128×128 image matrix size; 5 mm thickness. For the fMRI experiment, the gradient-echo planar image (GE-EPI) method (Mansfield, 1977) was used to acquire 3 adjacent coronal image slices (FOV = 20×20 cm^2; TR = 500; echo time (TE) = 30 ms; 64×64 image matrix size; 5 mm thickness, excitation pulse flip angle ≈ 45^o) covering the calcarine fissure in the human primary visual cortex, which was readily identified according to the anatomical images.

To identify the brain areas activated by the hemi-field stimulus and full-field stimulus, the first two runs of the fMRI experiment were conducted with a block-design paradigm (two task blocks interleaved with three control blocks, 60 GE-EPI volumes per block) with the hemi- and full-field stimuli, respectively, for each subject. Other imaging runs were performed under three desired conditions: (i) the resting state (RS); (ii) the

continuous hemi-field visual stimulus (CHVS); and (iii) the continuous full-field visual stimulus (CFVS) conditions. During the RS condition, the subjects were instructed to close their eyes and refrain from cognitive, language, or motor tasks as much as possible, but not to fall into sleep. For the CHVS and CFVS conditions, the visual stimuli were presented 10 seconds before the start of the fMRI acquisitions and kept on for the entire imaging run. The importance of the eye fixation to central white cross-mark, especially under the hemi-field stimulation, was repeatedly emphasized to the subjects before each fMRI run. The subjects' performance was judged based on the conventional fMRI maps obtained from the hemi-field visual stimulation for ensuring that the activation mainly occurred in the contralateral- rather ipsilateral-hemispheric visual cortical region. The fMRI measurement was repeated 2−4 runs for each condition; and each run acquired 300 or 550 GE-EPI volumes.

5.2.3 Data Processing

Motion correction was first performed on all of the fMRI datasets using the 3D registration tool (3dvolreg) of AFNI (Cox, 1996). Then, the motion corrected fMRI data acquired with the block-design paradigm were used to generate the functional activation maps for the hemi- and full-field stimuli, respectively, by using the period cross correlation method□the fMRI time courses were cross-correlated with the block-design template (Bandettini et al., 1993).

For fMRI data acquired under the CHVS, CFVS and RS conditions, the first 20 image volumes were discarded to ensure reaching a steady-state BOLD signal. The time courses of all image pixels were normalized by their means, and then band-pass filtered

(0.005~0.1 Hz) in frequency domain to remove the DC component, linear drift and reduce the possible fluctuations induced by cardiac and respiratory pulsations. Based on two fMRI activation maps, the most activated (the highest correlation with the block-design paradigm) 2-pixel × 2-pixel regions within the left- and right-hemisphere primary visual cortex were chosen as the left and right reference regions, respectively; and the image pixels near large vessels were carefully excluded from this selection. For each imaging run, the time courses from all image pixels were cross-correlated with the average time courses from the left and right reference regions to generate two correlation maps. A 3×3 Gaussian kernel was convoluted with the correlation maps to spatially smoothen them and reduce the salt-and-pepper phenomenon. These two correlation maps were then transformed to the left and right Z maps according to the well-established method (Vincent et al., 2007): the correlation coefficients were transformed to z score by Fisher's transformation, and then normalized by the theoretical standard deviation with the degree of freedom being adjusted according to Barlett's theory (Jenkins and Watts, 1968).

To summarize the results from the present study, the activated visual cortical regions in the left- and right-hemispheres were defined as two ROIs based on the functional activation maps. For each imaging run, the Z scores of the left Z map (quantifying the correlation to the left-hemisphere reference region) were averaged within the left and right ROIs to obtain two statistics: $\overline{Z}_{LL}$ and $\overline{Z}_{RL}$. The linear mixed model regarding the inter-subject variation as the random effect was used to combine the results from all subjects and to give the statistical inference. $\overline{Z}_{LL}$ and $\overline{Z}_{RL}$ were compared under

each condition, and each was also compared across conditions. All of statistical analyses were performed using the "nlme" package in R (Pinheiro et al., 2009, Team, 2008).

5.3 Results

5.3.1 Distinct Temporal Behaviors of BOLD Signals

Figure 5.1 summarizes the BOLD time courses measured under resting and activated conditions from one representative subject (Subject 1). As we expected, both left and right reference regions responded to the full-field visual stimulus in the conventional block-design fMRI experiment (Figure 5.1b); while only the left reference region showed the stimulus-evoked BOLD response when the hemi-field visual stimulus was presented in the contralateral (right-side) visual field (Figure 5.1a). The BOLD signals measured under the CHVS, CFVS and RS conditions (Figure 5.1c to 5.1h) exhibited strong (up to ±4%), low-frequency fluctuations in both activated and non-activated reference regions, and the fluctuation magnitudes are comparable to the stimulus-evoked BOLD changes (up to 8%) (Figure 5.1a and 5.1b). Under the CHVS condition, the temporal behavior of BOLD signals from the left (activated) and the right (non-activated) reference regions are not well correlated with each other (Figure 5.1c and 5.1d). In contrast, under the CFVS (both reference regions were activated) and RS (both reference regions were not activated) conditions, the fluctuations of BOLD time courses from two reference regions showed strong temporal correlations (Figure 5.1e to 5.1h). These observations were consistent among repeated measurements (e.g., run 1 versus run

2 in Figure 5.1) in the same subject as well as among inter-subjects. The characteristics of the BOLD temporal behavior imply distinct neural networks under different conditions as investigated in this study.

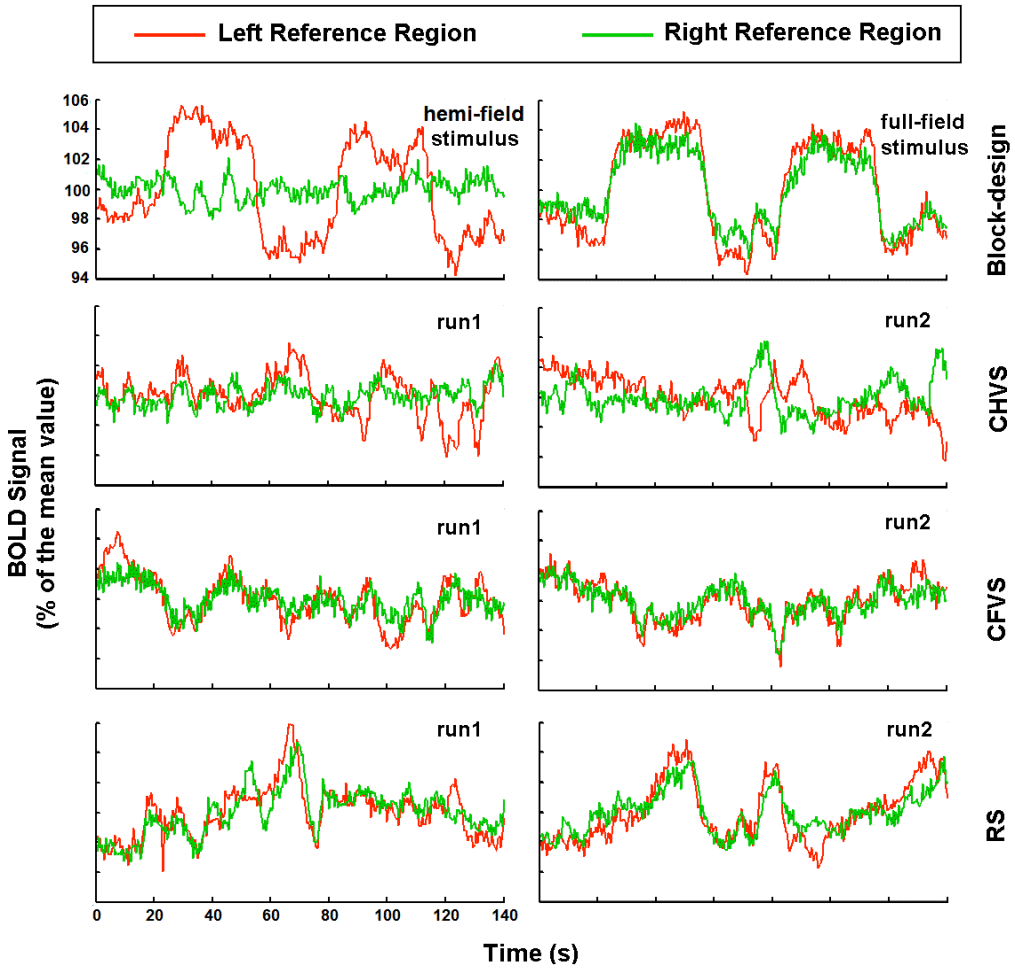

Figure 5.1 BOLD time courses from the left- (red) and right-hemisphere (green) reference regions under the resting and activated conditions. The BOLD time courses were normalized by the mean value without the use of the temporal filter. The first row is for the block-design fMRI runs with (a) hemi-field and (b) full-field visual stimuli; the second (c, d), third (e, f), and fourth (g, h) rows are for runs under the CHVS, CFVS and RS conditions, respectively.

5.3.2 Spatial Modulation of Coherent Neural Network under Stimulation

To further study the spatial relationship of BOLD signal fluctuations based on their temporal correlations, two correlation maps with respect to the left and right reference regions were computed and then transformed to the left (i.e., tightly correlated to the left reference region) and right (i.e., tightly correlated to the right reference region) Z maps. These two maps represented the coherent neural networks containing these two reference regions, respectively.

The conventional functional activation maps and the Z maps from two representative subjects (Subject 1 and Subject 2) are illustrated in Figure 5.2. For each condition studied, the left and right Z maps were superimposed on anatomical images using red (the left Z map) and green (the right Z map) colors, with the yellow color denoting the overlapped brain regions between two.

There was almost no overlap (i.e., yellow areas) between the left and right Z maps measured under the CHVS condition (Figure 5.2c), during which only the left-hemisphere visual cortex was continuously stimulated by the right-field visual stimulus. Moreover, the left Z map (red areas in Figure 5.2c), which represents the "activated" coherent network, is similar to the conventional fMRI activation map obtained during the hemi-field visual stimulus (Figure 5.2a); while the right Z map mainly covers the remaining non-activated regions of the visual cortex. In contrast, the left and right Z maps are largely overlapped with each other under the CFVS and RS conditions (Figure 5.2d and 5.2e), during which both of the left- and right-hemisphere visual cortices are either activated or not activated. Moreover, the Z maps for the CFVS condition (Figure 5.2d)

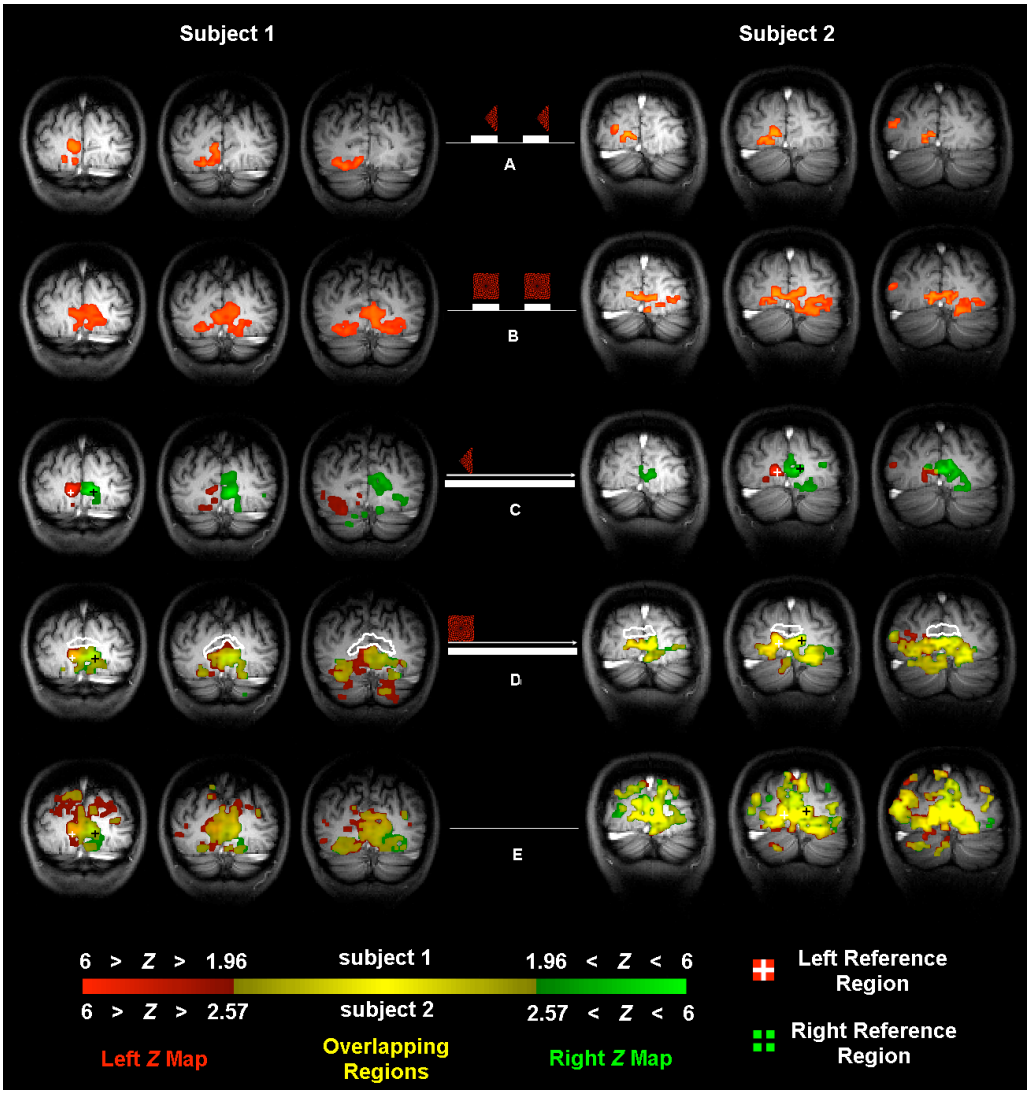

Figure 5.2 Functional activation maps and Z maps from two representative subjects. Left and right panel are for Subject 1 and Subject 2, respectively. The functional activation maps representing the evoked BOLD responses to the hemi-field visual stimulus (a) and the full-field visual stimulus (b) were superimposed on the anatomical images with a desired threshold; the left (red) and right (green) Z maps (with respect to left and right reference region, respectively) representing the spatial pattern of coherent BOLD fluctuations were combined and overlapped on the same anatomical images for the following conditions: (c) CHVS, (d) CFVS, and (e) RS. The locations of the left and right reference regions were marked by white and black cross-marks in (c), (d), and (e). The brain region of *cuneus* was outlined by a white line in (d).

are similar to the conventional fMRI activation map using the full-field visual stimulus (Figure 5.2b); in contrast, the Z maps for the RS (Figure 5.2e) cover much wider brain regions in the occipital lobe, especially the cuneus area (outlined by the white lines in Figure 5.2d), than those Z maps obtained under the CFVS condition.

These observations indicate that, under continuous, sustained visual stimulation, the resting-state coherent network is spatially reorganized into two distinct coherent networks: one covers the activated brain region, and the other covers the remaining, non-activated visual cortex with distinct BOLD temporal behaviors.

5.3.3 Modulation of Coherence Strength

Z scores of the left Z map were averaged within two ROIs to obtain two statistics $\overline{Z}_{LL}$ and $\overline{Z}_{RL}$, which quantify the intra-hemisphere coherence within the left-hemisphere visual cortex and inter-hemisphere coherence between the left- and right- hemisphere visual cortices, respectively. Figure 5.3a illustrates an example for choosing ROIs from Subject 1; and Figure 5.3b summarizes the statistical results of $\overline{Z}_{LL}$ and $\overline{Z}_{RL}$ from all subjects (nine subjects and ten datasets in total). When calculating the left Z map, the Z values within the left reference region were taken from the auto-correlation, which probably resulted in slightly higher $\overline{Z}_{LL}$ values than $\overline{Z}_{RL}$ values for the CFVS and RS conditions (Figure 5.3b). Even with this possible bias, the inter-hemisphere coherence (quantified by $\overline{Z}_{RL}$) is almost as strong as the intra-hemisphere coherence (quantified by $\overline{Z}_{LL}$) for the CFVS and RS conditions without a statistically significant difference (p = 0.589 for CFVS; and p = 0.471 for RS). In contrast, for the CHVS condition, the

$\bar{Z}_{RL}$ value is significantly lower than $\bar{Z}_{LL}$ ($p = 1.37\times10^{-9}$), indicating a much weaker inter-hemisphere coherence than intra-hemisphere coherence. These results are consistent with the observations shown in Figure 5.1c and 5.1d, and Figure 5.2c.

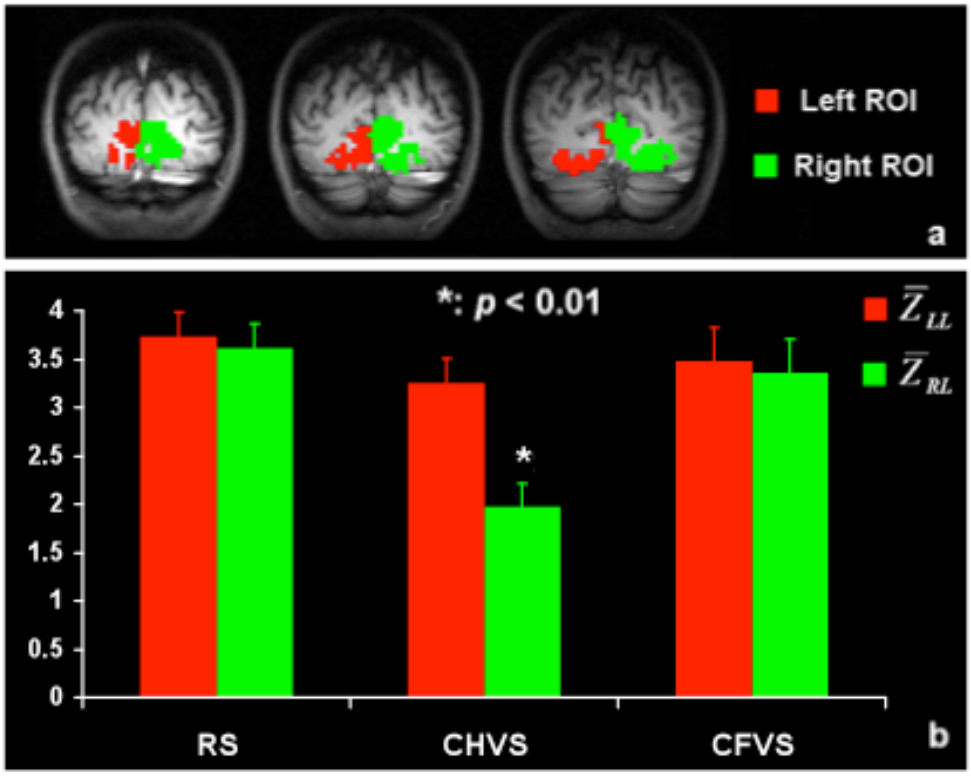

Figure 5.3 An example of defining ROIs and the summary of statistics $\bar{Z}_{LL}$ and $\bar{Z}_{RL}$. (a) The left and right ROIs from Subject 1; and (b) the summary of $\bar{Z}_{LL}$ and $\bar{Z}_{RL}$ from all subjects. $\bar{Z}_{LL}$ and $\bar{Z}_{RL}$ for CHVS and CFVS were compared with those for RS, $\bar{Z}_{LL}$ and $\bar{Z}_{RL}$ the statistically significant differences (p < 0.01) are marked by the star symbol. Note: the calculation of and were based only on left Z maps.

The $\bar{Z}_{LL}$ and $\bar{Z}_{RL}$ values were also statistically compared across different conditions. To reduce the possible bias caused by the ROI analysis method, a conservative significance level of p < 0.01 was used. The inter-hemisphere coherence ($\bar{Z}_{RL}$, the green columns in Figure 5.3b) decreased significantly under the CHVS

condition compared to the RS condition ($p = 1.77\times10^{-9}$), while no significant difference was found between the CFVS and RS conditions ($p = 0.381$). The cross-condition comparison of (the red columns in Figure 5.3b) can quantify the coherence strength modulation of BOLD fluctuations in the left-hemisphere ROI. It decreased slightly, but not significantly, under the CHVS and CFVS conditions as compared to the RS condition ($p = 0.053$ for CHVS; and p = 0.354 for CFVS).

5.4 Discussion and Conclusion

5.4.1 Modulation of BOLD coherence strength

In the present study, the temporal correlation of BOLD signals from activated brain regions decreased slightly, but not to a statistically significant level, under continuous visual stimulation when compared to the resting-state condition (Figure 5.3). This result is contradictory with several early reports (Hampson et al., 2002, Lowe et al., 2000), which reported that the correlation of BOLD signals increased when the resting-state coherent network was activated and the enhanced coherence strength was explained as the result of increased neuronal interactions.

There are at least two possible explanations for this discrepancy. The first is that the previous studies focused on the brain networks involving high-level cognitive functions, for instance memory and language; while the present study focused on the early stage of visual sensory system. These networks may behave differently. The second, perhaps more likely, possibility is that the tasks employed by previous studies,

like working memory task and continuously listening task, could potentially introduce slow, task-related fluctuations in the brain activity, evoke slow BOLD fluctuations in the activated brain regions, and thus increase the BOLD correlations. In contrast, the carefully designed visual stimuli and experimental paradigm of the present study are able to exclude slow and stimulus-evoked BOLD fluctuations for the following three reasons. First, the combination of a 2-Hz image sampling rate and a narrow, low frequency band filter (0.005~0.1 Hz) applied in data processing should minimize the folding problem resulting from the 8-Hz reversal visual stimuli as well as the potential contributions from cardiac and respiratory pulsations on the observed BOLD fluctuations. Only the heart beating ranging from 1.9~2.1 Hz can possibly fold back to the passing band of the filter, nevertheless, this range is beyond normal heart beating rate of ~1 Hz. Secondly, the linear summation of 8 Hz canonical hemodynamic response function only results in a 0.001% oscillation in the BOLD signals after the BOLD response approaches a steady-state level; such a small BOLD oscillation is not comparable with the large BOLD fluctuations (~4%) observed in this study (Figure 5.1); thus, its contribution is negligible. Thirdly, spectral analysis did not show any specific frequency component dominating the fluctuation of BOLD signals.

It is well known that a family of synchronized neuronal oscillations, which is called alpha family (8~12 Hz), exists in the primary sensory systems under the resting state. Upon stimulation, activated neurons could shift their synchronized oscillations to high frequency gamma-band (30~100 Hz) rather than simply increase their phase synchronization in all frequency bands (Rodriguez et al., 1999, Hoogenboom et al., 2006,

Buschman and Miller, 2007, Bressler et al., 1993, Aoki et al., 1999). It means that the synchronization of activated neuron groups is not necessary to be stronger than that of non-activated neuron groups. On the other hand, the BOLD signal does not measure fast electrical activity of neurons directly, but instead much slower hemodynamic response secondary to the neuronal activity change. Even if neurons increased their phase synchronization during activation, it is unlikely that the slow BOLD response is sensitive to such fast neuronal changes associated with phase synchronization. Therefore, it is possible that the "resting-state" coherent network measured by fMRI BOLD fluctuation could be modulated during brain activation with an insignificant change in the temporal coherence strength.

5.4.2 Spatial Reorganization of Resting-State Coherent Networks

A resting-state coherent network covering a large portion of the visual cortex was observed in this study. This observation is consistent with early studies (Lowe et al., 1998, Mantini et al., 2007). When the visual stimuli were continuously presented to subjects, we found that the original resting-state coherent network was dynamically modulated according to the retinotopic attributes of the visual stimulation. Specifically, the visual cortex was reorganized spatially to two distinct coherent networks during the continuous, sustained visual stimulation: one covering the activated visual cortex and the other covering the non-activated visual cortex as illustrated in Figure 5.2.

In conventional fMRI studies, stimulus is repeatedly presented several times interleaved with the control periods (e.g., block-design paradigm); then brain regions consistently showing evoked BOLD responses to the stimulation are identified as

activated regions for generating fMRI activation maps. Temporal correlations of the stimulus-evoked BOLD signals acquired with such paradigm has also been proposed for evaluating the "functional connectivity" or "effective connectivity" (with the information about the direction of brain processing) among activated brain regions (Friston, 1994, Buchel and Friston, 1997, Horwitz, 2003). This approach is based on the temporal correlation analysis of the stimulus-evoked BOLD time courses.

In contrast, using the continuous stimuli, we could evaluate the correlation of slow BOLD signal fluctuations among different brain regions without the confounding effect from stimulus-evoked BOLD signals. Surprisingly, the "activated" coherent network, which is identified through the spatiotemporal correlations of slow BOLD signal fluctuations under continuous stimulation, is spatially well matched with the activated brain regions showing the evoked BOLD responses to the same stimulus, as demonstrated in the conventional fMRI activation maps in Figure 5.2. More strikingly, this "activated" coherent network is spatially and temporally distinguishable from another coherent neural network covering the remaining non-activated visual cortex.

This finding may suggest that activated brain regions shown in the conventional fMRI maps are probably not just "activated regions" but also an "activated functional network", and it represents a dynamically-organized neuron population with modified neuronal interactions (or synchronized neuronal activity), which is dissociated from the resting-state coherent network.

5.4.3 Spatial Coverage of the Coherent Networks

Compared with the "activated" coherent network under the CFVS condition, the coherent network under the RS condition extends into much larger brain regions, such as the cuneus area, which belongs to visual association areas involved in the dorsal pathway and high-level visual functions. The simple reversal checkerboard stimuli used in the present study were unable to activate these areas even with full coverage of the visual field. For the CHVS condition, the coherent network covering the non-activated brain regions (the green map in Figure 5.2c) included those associated visual areas. These observations suggest that the neurons in the non-activated visual cortical regions remain similar neuronal interactions as under the RS condition.

The correlations of BOLD signals under the resting state may reflect a type of "intrinsic" interactions between neurons from a large portion of the visual cortex in the occipital lobe. The external stimulation or task performance will only selectively affect neurons in certain brain regions and switch their interactions to an "activated" state with much less profound effects on the "intrinsic" interactions in other non-activated brain regions. Therefore, the "activated" coherent network will only be a subset of the resting-state coherent network as demonstrated in Figure 5.2. Moreover, such transition from "intrinsic" to "activated" neuronal interaction mode may not need a large amount of the brain energy budget compared to the total energy consumed under the resting state, and this could provide an efficient working mechanism for brain function.

Since the stimuli with various retinotopic attributes were used in the present study, the eyes fixation is important for the outcome and interpretation of our results. In

this study, subjects were requested repeatedly to focus on the central cross (fixation point) before every fMRI run with stimuli, and both the functional activation maps and Z maps partly confirmed the subjects' compliance with this requirement. First, the functional activation map acquired with the hemi-field stimulus (Figure 5.2a) did not show activation in the ipsilateral-hemisphere visual cortex. Secondly, suppose the subject's focus was intermittently attracted by the hemi-field stimulus under the CHVS condition, which is most likely eye movement; the fovea area of the ipsilateral-hemisphere visual cortex would be intermittently activated and the peripheral area of the contralateral-hemisphere visual cortex would be intermittently de-activated correspondingly. Therefore, there would be two anti-correlated "coherent networks" on these two brain regions. However, none of Z maps under the CHVS condition (Figure 5.2c) have shown such patterns. The formation of two coherent networks in the activated and non-activated brain regions under continuous visual stimulation observed in the present study is hardly explained by visual focus deviation.

5.4.4 Neural basis of the reorganization of coherent networks

It has been suggested (Leopold et al., 2003) that the band-limited power (BLP) modulation of electroencephalogram (EEG) signals might make a significant contribution to spontaneous BOLD fluctuations. This notion has gained more supports from a series of studies. Correlations have been found between the spontaneous fluctuations of BOLD signals and the power modulation of alpha-band (Feige et al., 2005, Goldman et al., 2002, Moosmann et al., 2003) and gamma-band (Shmuel and Leopold, 2008) electrophysiological signals under conditions without any stimulation. These studies

provide important clues to the possible neural correlate of resting-state coherent networks. However, what happens when the brain is activated by external stimuli?

Many electrophysiological studies have demonstrated that the activated neurons would engage in synchronized oscillations at the gamma-band with decreased alpha-band activity (Aoki et al., 1999, Rodriguez et al., 1999, Hoogenboom et al., 2006, Fries et al., 2007). Two previous studies can potentially link such a frequency shift of synchronized neuronal oscillations to the change of hemodynamic signals. One magnetoencephalographic (MEG) study (Hoogenboom et al., 2006) having a similar experiment set-up as ours not only observed that the dominant frequency of MEG signals shifted from alpha-band towards gamma-band oscillations, but also confirmed that this shift happened mainly in the activated visual cortex regions identified by the conventional fMRI map. The other study (Niessing et al., 2005) observed a strong coupling between the gamma-band LFP oscillations and the evoked hemodynamic response recorded by optical imaging; more interestingly, this study also found that the strength of the hemodynamic responses to the same stimulus fluctuated over trails; and the range of such fluctuation is as large as that induced by the stimulus.

Based on these findings, we formulate the following conjecture regarding the neural basis for explaining our observations. Under the resting state, neurons within the resting-state network maintain their "intrinsic" interactions through synchronized LFP oscillations likely dominated by low-frequency bands (e.g., the alpha-band oscillations in the occipital lobe), and the slow power modulation of the synchronized oscillations results in low-frequency, coherent BOLD fluctuations within the resting-state coherent

network owing to a tight neurovascular coupling relationship. When the brain is activated continuously by sustained stimuli, the activated neurons change their interactions into the "activated" state by shifting the dominant LFP oscillations to high-frequency bands (e.g., gamma-band) and form a new synchronized network within the activated brain regions. The power modulation of the synchronized oscillations and thus the corresponding temporal behaviors of the BOLD signal fluctuations become distinct between the activated and non-activated brain regions; thus, two coherent neural networks can be differentiated between the activated and non-activated brain regions using slow-frequency BOLD signals and spatiotemporal correlation analysis.

Chapter 6

INFLUENCE OF SPONTANEOUS BOLD FLUCTUATION ON STIMULUS-EVOKED BOLD IN HUMAN VISUAL CORTEX USING SHORT STIMULATION

This chapter, together with the previous chapter, is being prepared as a manuscript.

6.1 Introduction

In a previous single-event fMRI study (Fox et al., 2006b) using the right-handed button-press task, after BOLD time courses from the right-hemisphere (ipsilateral and non-activated) somatomotor cortex were subtracted from those from the left-hemisphere (contralateral and activated) somatomotor cortex, the trial-to-trial variability of event-related BOLD responses in the activated somatomotor cortical region was reduced significantly. It was therefore suggested (Fox et al., 2006b, Fox et al., 2007) that the

spontaneous neural activity reflected by coherent BOLD fluctuations in the resting state could remain unchanged and be linearly superimposed on the stimulus-evoked neural activity under stimulation. However, this superposition hypothesis is not favored either by the results presented in the previous chapter or by previous electrophysiological studies (Varela et al., 2001, Engel et al., 2001). It has been shown in the previous chapter that under continuous, sustained visual stimulation the BOLD signals from the activated brain regions fluctuate differently from those from inactivated regions and formed a new coherent network in the activated visual cortex. The correlations between BOLD signals from the left and right visual cortex decreased significantly when a continuous hemi-field visual stimulus was presented to subjects. The reorganization hypothesis would be a better explanation for the dissociation of the "activated" coherent network from the resting-state coherent network observed under continuous stimulation.

There are at least two possible explanations for the discrepancy regarding the superposition hypothesis favored by the previous study (Fox et al., 2006b, Fox et al., 2007) using single, short motor task and the reorganization hypothesis favored by our study using the continuous, sustained visual stimulation. One is due to different brain sensory systems (i.e., motor versus visual system) investigated by the two studies, and they may behave differently; the other is related to the different (i.e., short versus continuous) stimulus paradigm designs to activate the brain in these two studies. The purpose of the present study is to test whether the linear superimposition hypothesis is also true for the visual system when instantaneous, short visual stimuli are used and thus the first possibility could be excluded.

6.2 Materials and Methods

6.2.1 Subjects and Visual Stimulus

Seven human subjects (five females and three males, 19−63 years old) participated in this study with written informed consent proved by the Institutional Review Board of the University of Minnesota. All of them were healthy and without history of neurological or psychiatric diseases. The hemi-field visual stimulus used in this study is identical to that used in the study presented in the previous chapter: 8-Hz reversal, radial red-black checkerboards (100 degree sector on the right side of visual field) with a white cross-mark at the center for visual fixation (see Section 5.2.1).

6.2.2 MRI Data Acquisition

Subjects were scanned on a 4T/90 cm bore magnet (Oxford, UK) with the Varian INOVA console (Varian Inc., Palo Alto, CA) and a RF surface coil. For the fMRI experiments, GE-EPI (FOV = 20×20 cm^2; TR/TE = 1000/30 ms) was used to acquire 3 adjacent coronal image slices (64×64 image matrix size; 5 mm thickness) covering the *calcarine fissure* based on the anatomical MRI information.

BOLD signals were acquired according three different paradigms. For the block-design fMRI runs (150 GE-EPI volumes per run), the hemi-field visual stimulus was applied during two stimulated blocks (30 second each) which were sandwiched by three control blocks with only the cross mark. For the resting-state runs (225 GE-EPI volumes per run), the subjects were instructed to close their eyes and refrain from cognitive,

language, or motor tasks. For the event-related fMRI runs (190 seconds), the single hemi-field visual stimulus was presented instantaneously every 30 seconds; and the GE-EPI data from those runs were normalized and cut into 30-second epochs. There are totally 240 epochs (trials) from seven subjects.

6.2.3 Data Processing

Functional activation maps for the block-design fMRI runs and correlation maps for the resting-state runs were generated according to pre-processing steps and strategies identical to those used in the previous chapter (see Section 5.2.3). Based on these maps, three ROIs were defined as the following. Left visual cortex (LVC) covers the primary visual cortex showing strong activation to the right hemi-field stimulus (defined based on the activation maps). Right visual cortex (RVC) covers the visual cortex in the right hemisphere showing strong correlations with the LVC in the resting state but not activation to the hemi-field stimulus (defined based on the resting-state correlation maps). Other brain region (OBR) was also a cortex region in the right hemisphere and had the similar SNR as the LVC and RVC, but it is outside the visual cortex and showed only weak correlations with the LVC in the resting state. The functional activation map, resting-state correlation map, and three defined ROIs from subject 1 are shown in Figure 6.1 as an example.

Similar to the subtraction method used by the previous event-related functional study (Fox et al., 2006b), the BOLD time courses were extracted from and averaged within the three ROIs defined above. Then, the averaged BOLD time courses of the RVC

and OBR were subtracted from that of the LVC, respectively. This step was done for total 240 trials from all seven subjects and the results were summarized in Figure 6.2.

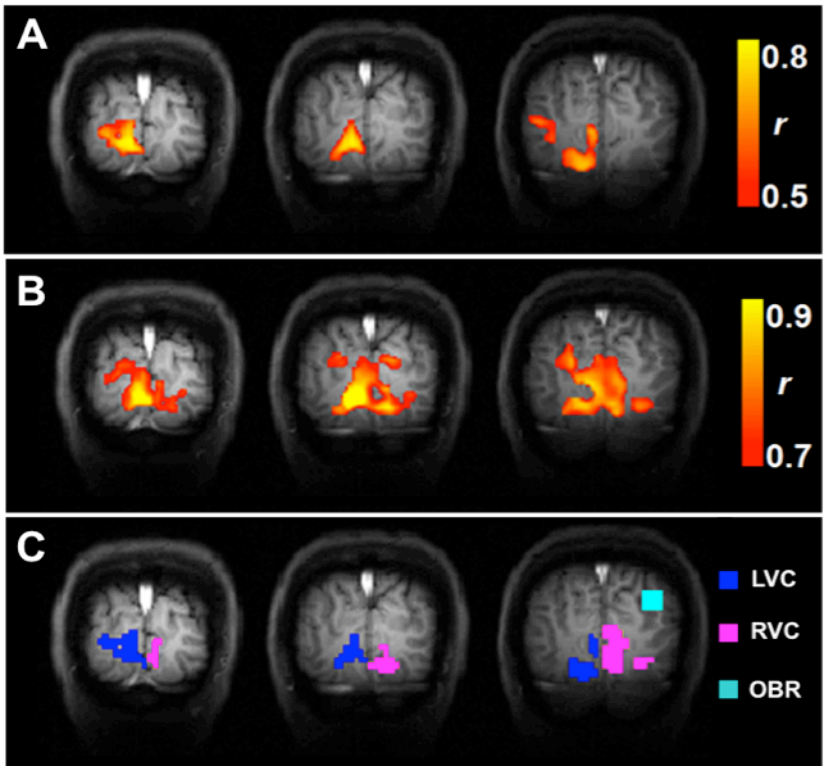

Figure 6.1 Definition of ROIs. For a representative subject, three ROIs in the left visual cortex (LVC), right visual cortex (RVC), and other brain region (ORB) were selected, based on the functional activation map (A) and the resting-state correlation map (B), and shown in (C).

The data from the study in the previous chapter was also processed using the subtraction method for comparison. BOLD signals were extracted from and averaged within the left and right ROIs defined previously (see Section 5.2.3). After normalization, the averaged BOLD time courses were intentionally cut into 35-second segments. Segments of the right ROI were subtracted from those of the left ROI; the difference and original BOLD segments were summarized in Figure 6.3.

6.3 Results

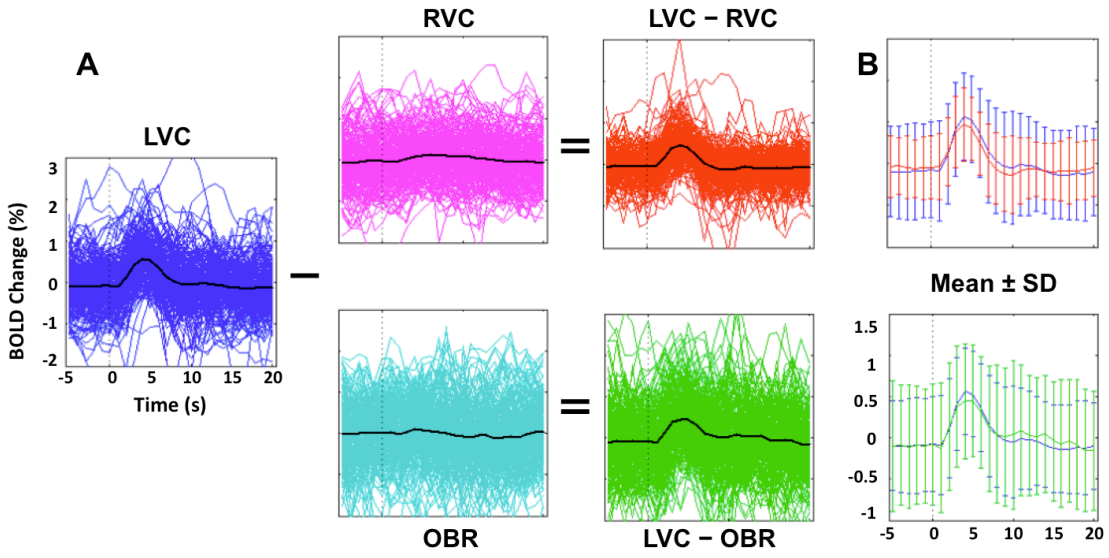

Figure 6.2 Subtraction reduces trial-to-trial variation in event-related BOLD signals. (A) The BOLD time courses (240 trials) and their averaged time courses (thicker black) from three ROIs, and their corresponding differences. (B) The mean and standard deviation of BOLD signals (across trials).

For each trial, the event-related fMRI data were spatially averaged within three ROIs to obtain BOLD time courses in each ROI and then plotted in Figure 6.2. It is obvious that the hemi-field visual stimulus presented in subjects' right visual field elicited BOLD responses in the LVC but not in the RVC or OBR; however, the BOLD response demonstrated very large variation across different trials. After the BOLD time courses of the RVC were subtracted from those of the LVC, the trial-to-trial variation was significantly reduced, suggesting a strong correlation between BOLD signals from the left and right visual cortex. In contrast, if the BOLD fluctuations in ORB were used for subtraction, the trial-to-trial variation was actually increased, presumably, owing to

the incoherent BOLD signal fluctuations between the LVC and ORB. These results suggest that the reduction of trial-to-trial variation is not due to the subtraction of global

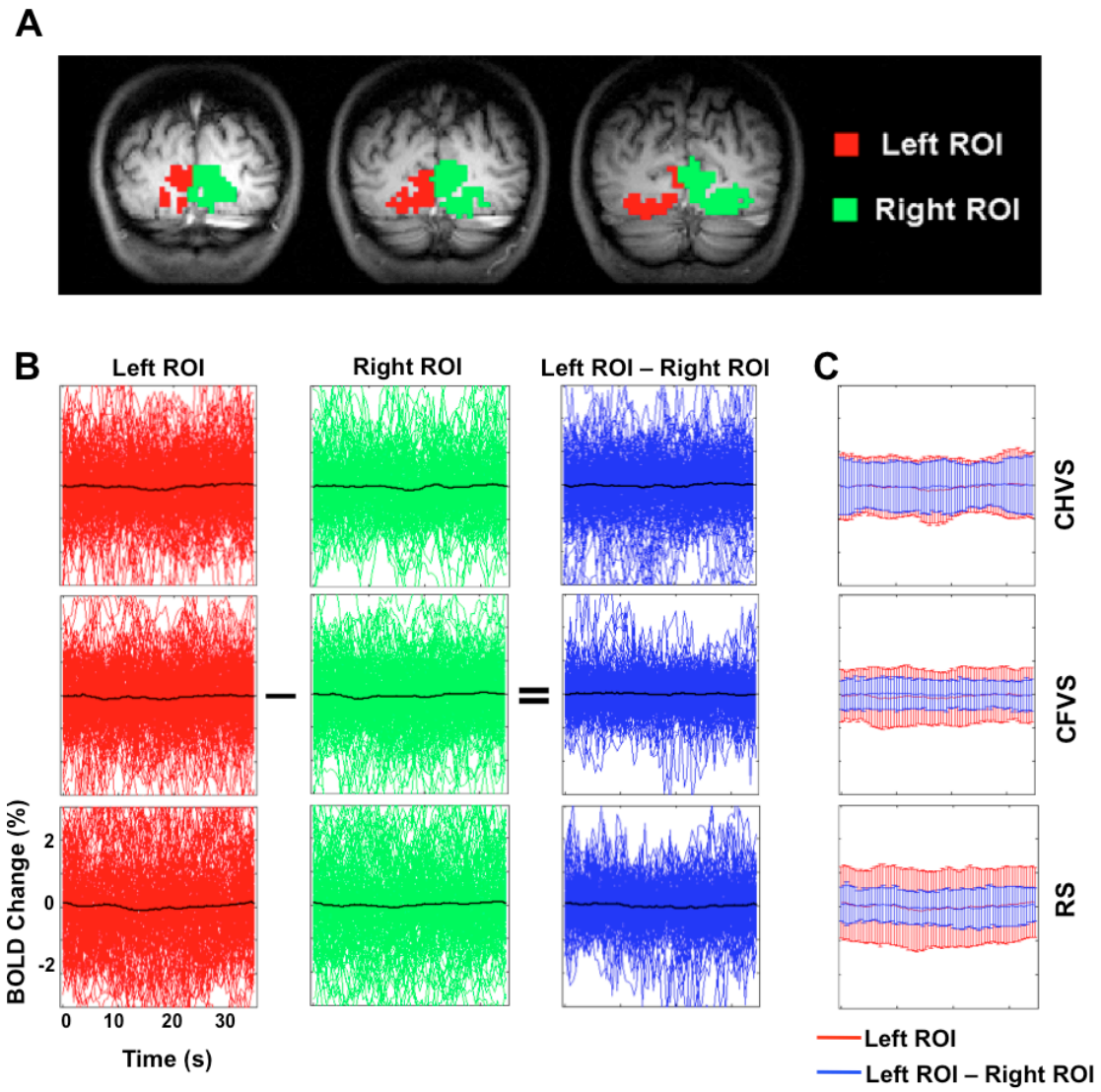

Figure 6.3 Segments (35 second each) of BOLD time courses extracted from left (red) and right (green) ROIs, and their difference (blue). (A) An example of ROIs from a representative subject, (B) the raw BOLD time courses were only normalized by the mean value without the use of the temporal filter, and (C) the averaged BOLD time courses with the error bars denoting standard deviations, which can be used to quantify the magnitudes of BOLD fluctuations.

brain fluctuations but owe to the removal of "spontaneous" BOLD fluctuations intrinsic to the resting-state visual networks.

The similar analysis has also been performed on the fMRI BOLD signals under conditions with continuous stimulation (from the study presented in the previous chapter) after cutting continuous BOLD signals into 35-second segments, and the results are shown in Figure 6.3. Under the resting state (RS) or the condition with the continuous full-field visual stimulus (CFVS), during which neither or both of the left and right ROIs were activated, the segment-to-segment variation can be reduced significantly by subtraction, due to the correlation between the left and right ROIs under these two conditions. However, subtraction did not successfully reduce the segment-to-segment variation under the condition with the continuous hemi-field visual stimulus (CHVS), indicating a reduced coherence between the left and right visual cortex under this condition compared with the other two conditions.

6.4 Discussion and Conclusion

Our results clearly show that the trial-to-trial variation of event-related BOLD responses in the activated visual cortex is largely due to the underlying spontaneous and coherent BOLD fluctuations. This finding is consistent with the former observation in human somatomotor system (Fox et al., 2006b). In addition, we also demonstrated that the trial-to-trial variation is specifically affected by the spontaneous BOLD fluctuations within the same resting-state network rather than the global brain BOLD fluctuations. In

future studies, such effect should be taken into account when interpreting the event-related BOLD responses.

Nevertheless, the similar analysis on the fMRI data acquired under continuous stimulation showed different results. When the identical hemi-field stimulus was presented to subjects continuously, the correlation between the left (activated) and right (not activated) visual cortex is not as strong as under the short stimulation. The discrepancy cannot be explained by difference in stimuli or brain systems investigated, but it may be explained from the basic mechanism of fMRI BOLD signal.

As aforementioned, the hemodynamic response measured by the BOLD signal is secondary to and much slower than the electrical activity of neurons, and it can last tens of seconds following the change of brain activity evoked by brain stimulation. Such a neurovascular coupling relationship is usually modeled as a linear time-invariant (LTI) system with the slow hemodynamic response function as the impulse function. When a single, short stimulus is applied, the activated neurons would temporarily modulate their activity within a short time window (e.g., hundreds of milliseconds) following the onset of the stimulus and then recover to the pre-stimulus state (spontaneous activity) rapidly (Pfurtscheller et al., 2000); while its influence on the BOLD signals will sustain for a much longer time (typically ~20 s) following neural activity changes, as illustrated in Figure 6.4A. Therefore, BOLD signals acquired from the activated brain region during a typical time window for event-related fMRI studies would actually include three components: the component induced by the stimulus-evoked neural activity and those induced by the spontaneous neuronal activities before and after the stimulus. Since the

magnitudes of the spontaneous BOLD fluctuation are comparable to the stimulus-evoked BOLD change, the latter two components could have a significant contribution to the total BOLD signals observed after the onset of the stimulus, and therefore may result in certain degree of coherence between the activated and non-activated (control) brain regions within the same resting-state coherent network. This notion would explain the persistent BOLD signal correlation within the resting-state networks under short simulation/tasks. In contrast, the continuous, sustained stimuli would continuously modulate the activity of activated neurons (Figure 6.4B). Therefore, the slow BOLD signal fluctuations obtained during the sustained, steady-sate stimulation condition mainly reflect the coherent neural activity of activated neurons without the confounding effects from the pre- and post-stimulus BOLD contributions. Under this circumstance, reorganization of the resting-state coherent network can be observed in the human visual cortex during activation.

According to the above argument, it may not be reasonable to infer the superimposition of spontaneous and evoked neural activity based on the superimposition of spontaneous and evoked BOLD signals. On the other hand, it is neither rational to completely deny the superimposition theory based on the argument. For example, for neurons in a specific brain region, if only certain subgroup is recruited (or reorganization) for brain activation with the others maintaining their spontaneous activity, but the two groups are spatially indistinguishable. Under this circumstance, spontaneous and evoked brain activity could be still superimposable from a macroscopic perspective, for example, at the typical spatial resolution of most neuroimaging techniques. To further understand

these issues, more studies, especially those involving the electrophysiological signal measurement, are needed.

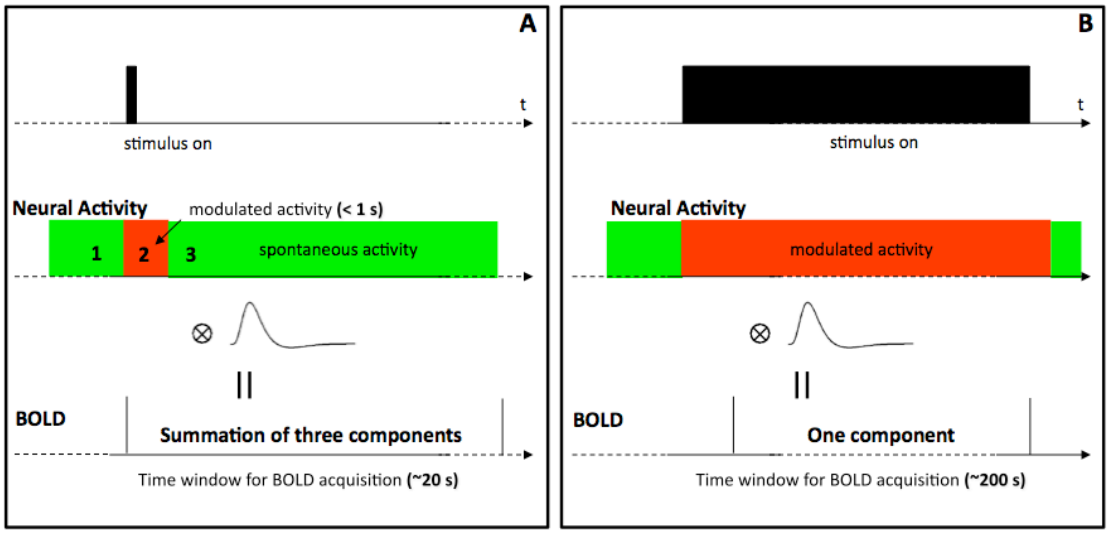

Figure 6.4 Illustration of the relationship between BOLD signal and underlying neural activity under short (A) and continuous (B) stimulation.

Chapter 7

BASELINE BOLD CORRELATION PREDICTS INDIVIDUALS' STIMULUS-EVOKED BOLD RESPONSES

This manuscript has been submitted to NeuroImage and under revision.

7.1 Introduction

In the past two decades, the functional magnetic resonance imaging (fMRI) technique based on the blood oxygenation level dependent (BOLD) contrast (Ogawa et al., 1990, Ogawa et al., 1992, Bandettini et al., 1992, Kwong et al., 1992) has been widely applied to noninvasive imaging of brain activity in numerous neuroscience and psychology studies. However, a major challenge in fMRI application is the large variability in the magnitude, shape, and location of stimulus-evoked BOLD responses commonly observed within or between subjects (White et al., 2001). Such large intra- and inter-subject variations make one difficult to quantify fMRI data and interpret outcomes,

and usually demand a large sample size for reaching a statistical significance level, particularly for comparative studies.

Many factors have been suggested to account for the large variability of stimulus-evoked BOLD responses, and most of them are from non-neural sources, such as the hematocrit level (Gustard et al., 2003), venous blood oxygenation level (Lu et al., 2008), vasculature (D'Esposito et al., 2003), and motion artifacts (Lund et al., 2005). This is probably because the fMRI BOLD contrast is mainly based on hemodynamic responses to brain activity changes (Ogawa et al., 1998). Nevertheless, possible contributions from neural-related factors should not be neglected. Previous electrophysiology studies have demonstrated that ongoing brain activity prior to brain stimulation may have a significant influence on stimulus-evoked brain responses (Makeig et al., 2002, Arieli et al., 1996). Therefore, the variability of ongoing brain activity could be another factor possibly relating to the variability of stimulus-evoked brain responses, including those measured with fMRI BOLD signal.

A number of recent fMRI studies have shown that baseline BOLD signals acquired in the resting state fluctuate slowly and coherently within a variety of anatomically connected and functionally specific brain networks (Biswal et al., 1995, Fox and Raichle, 2007). It has been suggested that such baseline BOLD fluctuations could result from ongoing brain activity and their spatiotemporal correlations reflect functional connectivity between different brain regions (Biswal et al., 1995, Fox and Raichle, 2007). Moreover, several fMRI studies have demonstrated that ongoing brain activity, reflected by pre-stimulus baseline BOLD signals, can influence behavioral responses of human

subjects to external stimuli (Boly et al., 2007, Sapir et al., 2005, Fox et al., 2007, Hesselmann et al., 2008b, Hesselmann et al., 2008a). These interesting findings not only suggest an interaction between the ongoing brain activity and evoked brain responses at a behavioral level, but also demonstrate the feasibility of measuring ongoing brain activity noninvasively using the BOLD-based fMRI technique. It would be essential to examine and quantify the relationship between ongoing and evoked brain activities, if it exists, at a more mechanistic level.

The purpose of this study is to quantitatively investigate the interaction between ongoing and evoked brain activity, and more specifically to examine the relationship between baseline BOLD signal fluctuation and stimulus-evoked BOLD response in the human visual cortex using fMRI. Our working hypothesis is that individuals' baseline BOLD fluctuation could influence the amplitude of their evoked BOLD responses to identical brain stimulation and their relationship is one of the major factors responsible for the large inter-subject variability in the stimulus-evoked BOLD amplitudes. To test this hypothesis, BOLD signals were imaged from the human visual cortex according to a two-stage paradigm design (see Figure 7.1A). The temporal correlation strength and fluctuation magnitude of baseline BOLD signals acquired during the control stage (i.e., the eyes-fixed condition in the absence of visual stimulation) were used to quantify ongoing brain activity, while the amplitude of evoked BOLD responses acquired during the block-design stage (i.e., the stimulus was presented according to the conventional block-design paradigm) was used to quantify evoked brain activity. Their relationships were then examined through a regression analysis to test the hypothesis. In addition, the

baseline BOLD signals were also imaged under the eyes-closed condition for a subgroup of subjects and compared with those acquired under the eyes-fixed condition.

7.2 Materials and Methods

7.2.1 Participants

Sixteen volunteers (6 males and 10 females; age: 28 ± 13 years) participated in this study with written informed consent proved by the Institutional Review Board of the University of Minnesota. All of them were healthy without histories of neurological or psychiatric diseases. One subject was excluded from the final data analysis because of large head motion during MRI data acquisition; therefore the results from fifteen subjects were summarized and presented herein.

7.2.2 Stimuli and Experimental Paradigm

A full-screen ($30^o \times 23^o$ visual angle) red-black checkerboard (spatial frequency 1.5^o per cycle) visual stimulus flashing at 8 Hz, with a small white cross in the screen center for eyes fixation, was used to activate visual cortices. The stimulus was back-projected onto a screen at a viewing distance of ~ 35 cm. A control image with only the small white cross on a black and uniform background was used for eyes fixation when the visual stimulus was off.

Each standard fMRI run consists of 300 image volumes with a total of 330 seconds of acquisition time. During each run, the visual stimulus was presented to

volunteers interleaved with the control image (a white cross on a black background) according to the experimental paradigm shown in Figure 7.1A: a long control block (150 fMRI volumes, 165 seconds) followed by six short blocks (25 volumes, 27.5 seconds each) switching between stimulus and control conditions. The first 150 and last 175 image volumes (25 overlapped volumes between them) were regarded as the control (Figure 7.1A, red shadow) and block-design (Figure 7.1A, green shadow) stages,

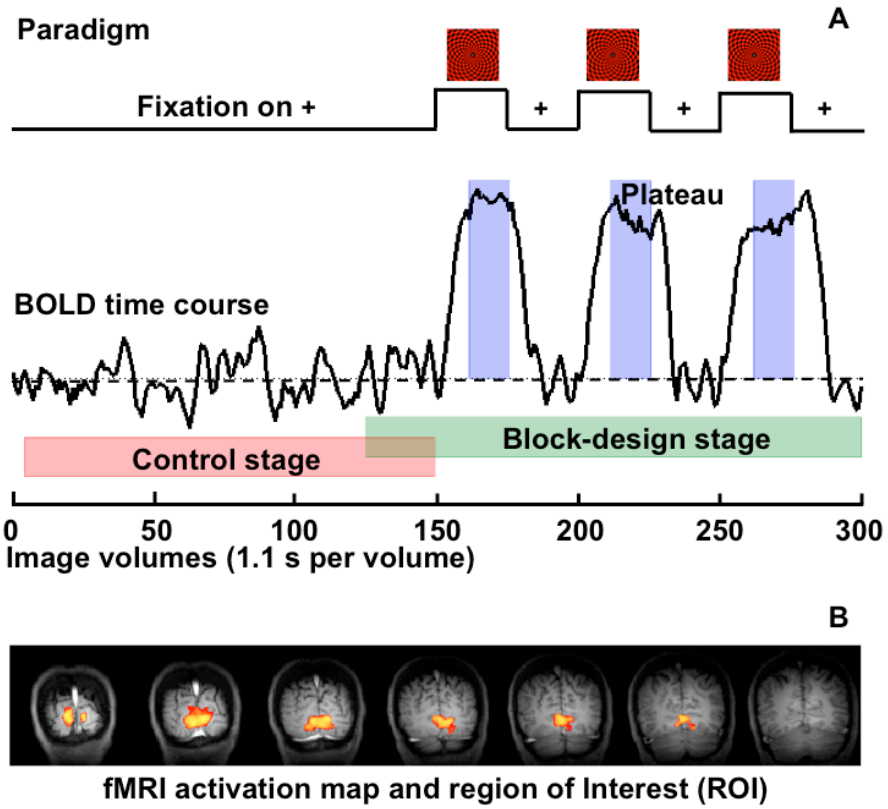

Figure 7.1 Standard experimental paradigm and an example of ROI selection. (A) The experimental paradigm for a standard fMRI run with the control (red shadow), block-design (green shadow), and BOLD plateau (blue shadow) stages being marked; (B) An example of functional activation maps generated based on the block-design stage data from a single fMRI run of a representative participant (Subject 1). The statistical threshold was adjusted to show the most activated (~10% of) brain regions, which defined the ROI utilized for quantification.

respectively; while the 160~175th, 210~225th, and 260~275th image volumes were assigned to the stimulus-evoked BOLD plateau stage (Figure 7.1A, blue shadow).

For a subgroup of five subjects, besides the standard fMRI runs, two additional fMRI runs were also acquired under the eyes-closed condition, during which the subjects were instructed to close their eyes and refrain from cognitive, language, and motor tasks as much as possible, but not to fall asleep. Each eyes-closed fMRI run consisted of 150 image volumes.

7.2.3 MRI Data Acquisition

All MRI experiments were performed on a 4 Tesla 90 cm bore human magnet (Oxford, UK) interfaced with the Varian INOVA console (Varian Inc., Palo Alto, CA). A single-loop radiofrequency (RF) surface coil (10 cm in diameter) was applied to detect brain MRI signals mainly from the occipital and parietal lobes and cerebrum for achieving high detection sensitivity.

At the beginning of each experiment, the T_1-weighted TurboFLASH MRI method (Haase, 1990) was used to acquire a set of anatomical images in transversal, sagittal, and coronal orientations with the following parameters: field of view (FOV) = 20 × 20 cm2; repetition time (TR) = 3 s; 128 × 128 image matrix size; and slice thickness = 5 mm. For the fMRI experiments, seven consecutive coronal gradient-echo echo-planar image (GE-EPI (Mansfield, 1977)) slices were acquired (FOV = 20 × 20 cm^2; TR/TE = 1100/30 ms; 64 × 64 matrix size; 5 mm slice thickness; and a nominal excitation pulse flip angle of ≈ 45^o) to cover the entire calcarine fissure, with reference to the anatomical images. Five

dummy scans were also added to the beginning of GE-EPI data acquisition to avoid the transient BOLD signal change at the initial acquisition period.

During fMRI data acquisition, the magnet room was kept dark and the only light source was the projector sitting in the next room. Before each standard fMRI run, the importance of eyes fixation on the white cross and minimizing head motion was re-emphasized to subjects. Four to seven standard fMRI runs were acquired for each subject and two additional eyes-closed fMRI runs were acquired for a subgroup of five subjects.

7.2.4 Preprocessing and Analysis of fMRI Data

Motion correction was performed on all fMRI data using the 3D registration tool (3dvolreg) of AFNI (Cox, 1996), and fMRI runs with large head motion (> 3 mm at any direction) were excluded from further analysis. All images were then spatially smoothened with a Gaussian kernel with 6 mm full width at half maximum (FWHM). The first five GE-EPI image volumes were excluded to further eliminate the transient BOLD signal complication at the initial GE-EPI acquisition period.

For each standard fMRI run, functional activation maps were generated by cross-correlating the block-design stage data (126th to 300th image volumes) with the convolution of the task paradigm and canonical hemodynamic response function (Bandettini et al., 1993). Then, based on each functional activation map, a corresponding region of interest (ROI) was drawn automatically based on three criteria: 1) to only include the activated fMRI voxels reaching a statistical significance: having high correlation with the task paradigm with a p value of < 0.05 (corrected for multiple comparison with Bonferroni correction); 2) to exclude the voxels showing an extremely

large BOLD percentage increase of >15% in response to the visual stimulation, thus, to reduce the large vessel BOLD contamination; 3) to limit the total number of the activated voxels for ensuring that the ROI size was 10% of the total brain region imaged by seven fMRI slices and the selected ROI mainly covered the calcarine fissure (see an example shown in Figure 7.1B). We did not use a fixed statistical threshold (p value) for determining the ROI, because it could result in considerable variations in both ROI size and large vessel BOLD contribution across subjects due to the nature of large inter-subject variability in the stimulus-evoked BOLD responses. The different ROI size over different subjects may significantly affect the quantification of evoked BOLD amplitude and lead to underestimation of the inter-subject variation. We neither applied a fixed number of activated fMRI voxels to determine the ROI, because the size of the brain as well as of the calcarine fissure also varies across subjects, even though to a much lesser extent than the evoked BOLD response. Instead, we used a fixed proportion of the brain volume we imaged, which can assure the consistence of the selected ROI size with the consideration of the inter-subject brain size variation (418 ± 58 voxels, Mean ± SD).

For each standard fMRI run acquired under the eyes-fixed condition, we calculated one quantity to quantify the amplitude of stimulus-evoked BOLD response and two quantities to quantify the magnitude and correlation strength of baseline BOLD signal fluctuation. For each fMRI run acquired under the eyes-closed condition for a subgroup of five subjects, two quantities were calculated to quantify the magnitude and correlation strength of baseline BOLD fluctuation.

To obtain the quantity of the stimulus-evoked BOLD amplitude, the mean fMRI signal averaged within the stimulus-evoked BOLD plateau stage was divided by the mean fMRI signal of the control stage for each voxel to generate a map of percentage BOLD increases, whose values were then averaged within the corresponding ROI to give the quantity.

To quantify the magnitude and correlation strength of baseline BOLD fluctuation under eyes-fixed (or eyes-closed) conditions, the fMRI signal time course acquired during the control stage of the standard fMRI run (or the eyes-closed fMRI run) were first normalized by their means and band-pass filtered (0.005~0.1 Hz) in the frequency domain to remove the DC component and very slow drift and to reduce the possible fluctuations induced by cardiac and respiratory pulsations. Next, the standard deviation (SD) of BOLD time course was calculated for each fMRI voxels to generate a SD map, and the average of the SD values within the ROI presents the magnitude of baseline BOLD fluctuation under the eyes-fixed (or eyes-closed condition). In addition, the mean of the correlation coefficients (CCs) of any pair of voxels within the corresponding ROI was calculated to quantify the correlation strength of baseline BOLD fluctuation under the eyes-fixed (or eyes-closed) condition.

For the quantification based on the standard fMRI run, the ROIs were determined for each run. While for the quantification based on the eyes-closed MRI run, which did not include the block-design stage, the ROI was therefore determined based on the averaged fMRI activation map across multiple runs of the same subject; and it is to some

extent an average of the single-run ROIs, which showed small variation across multiple runs for the same subject.

A group-based regression analysis was employed instead of individual-based analysis to examine the relationships between these quantities, since it is advantageous to utilize the large inter-subject variability to increase the dynamic range of evoked BOLD responses.

7.2.5 Correlation Maps and Independent Component Analysis (ICA)

Correlation maps were generated based on the GE-EPI data acquired during the control stage (eyes-fixed) and block-design stage of the standard fMRI runs, as well as under the eyes-closed condition. The most activated 2-voxel × 2-voxel region was selected first, based on the averaged functional activation map in response to visual stimulation, as the reference region. For each GE-EPI dataset, then, the signal time courses of all image voxels (after preprocessing) were correlated with the averaged signal time course extracted from the reference region to create a correlation map.

Spatial Independent Component Analysis (sICA) was also performed on the same fMRI datasets including seven coronal slices of GE-EPI images covering the visual cortex. FastICA (Hyvarinen, 1999), a fixed-point ICA algorithm, was implemented on the data by using a MATLAB package downloaded from http://www.cis.hut.fi/projects/ica/fastica/. A total of 30 components, which can account for more than 90% of original variance, were decomposed for each dataset. The meaningful components, which show certain spatial pattern but are not obvious artifacts, were extracted by visual inspection. There was usually only one component (out of 30

components) showing a "meaningful" spatial pattern, which is similar to the correlation map based on the reference (or seeding) analysis approach.

All data were analyzed using MATLAB7.5 (MathWorks, Natick, MA). A p value of < 0.05 was considered statistically significant.

7.3 Results

7.3.1 Baseline BOLD Fluctuation versus Evoked BOLD Response

Figure 7.1B illustrates a typical functional activation map from a representative subject (Subject 1), which was generated based on the fMRI data (single run) acquired during the block-design stage. The activated brain regions in the primary visual cortex represent the region of interest (ROI) used for data quantification. All subjects showed robust activations in the visual cortex, and the functional activation maps and corresponding ROIs were highly consistent across multiple fMRI runs for the same subjects.

For each fMRI run, the correlation strength and fluctuation magnitude of the control stage BOLD signals and the amplitude of the plateau BOLD signals acquired during the block-design stage (see Figure 7.1A) were quantified within the corresponding ROI. These three quantities were then averaged over multiple runs for the same subject and their relationships were examined through a linear regression analysis across all subjects. Figure 7.2 summarizes the results.

Figure 7.2A shows a significant, positive correlation ($R^2 = 0.69$, $p = 1.2 \times 10^{-4}$, n = 15) between the amplitude of subjects' evoked BOLD responses and the correlation strength of their baseline BOLD fluctuations. The subjects with more synchronized baseline BOLD fluctuations showed stronger evoked BOLD responses to the same visual stimulus, and vice versa. Such a correlation is still statistically significant ($R^2 = 0.37$, $p = 1.1 \times 10^{-9}$) if the regression analysis was based on pooled single-fMRI-run quantities without averaging them within the same subject (see Figure 7.S1B).

In contrast, no statistically significant correlation ($R^2 = 0.0001$, $p = 0.97$, n = 15) was found between the magnitude of baseline BOLD fluctuation and the amplitude of stimulus-evoked BOLD response (Figure 7.2B) in the present study. It suggests that the

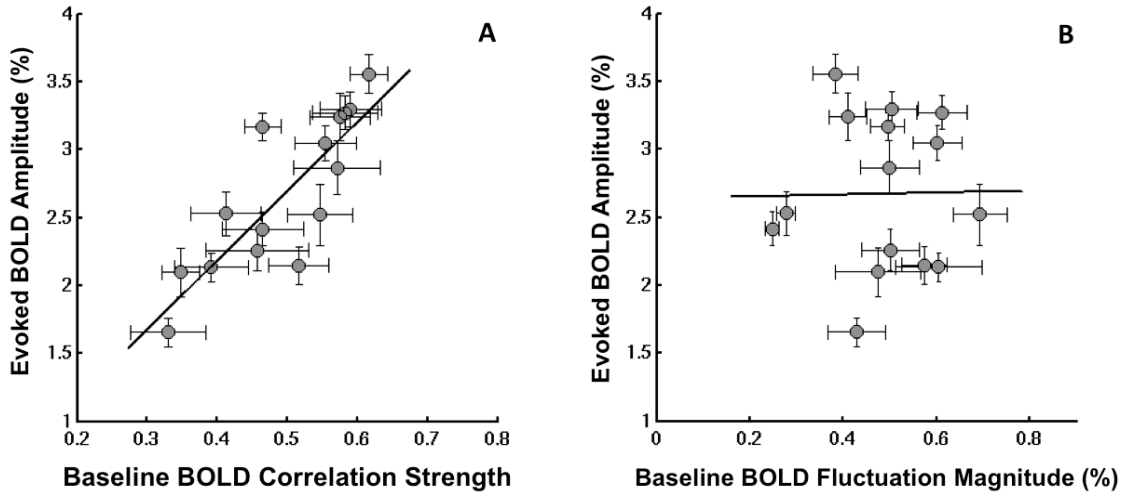

Figure 7.2 Scatter plots showing, for each subject, the amplitude of stimulus-evoked BOLD responses versus (A) the correlation strength and (B) fluctuation magnitude of baseline BOLD signals. Each gray circle in the plots represents the data from one subject with error bars standing for standard errors across multiple fMRI runs. The solid lines show the best linear fitting of experimental data (n = 15) using the least-square regression method: $R^2 = 0.69$ and $p = 1.2 \times 10^{-4}$ for (A); $R^2 = 0.0001$ and $p = 0.97$ for (B).

large inter-subject variability in evoked BOLD response observed in the present study may not be explained by the difference in subjects' vasculature within the selected ROI. Moreover, the correlation strength and fluctuation magnitude of baseline BOLD signals were found to be not correlated with each other either (R^2 = 0.053, p = 0.41, n = 15) based on the ROI analysis.

7.3.2 BOLD Coherent Networks under Eyes-Fixed and Eyes-Closed Conditions.

Spatiotemporal correlations of baseline BOLD fluctuations have been found to imply many "resting-state brain networks" including the one covering the visual cortex (Cordes et al., 2000, Greicius et al., 2003, Hampson et al., 2002, Lowe et al., 1998, Stein et al., 2000, Vincent et al., 2007). However, the resting-state visual network was usually identified using the fMRI BOLD signals acquired under the eyes-closed condition (Lowe et al., 1998, Mansfield, 1977). In contrast, the baseline BOLD signals in the present study were acquired when the subjects fixed their eyes on a small cross on a black background: a common control condition for most fMRI applications. To compare baseline BOLD fluctuations and their associated coherent networks in the human visual cortex under these two conditions, additional fMRI BOLD measurements under the eyes-closed condition were included for a subgroup of five subjects (Subject 11 to Subject 15).

Figure 7.3A shows a positive correlation (R^2 = 0.78, p = 0.046, n = 5) between the correlation strengths of baseline BOLD fluctuations measured under eyes-fixed and eyes-closed conditions. This result indicates a close relationship between these two baseline

brain states, and this notion is further supported by correlation maps showing the spatiotemporal correlations of BOLD signals as discussed below.

The correlation maps were generated based on the BOLD signals acquired during visual stimulation (the block-design stage), under the eyes-fixed (the control stage depicted in Figure 7.1A) and eyes-closed conditions (additional fMRI run), respectively. Figure 7.3B compares BOLD correlation maps (five coronal images) from a representative subject (Subject 12). The BOLD correlation map during visual stimulation mainly covers the activated brain regions showing evoked responses to the visual stimulus, and it is almost identical to the conventional fMRI activation map (not shown in Figure 7.3) as expected. The BOLD correlation maps under the eyes-fixed and eyes-closed conditions show almost identical patterns, which are substantially different from, even though largely overlapped with, the BOLD correlation map obtained during visual stimulation. The major difference lies in the cuneus gyrus region, which is clearly one part of the visual network obtained under either the eyes-fixed or eyes-closed condition but did not show an evoked BOLD response to the full-screen visual stimulus. This observation is consistent across all five subjects (see Figure 7.S2).

To further confirm the above observation, the spatial independent component analysis (sICA) was also performed on the same fMRI data to independently examine spatial coherent patterns of BOLD signals. The meaningful independent components (ICs) extracted under the three conditions (Figure 7.3C) resembled the pattern of the corresponding BOLD correlation maps (Figure 7.3B), supporting the results of the seed-based correlation analysis.

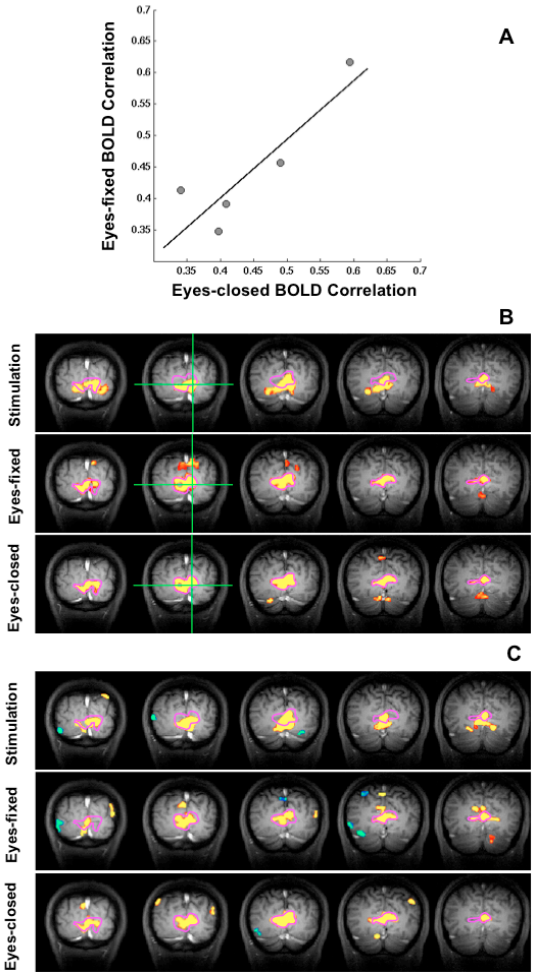

Figure 7.3 Comparison of BOLD correlation strength and correlation maps between the eyes-fixed and eyes-closed conditions. (A) A scatter plot showing, for each subject, the correlation strength of baseline BOLD fluctuations under these two conditions suggests a significant association between them (R^2 = 0.78, p = 0.046, n = 5). (B) Correlation maps from a representative participant (Subject 12) under the eyes-fixed (middle) and eyes-closed (bottom) conditions indicate two topographically undistinguishable coherent networks, which are different from the one during stimulation (top). These maps were generated with respect to a reference region (green cross), and their statistical thresholds were adjusted to show the same amount of voxels for better comparison of spatial pattern. (C) Independent components extracted from the same dataset using sICA method confirm the results of correlation analysis. All maps shown in this figure were averaged over multiple fMRI runs. The contour of the correlation map under the eyes-closed condition (the bottom of B) was outlined with magenta color and overlapped on all other maps.

The similarity between the baseline BOLD signal fluctuations measured under the eyes-fixed and eyes-closed conditions suggests that the relationship shown in Figure 7.2A could be further extended from the eyes-fixed (control) condition to the eyes-closed (resting-state) condition.

7.4 Discussion

7.4.1 Baseline BOLD Correlation Accounts for Large Inter-Subject Variability in Evoked BOLD Amplitude

Many factors have been shown to possibly contribute to the large inter-subject variability in hemodynamic responses during brain activation (Gustard et al., 2003, Lu et al., 2008, D'Esposito et al., 2003, Lund et al., 2005); a number of approaches, including spatial smoothing and motion correction, were applied in the present study to minimize possible variability induced by some of non-neural factors (White et al., 2001, Lund et al., 2005). Even so, the stimulus-evoked BOLD amplitude still exhibited considerably large variation across subjects, so did the baseline BOLD correlation strength. Interestingly, a significant association was found between these two BOLD measurements, which suggests that the inter-subject variability in the evoked BOLD amplitude can, at least substantially, be attributed to the large variation of baseline BOLD correlation across subjects.

In contrast to the large inter-subject variability, both baseline BOLD correlation and stimulus-evoked BOLD amplitude are relatively stable across multiple fMRI runs

within the same subject and this is evident by the small error bars shown in Figure 7.2. This result is consistent with previous observations that the intra-subject variability of both evoked BOLD responses (Aguirre et al., 1998) and baseline BOLD correlations (Zhang et al., 2007) is smaller than their inter-subject variability. For this reason, the relationship between the baseline BOLD correlation and evoked BOLD amplitude is not obvious based only on single-subject data (Figure 7.S1A), except for a few subjects (e.g., Subject 8 and Subject 11, Figure 7.S1A) showing relatively large inter-run variability in both evoked BOLD response and baseline BOLD correlation strength.

7.4.2 Coherent Networks Implied by Baseline BOLD Fluctuations under Eyes-Fixed and Eyes-Closed Conditions

Most studies on baseline BOLD fluctuations are conducted during a resting-state with eyes either fixed on a cross or closed (Fox et al., 2006a), and a number of resting-state networks have been found to remain similar under these two baseline conditions (Fox et al., 2005). Nevertheless, a few studies (Bianciardi et al., 2009a, Yang et al., 2007) have suggested that the magnitude and correlation of baseline BOLD fluctuations in the visual cortex might be different between the eyes-fixed and eyes-closed conditions. It is therefore interesting to examine this aspect quantitatively.

Our parallel correlation analyses on the baseline BOLD signals acquired under the eyes-fixed and eyes-closed conditions showed two spatially indistinguishable coherent networks mainly covering the visual cortex. They are, however, not completely overlapped with the cortical regions showing evoked BOLD responses to a full-screen visual stimulus (Figure 7.3). The main difference is in the cuneus gyrus region, which

belongs to visual association areas involved in the dorsal pathway and high-level visual functions and was not activated by the reversal checkerboard stimuli with full coverage of visual field. Furthermore, quantitative analysis also suggests a correlation between the correlation strengths within the visual coherent network under these two conditions (Figure 7.3A). These results suggest a similar neurophysiologic basis for the baseline coherent networks under the eyes-fixed and eyes-closed conditions.

7.4.3 Interaction between Ongoing Brain Activity and Evoked Brain Response

The coherent visual network as observed in the present study is just one of many "resting-state networks" mapped through baseline BOLD fluctuations. Although the exact mechanism underlying the baseline BOLD fluctuation remains elusive, several studies have linked it to spontaneous neural activity (Mantini et al., 2007, Goldman et al., 2002, Feige et al., 2005, Liu et al., 2010, Shmuel and Leopold, 2008).

More interestingly, recent fMRI studies have demonstrated how human behaviors could be influenced by pre-stimulus baseline BOLD signals acquired under the eyes-fixed condition (the same as in the present study) (Boly et al., 2007, Fox et al., 2007, Hesselmann et al., 2008b, Hesselmann et al., 2008a, Sapir et al., 2005). These studies have shown, for example, that differences in the pre-stimulus BOLD signal can predict whether: a motion discrimination judgment is right or wrong (Sapir et al., 2005), a sensory stimulus will be perceived or missed (Boly et al., 2007), an ambiguous visual stimulus will be perceived as a face or object (Hesselmann et al., 2008a), or a group of dots will move coherently or randomly (Hesselmann et al., 2008b). These important

findings clearly suggest an interaction between ongoing brain activity and evoked brain response at a behavioral level.

Compared to those behavioral studies, our study aims to understand the quantitative relationship between ongoing and evoked brain activities from a more mechanistic perspective by measuring and examining the relationship between baseline and evoked BOLD signals. We found that synchronization strength within a resting-state coherent network (implied by the baseline BOLD signal fluctuation associated with the underlying ongoing brain activity) has an important influence on the amplitude of its evoked response (evoked brain activity) to external stimulation, even at the early stage of the visual system.

We were unable to directly draw conclusions in regard to the quantitative relationship between the evoked BOLD amplitude in the visual cortex and associated visual behaviors, which were not measured in this study. However, several previous studies have provided evidence to link them (Buchel et al., 2002, Dehaene et al., 2001, Ress et al., 2000). For example, the amplitude of evoked BOLD responses in the primary visual cortex was found to be able to predict how well subjects performed a visual perception task (Ress et al., 2000).

The present study is also distinct from the previous studies aiming to link baseline BOLD signal with human behavior in the aspect of ongoing brain activity quantification. The majority of previous behavior studies employed an event-related fMRI paradigm, and a short period of baseline BOLD signals (or even a single image time point) prior to the stimulation (or task) onset was utilized to quantify the relative level of ongoing brain

activity, which may only reflect an instantaneous status of the resting brain. In contrast, we used a relatively long period (165 seconds) of baseline BOLD signals to quantify the correlation of ongoing brain activity, which is likely to reflect a more general status of the resting brain. From this perspective, our study is closer to previous studies relying on the quantification of correlation strength (functional connectivity) of resting-state networks. For instance, the correlation strength of individuals' resting-state default mode networks has been successfully applied to predict how well subjects perform a working memory task (Hampson et al., 2006), to distinguish schizophrenia patients from healthy subjects, or to correlate with the schizophrenia psychopathology (Whitfield-Gabrieli et al., 2009). Together with those findings, our study reveals potential roles of resting-state networks and neuronal synchronization in brain activation, function, and behavior.

7.4.4 Neurophysiologic Basis of Baseline BOLD Fluctuations

Converged evidence from a number of studies using simultaneous EEG-fMRI measurements (Feige et al., 2005, Goldman et al., 2002, Moosmann et al., 2003) has consistently shown that the baseline BOLD signal measured in the human visual cortex is negatively correlated with the power of occipital alpha-band EEG oscillations under the eyes-closed condition. Interestingly, even though it is known that the occipital alpha-band EEG power will decrease drastically when subjects open their eyes, its topographic distribution has not been shown to change significantly (Barry et al., 2007). To some extent, this finding is in line with our observation that the coherent networks implied by baseline BOLD fluctuations are spatially indistinguishable under the eyes-fixed and eyes-closed conditions. Moreover, the individual alpha-frequency (IAF) under the resting-state

has been shown to negatively correlate with: (i) the amplitude of alpha-band EEG oscillations at rest; (ii) the amplitude of the visual evoked potential (VEP); and (iii) the amplitude of hemoglobin oxygenation level change, which was measured by the near-infrared spectroscopy (NIRS) technique, in response to visual stimulation (Koch et al., 2008). All of these findings suggest that the ongoing occipital alpha-band brain activity may be linked to the baseline BOLD fluctuations under both the eyes-fixed and the eyes-closed condition.

Besides the alpha-band activity at rest, the amplitude of stimulus-evoked BOLD responses has also been correlated with a number of other neurophysiologic measurements, for example, the stimulus-induced gamma oscillation frequency and the resting-state concentration of GABA (Muthukumaraswamy et al., 2009), which is a neurotransmitter essential for inhibitory interneurons and the generation of synchronized neuronal oscillations (Buzsaki et al., 2007). Understanding how the baseline BOLD correlation is associated with these neuro- and electro-physiology parameters should provide an important step for revealing the underlying mechanism of ongoing and evoked brain activity interaction. This remains an interesting topic for future studies.

7.4.5 Methodology Considerations and Perspectives

Since a correlation, but not causality, was found between the baseline BOLD correlation and stimulus-evoked BOLD amplitude in the present study, one possible argument on our results is that the visual input under the eyes-fixed condition (i.e., a white cross on a black screen), if considered as a weak "stimulus", might evoke stronger fluctuations and thus higher correlation (due to a higher temporal contrast-to-noise ratio)

of baseline BOLD signals for the subjects showing a stronger stimulus-evoked BOLD response. However, this possibility could be excluded for the following reasons. First, we minimized the effect of visual input under the eyes-fixed condition by using a very small cross-mark with moderate illumination on a dark screen with minimum illumination. The BOLD correlation maps for the eyes-fixed condition, which are almost identical to those obtained under the eyes-closed condition but different from those during visual stimulation (Figure 7.3), are very unlikely to be induced by the very small fixation cross on a dark screen. Secondly, no significant correlation was found between the magnitude of the baseline BOLD fluctuation and stimulus-evoked BOLD amplitude (Figure 7.2B), which means subjects showing stronger evoked BOLD responses do not necessarily have stronger baseline BOLD fluctuations in the same ROI – another line of evidence against the argument.

In fact, when the ROI was reduced to cover mainly the large-vessel GE-EPI voxels, the relationship between the magnitude of the baseline BOLD fluctuation and evoked BOLD amplitude is still not statistically significant (see Figure 7.S3). One implication of this finding is that the vasculature (especially in the venous side) variation is unlikely to contribute significantly to the large inter-subject variability in evoked BOLD amplitude observed in the present study, presumably due to: i) the large suppression of the large-vessel BOLD contribution at high magnetic field (Ogawa et al., 1998); ii) the further exclusion of large-vessel voxels in the ROI selection and data analysis; and iii) the narrow age distribution of the subjects (13 out of 15 subjects are aged between 20 and 30). For these reasons, the large inter-subject variability in baseline

BOLD correlation and evoked BOLD amplitude cannot be explained from a vascular-origin perspective. Furthermore, our results should not conflict with a previous study (Kannurpatti and Biswal, 2008) showing a correlation between the magnitude of baseline BOLD fluctuation and hypercapnia-induced BOLD responses, in which the relationship was established on intra-subject and voxel-based analysis, and thus a strong correlation is logically expected based on the underlying BOLD mechanism (Ogawa et al., 1998).

It has been shown previously that the spontaneous BOLD signal fluctuation was not only contributed by ongoing brain activity but also other sources including physiologic noise (Bianciardi et al., 2009b). Although certain measures, for example, the combination of short TR and band-pass filter, have been taken to minimize possible contributions from these sources; some of them, for example, very low-frequency variation of respiration volume (Birn et al., 2006), cannot be removed completely from the image data. However, our conclusion is likely less affected by those noise sources for the following three reasons. First, a previous study had shown that the spontaneous BOLD signal fluctuation in the human visual cortex is contributed dominantly by ongoing brain activity if high-frequency thermal noise and low-frequency drift are removed (Bianciardi et al., 2009b). Second, the present study focused on the relative correlation strength of baseline BOLD fluctuation (inter-subject difference); therefore, if the contribution from noise sources is relatively consistent across subjects, it would not affect our conclusion. Thirdly, the relationship between the evoked BOLD amplitude and correlation strength of baseline BOLD fluctuation observed in the present study cannot be explained only from the noise perspective.

Another impact of our finding that baseline BOLD correlation accounts for large inter-subject variability in stimulus-evoked BOLD amplitude is on fMRI quantification, especially for those studies aiming to compare differences between evoked BOLD amplitudes from different groups of subjects (e.g., healthy versus deiased groups). Our analysis suggests that 69% inter-subject variation in the stimulus-evoked BOLD response could be explained by the inter-subject variability in the baseline BOLD correlation (based on $R^2 = 0.69$). By monitoring baseline BOLD signals and removing the variation they cause by regression, the inter-subject (or within-group) variability in the stimulus-evoked BOLD signals could be significantly reduced, and therefore the sample size required to identify certain group difference could be effectively reduced.

7.5 Conclusion

In the present study, we found that the spatiotemporal correlations of baseline BOLD signals acquired under the eyes-fixed condition from the human visual cortex imply an organized, coherent network that is topographically indistinguishable from the resting-state visual network observed under the eyes-closed condition. More strikingly, the correlation strength of this ongoing visual network can significantly influence the amplitude of subjects' evoked BOLD responses to visual stimulation. The subject with a more synchronized ongoing network tends to show a stronger response to identical stimulation. The overall findings indicate a strong interaction between ongoing and evoked brain activities, and they also suggest the importance of the coherent networks implied by low-frequency baseline BOLD fluctuations under either the eyes-fixed or

eyes-closed condition for linking brain activation, function and dysfunction. This study highlights the importance to integrate the information from both resting-state coherent networks and task-evoked neural responses for a better understanding of how the brain works.

7.6 Supplementary Figures

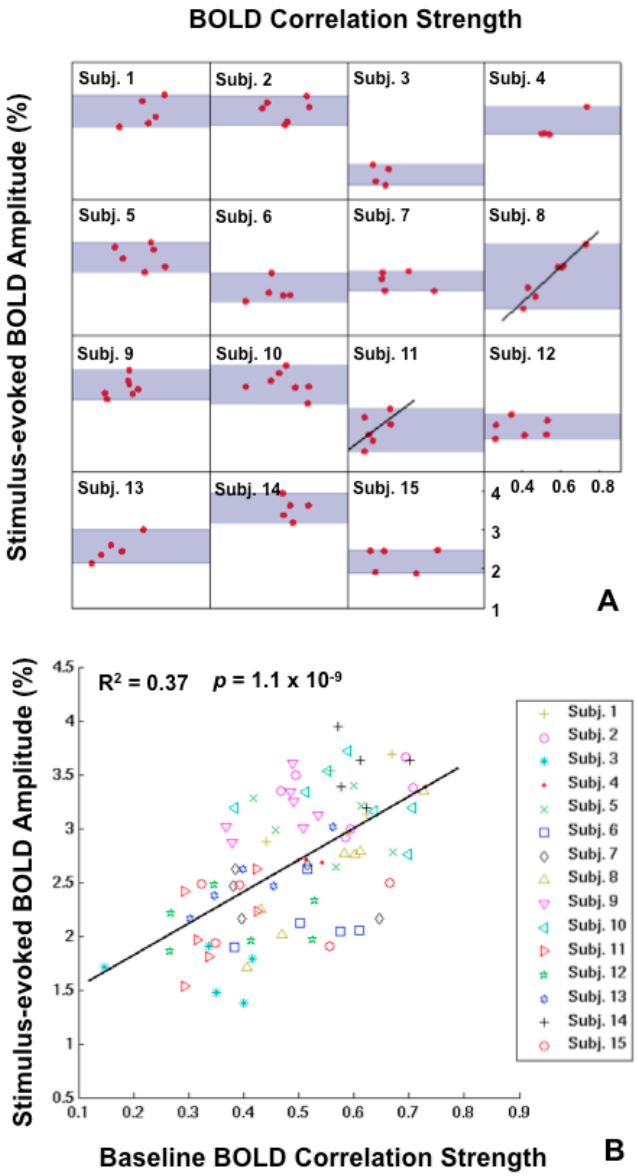

Figure 7.S1 Scatter plots showing, for each fMRI run, the amplitude of evoked BOLD responses versus the correlation strength of baseline BOLD fluctuations. Each symbol represents the data from a single standard fMRI run. (A) Scatter plot matrix with each element representing data from one subject. The blue shadows emphasize the range of evoked BOLD amplitude, and the LS fitting line was also plotted for two subjects with the widest ranges. (B) A scatter plot pooling the data from all the subjects.

Δ

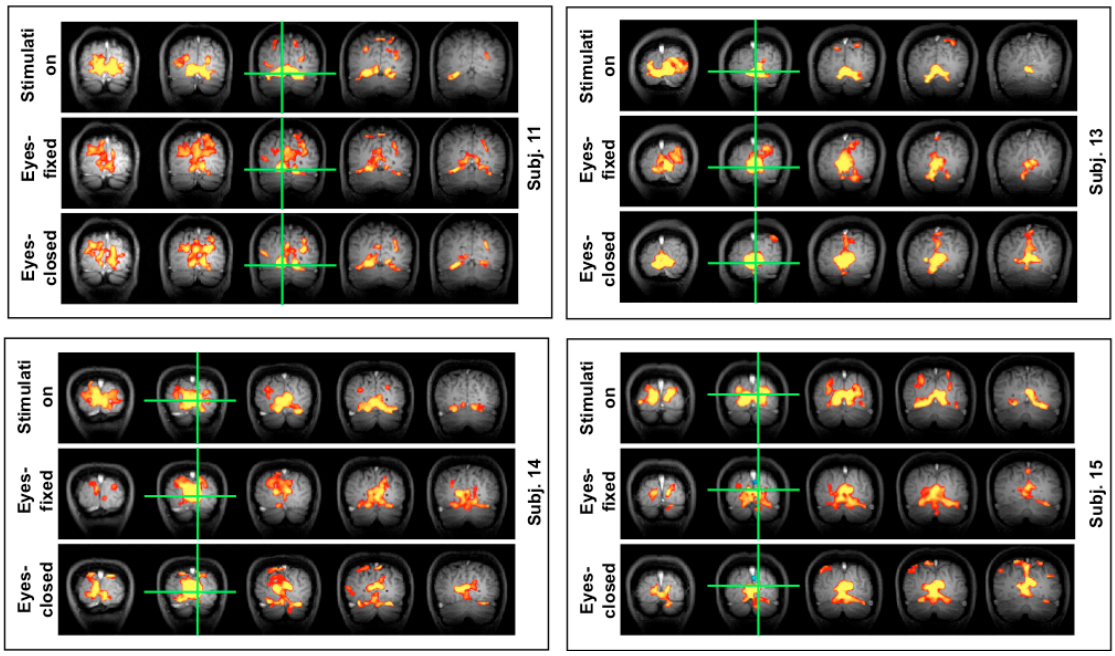

Figure 7.S2 Correlation maps with respect to a reference region (green cross) in the visual cortex under stimulation (the block-design stage), eyes-fixed, and eyes-closed conditions from the other four subjects (except for Subject 12 in Figure 3), whose baseline BOLD signals were acquired under both eyes-fixed and eyes-closed conditions. The thresholds were adjusted for each map to show only the most correlated 20% brain regions. All maps shown in this figure were averaged over multiple runs.

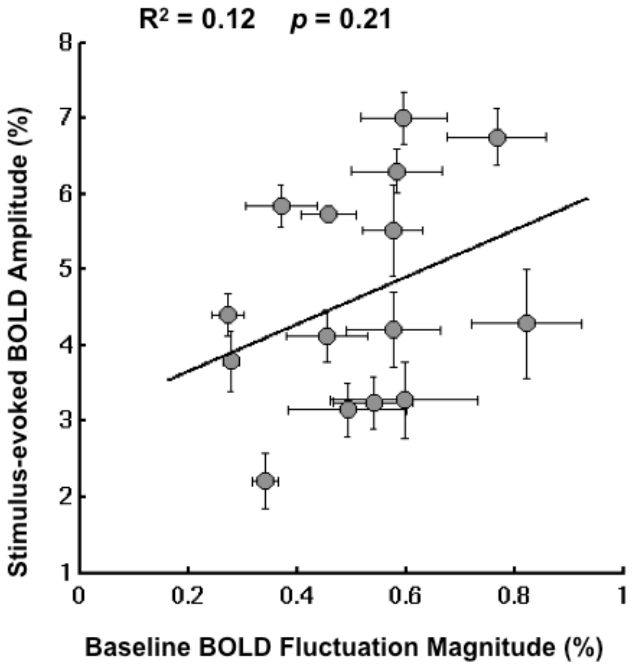

Figure 7.S3 Scatter plots showing, for each subject, the amplitude of stimulus-evoked BOLD responses versus magnitude of baseline BOLD fluctuation in the large-vessel voxels. No significant association was found between these two statistics (p = 0.21). The only difference between this plot and Figure 7.2*B* lies in the ROI used for data quantification. The ROI used here was selected to cover most activated 0.5% brain voxels (24 ± 3 voxels, Mean ± SD), which are supposed to be dominated by large-vessel brain voxels; and majority of these voxels are actually excluded from the ROI used for Figure 7.2.

Chapter 8

SUMMARY AND FUTURE DIRECTIONS

The rapid increase in research on spontaneous BOLD fluctuation during the past several years reflects peoples' growing interests in the brain's functional connectivity and ongoing activity. Even though some controversies and debates remain, the most of studies on spontaneous BOLD fluctuation concurred with its importance for brain functions. Based on the results of these studies, now we know that low-frequency spontaneous BOLD fluctuation is not from physiologic or thermal noise but reflects the underlying spontaneous neural activity. Though with certain modulations, it is preserved under a variety of brain conditions, such as anesthesia, sleep, and vegetative state, suggesting it is intrinsic to a live brain. It alters in a variety of brain diseases and metal disorders, indicating it is critical for the brain's functioning. It can influence subjects' responses to external stimulation/tasks, suggesting it is related to basic working mechanisms of the brain. All these findings support a new theory in system neuroscience

that the brain is a perpetually active and self-organized system and ongoing brain activity playing an essential role in this system. They also suggest a promising future for spontaneous BOLD fluctuation research in helping us to understand the neurophysiology behind many complex brain diseases and to find its applications in clinical diagnosis.

My dissertation made some contributions to this field, which are summarized as follows:

We have found that spontaneous BOLD fluctuation under deep anesthesia with burst-suppression activity mainly results from underlying neural activity and reveal the organization of ongoing brain activity.

We have also demonstrated that spontaneous BOLD fluctuation is extremely sensitive to the level of anesthesia. The coherent networks implied by its spatiotemporal correlations experience a specific-to-less-specific transition as the depth of anesthesia increases, giving a good illustration for a theory regarding consciousness and anesthesia. The transition may reflect a reorganization of ongoing brain activity under different brain states. The finding also suggests that the network specificity is a very important aspect for the quantification of spontaneous BOLD fluctuations and thus brain states.

In awake human subjects, we have observed that the resting-state coherent network is spatially reorganized into two distinct coherent networks covering activated and non-activated brain regions, respectively, under continuous stimulation. It implies that the brain regions showing evoked BOLD responses to external stimulation is actually a coherent network with strong synchronized activity. We also showed that the reduced correlation between activated and non-activated regions was, however, not observed

when presenting a short visual stimulus in event-related paradigm. We gave an explanation for the discrepant based on the basic mechanism of BOLD contrast.

We finally showed that the correlation strength within the resting-state network of subjects could affect the amplitude of their evoked BOLD responses to identical stimulation, suggesting an interaction between ongoing and evoked brain activity. The finding also provides a new explanation for the large inter-subject variability in evoked BOLD responses commonly observed in fMRI studies and can probably be utilized to reduce the inter-subject BOLD variation in the future.

The overall findings from my thesis are in three layers: i) to bridge the spontaneous BOLD signal to the underlying ongoing neuronal activity; and ii) to provide new insights into the functional connectivity implied by spontaneous BOLD signal; and iii) to bridge the resting and activated brain states. They clearly suggest that both resting-state and activated neuronal activities are essential for brain function or dysfunction, and fMRI should provide a vital tool for noninvasively mapping these activities.

In future, we would like to extend our current projects into a deeper and broader domain to better understand the mechanisms of spontaneous BOLD fluctuation. More specifically, for animal studies we would like to investigate the neural origin of spontaneous BOLD fluctuation under relatively light anesthesia condition using multi-modality methods. We would like to replace the intracranial-EEG recording with electrophysiology recording to give more information about the brain's electrical activity.

We would also like to know whether the specific-to-less-specific transition of resting-state functional connectivity is a general phenomenon related to changes in the consciousness level. Towards this goal, we would like to examine how spontaneous BOLD fluctuation changes under anesthesia conditions induced by other anesthetics or under non-anesthetic unconsciousness or awake state.

For human projects, we would like to link individuals' spontaneous BOLD fluctuation to other neural-related parameters, which have been found to correlate to subjects' evoked BOLD response. For example, we would like to investigate whether difference in spontaneous BOLD correlation strength is associated with the band-limited EEG activity, such as the power or frequency of alpha-band oscillation, or with the concentrations of neural-related metabolites or transmitters, for example, the concentration of GABA at rest. These researches should provide new and comprehensive information about spontaneous BOLD fluctuation.

BIBLIOGRAPHY

ACHARD, S., SALVADOR, R., WHITCHER, B., SUCKLING, J. & BULLMORE, E. 2006. A resilient, low-frequency, small-world human brain functional network with highly connected association cortical hubs. *J Neurosci,* 26**,** 63-72.

AGUIRRE, G. K., ZARAHN, E. & D'ESPOSITO, M. 1998. The variability of human, BOLD hemodynamic responses. *Neuroimage,* 8**,** 360-9.

ALKIRE, M. T., HUDETZ, A. G. & TONONI, G. 2008. Consciousness and anesthesia. *Science,* 322**,** 876-80.

ALOIMONOS, Y. & ROSENFELD, A. 1991. Computer vision. *Science,* 253**,** 1249-54.

ANAND, A., LI, Y., WANG, Y., WU, J., GAO, S., BUKHARI, L., MATHEWS, V. P., KALNIN, A. & LOWE, M. J. 2005. Activity and connectivity of brain mood regulating circuit in depression: a functional magnetic resonance study. *Biol Psychiatry,* 57**,** 1079-88.

AOKI, F., FETZ, E. E., SHUPE, L., LETTICH, E. & OJEMANN, G. A. 1999. Increased gamma-range activity in human sensorimotor cortex during performance of visuomotor tasks. *Clin Neurophysiol,* 110**,** 524-37.

ARIELI, A., STERKIN, A., GRINVALD, A. & AERTSEN, A. 1996. Dynamics of ongoing activity: explanation of the large variability in evoked cortical responses. *Science,* 273**,** 1868-71.

ARTHURS, O. J. & BONIFACE, S. 2002. How well do we understand the neural origins of the fMRI BOLD signal? *Trends Neurosci,* 25**,** 27-31.

BANDETTINI, P. A., JESMANOWICZ, A., WONG, E. C. & HYDE, J. S. 1993. Processing strategies for time-course data sets in functional MRI of the human brain. *Magn Reson Med,* 30**,** 161-73.

BANDETTINI, P. A., WONG, E. C., HINKS, R. S., TIKOFSKY, R. S. & HYDE, J. S. 1992. Time course EPI of human brain function during task activation. *Magn. Reson. Med.,* 25**,** 390-397.

BARRY, R. J., CLARKE, A. R., JOHNSTONE, S. J., MAGEE, C. A. & RUSHBY, J. A. 2007. EEG differences between eyes-closed and eyes-open resting conditions. *Clin Neurophysiol,* 118**,** 2765-73.

BEER, R. D. 2000. Dynamical approaches to cognitive science. *Trends Cogn Sci,* 4**,** 91-99.

BETTUS, G., GUEDJ, E., JOYEUX, F., CONFORT-GOUNY, S., SOULIER, E., LAGUITTON, V., COZZONE, P. J., CHAUVEL, P., RANJEVA, J. P., BARTOLOMEI, F. & GUYE, M. 2009. Decreased basal fMRI functional connectivity in epileptogenic networks and contralateral compensatory mechanisms. *Hum Brain Mapp,* 30**,** 1580-91.

BIANCIARDI, M., FUKUNAGA, M., VAN GELDEREN, P., HOROVITZ, S. G., DE ZWART, J. A. & DUYN, J. H. 2009a. Modulation of spontaneous fMRI activity in human visual cortex by behavioral state. *Neuroimage,* 45**,** 160-8.

BIANCIARDI, M., FUKUNAGA, M., VAN GELDEREN, P., HOROVITZ, S. G., DE ZWART, J. A., SHMUELI, K. & DUYN, J. H. 2009b. Sources of functional magnetic resonance imaging signal fluctuations in the human brain at rest: a 7 T study. *Magn Reson Imaging,* 27**,** 1019-29.

BIRN, R. M., DIAMOND, J. B., SMITH, M. A. & BANDETTINI, P. A. 2006. Separating respiratory-variation-related fluctuations from neuronal-activity-related fluctuations in fMRI. *Neuroimage,* 31**,** 1536-48.

BISWAL, B., HUDETZ, A. G., YETKIN, F. Z., HAUGHTON, V. M. & HYDE, J. S. 1997. Hypercapnia reversibly suppresses low-frequency fluctuations in the human motor cortex during rest using echo-planar MRI. *J Cereb Blood Flow Metab,* 17**,** 301-8.

BISWAL, B., YETKIN, F. Z., HAUGHTON, V. M. & HYDE, J. S. 1995. Functional connectivity in the motor cortex of resting human brain using echo-planar MRI. *Magn Reson Med,* 34**,** 537-41.

BLOCH, F., HANSEN, W. W. & PACKARD, M. E. 1946. Nuclear Induction. *Phys Rev* 460-73.

BLUHM, R. L., WILLIAMSON, P. C., OSUCH, E. A., FREWEN, P. A., STEVENS, T. K., BOKSMAN, K., NEUFELD, R. W., THEBERGE, J. & LANIUS, R. A. 2009. Alterations in default network connectivity in posttraumatic stress disorder related to early-life trauma. *J Psychiatry Neurosci,* 34**,** 187-94.

BOLY, M., BALTEAU, E., SCHNAKERS, C., DEGUELDRE, C., MOONEN, G., LUXEN, A., PHILLIPS, C., PEIGNEUX, P., MAQUET, P. & LAUREYS, S. 2007. Baseline brain activity fluctuations predict somatosensory perception in humans. *Proc Natl Acad Sci U S A,* 104**,** 12187-92.

BOLY, M., TSHIBANDA, L., VANHAUDENHUYSE, A., NOIRHOMME, Q., SCHNAKERS, C., LEDOUX, D., BOVEROUX, P., GARWEG, C., LAMBERMONT, B., PHILLIPS, C., LUXEN, A., MOONEN, G., BASSETTI, C., MAQUET, P. & LAUREYS, S. 2009. Functional connectivity in the default network during resting state is preserved in a vegetative but not in a brain dead patient. *Hum Brain Mapp,* 30**,** 2393-400.

BRESSLER, S. L., COPPOLA, R. & NAKAMURA, R. 1993. Episodic multiregional cortical coherence at multiple frequencies during visual task performance. *Nature,* 366**,** 153-6.

BUCHEL, C., BORNHOVD, K., QUANTE, M., GLAUCHE, V., BROMM, B. & WEILLER, C. 2002. Dissociable neural responses related to pain intensity, stimulus intensity, and stimulus awareness within the anterior cingulate cortex: a parametric single-trial laser functional magnetic resonance imaging study. *J Neurosci,* 22**,** 970-6.

BUCHEL, C. & FRISTON, K. J. 1997. Modulation of connectivity in visual pathways by attention: cortical interactions evaluated with structural equation modelling and fMRI. *Cereb Cortex,* 7**,** 768-78.

BUSCHMAN, T. J. & MILLER, E. K. 2007. Top-down versus bottom-up control of attention in the prefrontal and posterior parietal cortices. *Science,* 315**,** 1860-2.

BUZSAKI, G. & DRAGUHN, A. 2004. Neuronal oscillations in cortical networks. *Science,* 304**,** 1926-9.

BUZSAKI, G., KAILA, K. & RAICHLE, M. 2007. Inhibition and brain work. *Neuron,* 56**,** 771-83.

CAESAR, K., GOLD, L. & LAURITZEN, M. 2003. Context sensitivity of activity-dependent increases in cerebral blood flow. *Proc Natl Acad Sci U S A,* 100**,** 4239-44.

CHERKASSKY, V. L., KANA, R. K., KELLER, T. A. & JUST, M. A. 2006. Functional connectivity in a baseline resting-state network in autism. *Neuroreport,* 17**,** 1687-90.

CONTRERAS, D. & STERIADE, M. 1997. State-dependent fluctuations of low-frequency rhythms in corticothalamic networks. *Neuroscience,* 76**,** 25-38.

CORDES, D., HAUGHTON, V., CAREW, J. D., ARFANAKIS, K. & MARAVILLA, K. 2002. Hierarchical clustering to measure connectivity in fMRI resting-state data. *Magn Reson Imaging,* 20**,** 305-17.

CORDES, D., HAUGHTON, V. M., ARFANAKIS, K., WENDT, G. J., TURSKI, P. A., MORITZ, C. H., QUIGLEY, M. A. & MEYERAND, M. E. 2000. Mapping functionally related regions of brain with functional connectivity MR imaging. *AJNR Am J Neuroradiol,* 21**,** 1636-44.

COX, R. W. 1996. AFNI: software for analysis and visualization of functional magnetic resonance neuroimages. *Comput Biomed Res,* 29**,** 162-73.

D'ESPOSITO, M., DEOUELL, L. Y. & GAZZALEY, A. 2003. Alterations in the BOLD fMRI signal with ageing and disease: a challenge for neuroimaging. *Nat Rev Neurosci,* 4**,** 863-72.

DAVIS, T. L., KWONG, K. K., WEISSKOFF, R. M. & ROSEN, B. R. 1998. Calibrated functional MRI: mapping the dynamics of oxidative metabolism. *Proc Natl Acad Sci U S A,* 95**,** 1834-9.

DEHAENE, S., NACCACHE, L., COHEN, L., BIHAN, D. L., MANGIN, J. F., POLINE, J. B. & RIVIERE, D. 2001. Cerebral mechanisms of word masking and unconscious repetition priming. *Nat Neurosci,* 4**,** 752-8.

DOSENBACH, N. U., FAIR, D. A., MIEZIN, F. M., COHEN, A. L., WENGER, K. K., DOSENBACH, R. A., FOX, M. D., SNYDER, A. Z., VINCENT, J. L., RAICHLE, M. E., SCHLAGGAR, B. L. & PETERSEN, S. E. 2007. Distinct brain networks for adaptive and stable task control in humans. *Proc Natl Acad Sci U S A,* 104**,** 11073-8.

DU, F., ZHU, X. H., ZHANG, Y., FRIEDMAN, M., ZHANG, N., UGURBIL, K. & CHEN, W. 2008. Tightly coupled brain activity and cerebral ATP metabolic rate. *Proc Natl Acad Sci U S A,* 105**,** 6409-14.

ENGEL, A. K., FRIES, P. & SINGER, W. 2001. Dynamic predictions: oscillations and synchrony in top-down processing. *Nat Rev Neurosci,* 2**,** 704-16.

FAIR, D. A., COHEN, A. L., DOSENBACH, N. U., CHURCH, J. A., MIEZIN, F. M., BARCH, D. M., RAICHLE, M. E., PETERSEN, S. E. & SCHLAGGAR, B. L. 2008. The maturing architecture of the brain's default network. *Proc Natl Acad Sci U S A,* 105**,** 4028-32.

FAIR, D. A., DOSENBACH, N. U., CHURCH, J. A., COHEN, A. L., BRAHMBHATT, S., MIEZIN, F. M., BARCH, D. M., RAICHLE, M. E., PETERSEN, S. E. & SCHLAGGAR, B. L. 2007. Development of distinct control networks through segregation and integration. *Proc Natl Acad Sci U S A,* 104**,** 13507-12.

FEIGE, B., SCHEFFLER, K., ESPOSITO, F., DI SALLE, F., HENNIG, J. & SEIFRITZ, E. 2005. Cortical and subcortical correlates of electroencephalographic alpha rhythm modulation. *J Neurophysiol,* 93**,** 2864-72.

FOX, M. D., CORBETTA, M., SNYDER, A. Z., VINCENT, J. L. & RAICHLE, M. E. 2006a. Spontaneous neuronal activity distinguishes human dorsal and ventral attention systems. *Proc Natl Acad Sci U S A,* 103**,** 10046-51.

FOX, M. D. & RAICHLE, M. E. 2007. Spontaneous fluctuations in brain activity observed with functional magnetic resonance imaging. *Nat Rev Neurosci,* 8**,** 700-11.

FOX, M. D., SNYDER, A. Z., VINCENT, J. L., CORBETTA, M., VAN ESSEN, D. C. & RAICHLE, M. E. 2005. The human brain is intrinsically organized into dynamic, anticorrelated functional networks. *Proc Natl Acad Sci U S A,* 102**,** 9673-8.

FOX, M. D., SNYDER, A. Z., VINCENT, J. L. & RAICHLE, M. E. 2007. Intrinsic fluctuations within cortical systems account for intertrial variability in human behavior. *Neuron,* 56**,** 171-84.

FOX, M. D., SNYDER, A. Z., ZACKS, J. M. & RAICHLE, M. E. 2006b. Coherent spontaneous activity accounts for trial-to-trial variability in human evoked brain responses. *Nat Neurosci,* 9**,** 23-5.

FOX, M. D., ZHANG, D., SNYDER, A. Z. & RAICHLE, M. E. 2009. The global signal and observed anticorrelated resting state brain networks. *J Neurophysiol,* 101**,** 3270-83.

FOX, P. T. & RAICHLE, M. E. 1986. Focal physiological uncoupling of cerebral blood flow and oxidative metabolism during somatosensory stimulation in human subjects. *Proc Natl Acad Sci U S A,* 83**,** 1140-4.

FOX, P. T., RAICHLE, M. E., MINTUN, M. A. & DENCE, C. 1988. Nonoxidative glucose consumption during focal physiologic neural activity. *Science,* 241**,** 462-464.

FRANSSON, P. 2005. Spontaneous low-frequency BOLD signal fluctuations: an fMRI investigation of the resting-state default mode of brain function hypothesis. *Hum Brain Mapp,* 26**,** 15-29.

FRIES, P., NIKOLIC, D. & SINGER, W. 2007. The gamma cycle. *Trends Neurosci,* 30**,** 309-16.

FRISTON, K. J. 1994. Functional and Effective Connectivity in Neuroimaging: A Synthesis. *Hum Brain Mapp,* 2**,** 56-78.

FRISTON, K. J., FRITH, C. D., LIDDLE, P. F. & FRACKOWIAK, R. S. 1993. Functional connectivity: the principal-component analysis of large (PET) data sets. *J Cereb Blood Flow Metab,* 13**,** 5-14.

FUKUNAGA, M., HOROVITZ, S. G., VAN GELDEREN, P., DE ZWART, J. A., JANSMA, J. M., IKONOMIDOU, V. N., CHU, R., DECKERS, R. H., LEOPOLD, D. A. & DUYN, J. H. 2006. Large-amplitude, spatially correlated fluctuations in BOLD fMRI signals during extended rest and early sleep stages. *Magn Reson Imaging,* 24**,** 979-92.

GOLANOV, E. V., YAMAMOTO, S. & REIS, D. J. 1994. Spontaneous waves of cerebral blood flow associated with a pattern of electrocortical activity. *Am J Physiol,* 266**,** R204-14.

GOLDMAN, R. I., STERN, J. M., ENGEL, J., JR. & COHEN, M. S. 2002. Simultaneous EEG and fMRI of the alpha rhythm. *Neuroreport,* 13**,** 2487-92.

GREICIUS, M. D., FLORES, B. H., MENON, V., GLOVER, G. H., SOLVASON, H. B., KENNA, H., REISS, A. L. & SCHATZBERG, A. F. 2007. Resting-state functional connectivity in major depression: abnormally increased contributions from subgenual cingulate cortex and thalamus. *Biol Psychiatry,* 62**,** 429-37.

GREICIUS, M. D., KIVINIEMI, V., TERVONEN, O., VAINIONPAA, V., ALAHUHTA, S., REISS, A. L. & MENON, V. 2008. Persistent default-mode network connectivity during light sedation. *Hum Brain Mapp,* 29**,** 839-47.

GREICIUS, M. D., KRASNOW, B., REISS, A. L. & MENON, V. 2003. Functional connectivity in the resting brain: a network analysis of the default mode hypothesis. *Proc Natl Acad Sci U S A,* 100**,** 253-8.

GUSTARD, S., WILLIAMS, E. J., HALL, L. D., PICKARD, J. D. & CARPENTER, T. A. 2003. Influence of baseline hematocrit on between-subject BOLD signal change using gradient echo and asymmetric spin echo EPI. *Magn Reson Imaging,* 21**,** 599-607.

HAASE, A. 1990. Snapshot FLASH MRI. Applications to T1, T2, and chemical-shift imaging. *Magn Reson Med,* 13**,** 77-89.

HAMPSON, M., DRIESEN, N. R., SKUDLARSKI, P., GORE, J. C. & CONSTABLE, R. T. 2006. Brain connectivity related to working memory performance. *J Neurosci,* 26**,** 13338-43.

HAMPSON, M., PETERSON, B. S., SKUDLARSKI, P., GATENBY, J. C. & GORE, J. C. 2002. Detection of functional connectivity using temporal correlations in MR images. *Hum Brain Mapp,* 15**,** 247-62.

HARTIKAINEN, K. M., RORARIUS, M., PERAKYLA, J. J., LAIPPALA, P. J. & JANTTI, V. 1995. Cortical reactivity during isoflurane burst-suppression anesthesia. *Anesth Analg,* 81**,** 1223-8.

HEEGER, D. J., HUK, A. C., GEISLER, W. S. & ALBRECHT, D. G. 2000. Spikes versus BOLD: what does neuroimaging tell us about neuronal activity? *Nat Neurosci,* 3**,** 631-3.

HESSELMANN, G., KELL, C. A., EGER, E. & KLEINSCHMIDT, A. 2008a. Spontaneous local variations in ongoing neural activity bias perceptual decisions. *Proc Natl Acad Sci U S A,* 105**,** 10984-9.

HESSELMANN, G., KELL, C. A. & KLEINSCHMIDT, A. 2008b. Ongoing activity fluctuations in hMT+ bias the perception of coherent visual motion. *J Neurosci,* 28**,** 14481-5.

HONEY, C. J., SPORNS, O., CAMMOUN, L., GIGANDET, X., THIRAN, J. P., MEULI, R. & HAGMANN, P. 2009. Predicting human resting-state functional

connectivity from structural connectivity. *Proc Natl Acad Sci U S A,* 106**,** 2035-40.

HOOGENBOOM, N., SCHOFFELEN, J. M., OOSTENVELD, R., PARKES, L. M. & FRIES, P. 2006. Localizing human visual gamma-band activity in frequency, time and space. *Neuroimage,* 29**,** 764-73.

HOROVITZ, S. G., BRAUN, A. R., CARR, W. S., PICCHIONI, D., BALKIN, T. J., FUKUNAGA, M. & DUYN, J. H. 2009. Decoupling of the brain's default mode network during deep sleep. *Proc Natl Acad Sci U S A,* 106**,** 11376-81.

HOROVITZ, S. G., FUKUNAGA, M., DE ZWART, J. A., VAN GELDEREN, P., FULTON, S. C., BALKIN, T. J. & DUYN, J. H. 2008. Low frequency BOLD fluctuations during resting wakefulness and light sleep: a simultaneous EEG-fMRI study. *Hum Brain Mapp,* 29**,** 671-82.

HORWITZ, B. 2003. The elusive concept of brain connectivity. *Neuroimage,* 19**,** 466-70.

HUBEL, D. H. & WIESEL, T. N. 1965. Receptive Fields and Functional Architecture in Two Nonstriate Visual Areas (18 and 19) of the Cat. *J Neurophysiol,* 28**,** 229-89.

HUDETZ, A. G. 2006. Suppressing consciousness: Mechanisms of general anesthesia. *Seminars Anesth Periop Med Pain,* 25**,** 196-204.

HUDETZ, A. G. & IMAS, O. A. 2007. Burst activation of the cerebral cortex by flash stimuli during isoflurane anesthesia in rats. *Anesthesiology,* 107**,** 983-91.

HUDETZ, A. G., ROMAN, R. J. & HARDER, D. R. 1992. Spontaneous flow oscillations in the cerebral cortex during acute changes in mean arterial pressure. *J Cereb Blood Flow Metab,* 12**,** 491-9.

HYVARINEN, A. 1999. Fast and robust fixed-point algorithms for independent component analysis. *IEEE Trans Neural Netw,* 10**,** 626-34.

JAFRI, M. J., PEARLSON, G. D., STEVENS, M. & CALHOUN, V. D. 2008. A method for functional network connectivity among spatially independent resting-state components in schizophrenia. *Neuroimage,* 39**,** 1666-81.

JENKINS, G. M. & WATTS, D. G. 1968. Spectral Analysis and its Applications. *Emerson-Adams Press, Boca Raton*.

JEZZARD, P., LEBIHAN, D., CUENOD, D., PANNIER, L., PRINSTER, A. & TURNER, R. 1993. An investigation of the contribution of physiological noise in human functional MRI studies at 1.5 tesla and 4 tesla. *The proceeding of 12th SMRM annual meeting, New York***,** 1392.

JOHNSTON, J. M., VAISHNAVI, S. N., SMYTH, M. D., ZHANG, D., HE, B. J., ZEMPEL, J. M., SHIMONY, J. S., SNYDER, A. Z. & RAICHLE, M. E. 2008. Loss of resting interhemispheric functional connectivity after complete section of the corpus callosum. *J Neurosci,* 28**,** 6453-8.

KANNURPATTI, S. S. & BISWAL, B. B. 2008. Detection and scaling of task-induced fMRI-BOLD response using resting state fluctuations. *Neuroimage,* 40**,** 1567-74.

KANNURPATTI, S. S., BISWAL, B. B., KIM, Y. R. & ROSEN, B. R. 2008. Spatio-temporal characteristics of low-frequency BOLD signal fluctuations in isoflurane-anesthetized rat brain. *Neuroimage,* 40**,** 1738-47.

KIM, S. G. & UGURBIL, K. 1997. Comparison of blood oxygenation and cerebral blood flow effects in fMRI: estimation of relative oxygen consumption change. *Magn Reson Med,* 38**,** 59-65.

KIVINIEMI, V., JAUHIAINEN, J., TERVONEN, O., PAAKKO, E., OIKARINEN, J., VAINIONPAA, V., RANTALA, H. & BISWAL, B. 2000. Slow vasomotor fluctuation in fMRI of anesthetized child brain. *Magn Reson Med,* 44**,** 373-8.

KIVINIEMI, V. J., HAANPAA, H., KANTOLA, J. H., JAUHIAINEN, J., VAINIONPAA, V., ALAHUHTA, S. & TERVONEN, O. 2005. Midazolam sedation increases fluctuation and synchrony of the resting brain BOLD signal. *Magn Reson Imaging,* 23**,** 531-7.

KOCH, S. P., KOENDGEN, S., BOURAYOU, R., STEINBRINK, J. & OBRIG, H. 2008. Individual alpha-frequency correlates with amplitude of visual evoked potential and hemodynamic response. *Neuroimage,* 41**,** 233-42.

KROEGER, D. & AMZICA, F. 2007. Hypersensitivity of the anesthesia-induced comatose brain. *J Neurosci,* 27**,** 10597-607.

KUMAR, A., WELTI, D. & ERNST, R. R. 1975. NMR Fourier zeugmatography. *J Magn Reson,* 18**,** 69-83.

KWONG, K. K., BELLIVEAU, J. W., CHESLER, D. A., GOLDBERG, I. E., WEISSKOFF, R. M., PONCELET, B. P., KENNEDY, D. N., HOPPEL, B. E., COHEN, M. S., TURNER, R., CHENG, H. M., BRADY, T. J. & ROSEN, B. R. 1992. Dynamic magnetic resonance imaging of human brain activity during primary sensory stimulation. *Proc. Natl. Acad. Sci. USA,* **89,** 5675-5679.

LAMBRAKIS, C. C., LANCMAN, M. E. & ROMANO, C. 1999. Asynchronous and asymmetric burst-suppression in a patient with a corpus callosum lesion. *Clin Neurophysiol,* 110**,** 103-5.

LAUTERBUR, P. C. 1973. Image formation by induce local interactions: examples employing nuclear magnetic resonance. *Nature,* 242**,** 190-1.

LAZAR, L. M., MILROD, L. M., SOLOMON, G. E. & LABAR, D. R. 1999. Asynchronous pentobarbital-induced burst suppression with corpus callosum hemorrhage. *Clin Neurophysiol,* 110**,** 1036-40.

LENZ, C., REBEL, A., VAN ACKERN, K., KUSCHINSKY, W. & WASCHKE, K. F. 1998. Local cerebral blood flow, local cerebral glucose utilization, and flow-metabolism coupling during sevoflurane versus isoflurane anesthesia in rats. *Anesthesiology,* 89**,** 1480-8.

LEOPOLD, D. A., MURAYAMA, Y. & LOGOTHETIS, N. K. 2003. Very slow activity fluctuations in monkey visual cortex: implications for functional brain imaging. *Cereb Cortex,* 13**,** 422-33.

LI, S. J., LI, Z., WU, G., ZHANG, M. J., FRANCZAK, M. & ANTUONO, P. G. 2002. Alzheimer Disease: evaluation of a functional MR imaging index as a marker. *Radiology,* 225**,** 253-9.

LINKENKAER-HANSEN, K., NIKULIN, V. V., PALVA, S., ILMONIEMI, R. J. & PALVA, J. M. 2004. Prestimulus oscillations enhance psychophysical performance in humans. *J Neurosci,* 24**,** 10186-90.

LIU, X., ZHU, X. H. & CHEN, W. 2009. Insights into the Origin of Spontaneous Coherent BOLD fluctuations in a Resting Rat Brain under Varied Isoflurane Anesthesia Depth. *In proceedings of 16th ISMRM Annual Meeting, Honolulu, Hawaii, USA***,** 123.

LIU, X., ZHU, X. H., ZHANG, Y. & CHEN, W. 2010. Neural Origin of Spontaneous Hemodynamic Fluctuations in Rats under Burst-Suppression Anesthesia Condition. *Cereb Cortex*.

LIU, Y., LIANG, M., ZHOU, Y., HE, Y., HAO, Y., SONG, M., YU, C., LIU, H., LIU, Z. & JIANG, T. 2008. Disrupted small-world networks in schizophrenia. *Brain,* 131**,** 945-61.

LIU, Z. M., SCHMIDT, K. F., SICARD, K. M. & DUONG, T. Q. 2004. Imaging oxygen consumption in forepaw somatosensory stimulation in rats under isoflurane anesthesia. *Magn Reson Med,* 52**,** 277-85.

LOGOTHETIS, N. K., MURAYAMA, Y., AUGATH, M., STEFFEN, T., WERNER, J. & OELTERMANN, A. 2009. How not to study spontaneous activity. *Neuroimage,* 45**,** 1080-9.

LOGOTHETIS, N. K., PAULS, J., AUGATH, M., TRINATH, T. & OELTERMANN, A. 2001. Neurophysiological investigation of the basis of the fMRI signal. *Nature,* 412**,** 150-7.

LOWE, M. J., DZEMIDZIC, M., LURITO, J. T., MATHEWS, V. P. & PHILLIPS, M. D. 2000. Correlations in low-frequency BOLD fluctuations reflect cortico-cortical connections. *Neuroimage,* 12**,** 582-7.

LOWE, M. J., MOCK, B. J. & SORENSON, J. A. 1998. Functional connectivity in single and multislice echoplanar imaging using resting-state fluctuations. *Neuroimage,* 7**,** 119-32.

LOWE, M. J., PHILLIPS, M. D., LURITO, J. T., MATTSON, D., DZEMIDZIC, M. & MATHEWS, V. P. 2002. Multiple sclerosis: low-frequency temporal blood oxygen level-dependent fluctuations indicate reduced functional connectivity initial results. *Radiology,* 224**,** 184-92.

LU, H., ZHAO, C., GE, Y. & LEWIS-AMEZCUA, K. 2008. Baseline blood oxygenation modulates response amplitude: Physiologic basis for intersubject variations in functional MRI signals. *Magn Reson Med,* 60**,** 364-72.

LU, H., ZUO, Y., GU, H., WALTZ, J. A., ZHAN, W., SCHOLL, C. A., REA, W., YANG, Y. & STEIN, E. A. 2007. Synchronized delta oscillations correlate with the resting-state functional MRI signal. *Proc Natl Acad Sci U S A,* 104**,** 18265-9.

LUND, T. E. 2001. fcMRI--mapping functional connectivity or correlating cardiac-induced noise? *Magn Reson Med,* 46**,** 628-9.

LUND, T. E., NORGAARD, M. D., ROSTRUP, E., ROWE, J. B. & PAULSON, O. B. 2005. Motion or activity: their role in intra- and inter-subject variation in fMRI. *Neuroimage,* 26**,** 960-4.

MAKEIG, S., WESTERFIELD, M., JUNG, T. P., ENGHOFF, S., TOWNSEND, J., COURCHESNE, E. & SEJNOWSKI, T. J. 2002. Dynamic brain sources of visual evoked responses. *Science,* 295**,** 690-4.

MANSFIELD, P. 1977. Multi-planar image formation using NMR spin-echos. *J. Phys. C: Solid State Physics* 10**,** L55-L58.

MANTINI, D., PERRUCCI, M. G., DEL GRATTA, C., ROMANI, G. L. & CORBETTA, M. 2007. Electrophysiological signatures of resting state networks in the human brain. *Proc Natl Acad Sci U S A,* 104**,** 13170-5.

MARTIN, C., MARTINDALE, J., BERWICK, J. & MAYHEW, J. 2006. Investigating neural-hemodynamic coupling and the hemodynamic response function in the awake rat. *Neuroimage,* 32**,** 33-48.

MARTUZZI, R., RAMANI, R., QIU, M., RAJEEVAN, N. & CONSTABLE, R. T. 2010. Functional connectivity and alterations in baseline brain state in humans. *Neuroimage,* 49**,** 823-34.

MASAMOTO, K., KIM, T., FUKUDA, M., WANG, P. & KIM, S. G. 2007. Relationship between neural, vascular, and BOLD signals in isoflurane-anesthetized rat somatosensory cortex. *Cereb Cortex,* 17**,** 942-50.

MASSIMINI, M., FERRARELLI, F., ESSER, S. K., RIEDNER, B. A., HUBER, R., MURPHY, M., PETERSON, M. J. & TONONI, G. 2007. Triggering sleep slow waves by transcranial magnetic stimulation. *Proc Natl Acad Sci U S A,* 104**,** 8496-501.

MATHIESEN, C., CAESAR, K., AKGOREN, N. & LAURITZEN, M. 1998. Modification of activity-dependent increases of cerebral blood flow by excitatory synaptic activity and spikes in rat cerebellar cortex. *J Physiol,* 512 (Pt 2)**,** 555-66.

MONK, C. S., PELTIER, S. J., WIGGINS, J. L., WENG, S. J., CARRASCO, M., RISI, S. & LORD, C. 2009. Abnormalities of intrinsic functional connectivity in autism spectrum disorders. *Neuroimage,* 47**,** 764-72.

MOOSMANN, M., RITTER, P., KRASTEL, I., BRINK, A., THEES, S., BLANKENBURG, F., TASKIN, B., OBRIG, H. & VILLRINGER, A. 2003. Correlates of alpha rhythm in functional magnetic resonance imaging and near infrared spectroscopy. *Neuroimage,* 20**,** 145-58.

MORCOM, A. M. & FLETCHER, P. C. 2007. Does the brain have a baseline? Why we should be resisting a rest. *Neuroimage,* 37**,** 1073-82.

MORGAN, V. L. & PRICE, R. R. 2004. The effect of sensorimotor activation on functional connectivity mapping with MRI. *Magn Reson Imaging,* 22**,** 1069-75.

MUKAMEL, R., GELBARD, H., ARIELI, A., HASSON, U., FRIED, I. & MALACH, R. 2005. Coupling between neuronal firing, field potentials, and FMRI in human auditory cortex. *Science,* 309**,** 951-4.

MUTHUKUMARASWAMY, S. D., EDDEN, R. A., JONES, D. K., SWETTENHAM, J. B. & SINGH, K. D. 2009. Resting GABA concentration predicts peak gamma frequency and fMRI amplitude in response to visual stimulation in humans. *Proc Natl Acad Sci U S A,* 106**,** 8356-61.

NIESSING, J., EBISCH, B., SCHMIDT, K. E., NIESSING, M., SINGER, W. & GALUSKE, R. A. 2005. Hemodynamic signals correlate tightly with synchronized gamma oscillations. *Science,* 309**,** 948-51.

OGAWA, S., LEE, T.-M., KAY, A. R. & TANK, D. W. 1990. Brain magnetic resonance imaging with contrast dependent on blood oxygenation. *Proc. Natl. Acad. Sci. USA,* 87**,** 9868-9872.

OGAWA, S., MENON, R. S., KIM, S.-G. & UGURBIL, K. 1998. On the characteristics of functional magnetic resonance imaging of the brain. *Annu. Rev. Biophys. Biomol. Struct.,* 27**,** 447-474.

OGAWA, S., TANK, D. W., MENON, R., ELLERMANN, J. M., KIM, S. G., MERKLE, H. & UGURBIL, K. 1992. Intrinsic signal changes accompanying sensory stimulation: functional brain mapping with magnetic resonance imaging. *Proc Natl Acad Sci U S A,* 89**,** 5951-5.

PALVA, S., LINKENKAER-HANSEN, K., NAATANEN, R. & PALVA, J. M. 2005. Early neural correlates of conscious somatosensory perception. *J Neurosci,* 25**,** 5248-58.

PAULING, L. & CORYELL, C. D. 1936. The magnetic properties and structure of hemoglobin, oxyhe- moglobin and carbonmonoxyhemoglobin. *Proc Natl Acad Sci U S A,* 22.

PAXINOS, G. & WATSON, C. 1998. The Rat Brain in Stereotaxic Coordinates. *Academic Press, San Diego, California*.

PELTIER, S. J., KERSSENS, C., HAMANN, S. B., SEBEL, P. S., BYAS-SMITH, M. & HU, X. 2005. Functional connectivity changes with concentration of sevoflurane anesthesia. *Neuroreport,* 16**,** 285-8.

PFURTSCHELLER, G., NEUPER, C. & KRAUSZ, G. 2000. Functional dissociation of lower and upper frequency mu rhythms in relation to voluntary limb movement. *Clin Neurophysiol,* 111**,** 1873-9.

PINHEIRO, J., BATES, D., DEBROY, S., SARKAR, D. & TEAM, T. R. C. 2009. nlme: Linear and Nonlinear Mixed Effects Models. *R package version 3.1-92.*

PURCELL, E. M., TORREY, H. C. & POUND, R. V. 1946. Resonance absorption by nuclear magnetic moments in a solid. *Phys Rev* 37-38.

QUIGLEY, M., CORDES, D., TURSKI, P., MORITZ, C., HAUGHTON, V., SETH, R. & MEYERAND, M. E. 2003. Role of the corpus callosum in functional connectivity. *AJNR Am J Neuroradiol,* 24**,** 208-12.

RABI, I. I., ZACHARIAS, J. R., MILLMAN, S. & KUSCH, P. 1938. A New Method of Measuring Nuclear Magnetic Moment. *Physical Review,* 53**,** 318.

RAICHLE, M. E. 2006. Neuroscience. The brain's dark energy. *Science,* 314**,** 1249-50.

RAICHLE, M. E. & MINTUN, M. A. 2006. Brain work and brain imaging. *Annu Rev Neurosci,* 29**,** 449-76.

REES, G., FRISTON, K. & KOCH, C. 2000. A direct quantitative relationship between the functional properties of human and macaque V5. *Nat Neurosci,* 3**,** 716-23.

RESS, D., BACKUS, B. T. & HEEGER, D. J. 2000. Activity in primary visual cortex predicts performance in a visual detection task. *Nat Neurosci,* 3**,** 940-5.

RIVA, C., ROSS, B. & BENEDEK, G. B. 1972. Laser Doppler measurements of blood flow in capillary tubes and retinal arteries. *Invest Ophthalmol,* 11**,** 936-44.

RODRIGUEZ, E., GEORGE, N., LACHAUX, J. P., MARTINERIE, J., RENAULT, B. & VARELA, F. J. 1999. Perception's shadow: long-distance synchronization of human brain activity. *Nature,* 397**,** 430-3.

ROY, C. S. & SHERRINGTON, C. S. 1890. On the Regulation of the Blood-supply of the Brain. *J Physiol,* 11**,** 85-158 17.

SALVADOR, R., MARTINEZ, A., POMAROL-CLOTET, E., SARRO, S., SUCKLING, J. & BULLMORE, E. 2007. Frequency based mutual information measures between clusters of brain regions in functional magnetic resonance imaging. *Neuroimage,* 35**,** 83-8.

SALVADOR, R., SUCKLING, J., COLEMAN, M. R., PICKARD, J. D., MENON, D. & BULLMORE, E. 2005. Neurophysiological architecture of functional magnetic resonance images of human brain. *Cereb Cortex,* 15**,** 1332-42.

SAPIR, A., D'AVOSSA, G., MCAVOY, M., SHULMAN, G. L. & CORBETTA, M. 2005. Brain signals for spatial attention predict performance in a motion discrimination task. *Proc Natl Acad Sci U S A,* 102**,** 17810-5.

SCHWARTZ, W. J., SMITH, C. B., DAVIDSEN, L., SAVAKI, H., SOKOLOFF, L., MATA, M., FINK, D. J. & GAINER, H. 1979. Metabolic mapping of functional activity in the hypothalamo-neurohypophysial system of the rat. *Science,* 205**,** 723-5.

SHMUEL, A. & LEOPOLD, D. A. 2008. Neuronal correlates of spontaneous fluctuations in fMRI signals in monkey visual cortex: Implications for functional connectivity at rest. *Hum Brain Mapp,* 29**,** 751-61.

SHULMAN, R. G. & ROTHMAN, D. L. 1998. Interpreting functional imaging studies in terms of neurotransmitter cycling. *Proc Natl Acad Sci U S A,* 95**,** 11993-8.

SHULMAN, R. G., ROTHMAN, D. L. & HYDER, F. 2007. A BOLD search for baseline. *Neuroimage,* 36**,** 277-81.

SIBSON, N. R., DHANKHAR, A., MASON, G. F., ROTHMAN, D. L., BEHAR, K. L. & SHULMAN, R. G. 1998. Stoichiometric coupling of brain glucose metabolism and glutamatergic neuronal activity. *Proc Natl Acad Sci U S A,* 95**,** 316-21.

SOMMERS, M. G., VAN EGMOND, J., BOOIJ, L. H. & HEERSCHAP, A. 2009. Isoflurane anesthesia is a valuable alternative for alpha-chloralose anesthesia in the forepaw stimulation model in rats. *NMR Biomed,* 22**,** 414-8.

SORG, C., RIEDL, V., MUHLAU, M., CALHOUN, V. D., EICHELE, T., LAER, L., DRZEZGA, A., FORSTL, H., KURZ, A., ZIMMER, C. & WOHLSCHLAGER, A. M. 2007. Selective changes of resting-state networks in individuals at risk for Alzheimer's disease. *Proc Natl Acad Sci U S A,* 104**,** 18760-5.

STEIN, T., MORITZ, C., QUIGLEY, M., CORDES, D., HAUGHTON, V. & MEYERAND, E. 2000. Functional connectivity in the thalamus and hippocampus studied with functional MR imaging. *AJNR Am J Neuroradiol,* 21**,** 1397-401.

STERIADE, M., AMZICA, F. & CONTRERAS, D. 1994. Cortical and thalamic cellular correlates of electroencephalographic burst-suppression. *Electroencephalogr Clin Neurophysiol,* 90**,** 1-16.

STERN, J. M. & ENGEL, J. 2005. Atlas of EEG patterns. *Philadelphia, Lippincott Williams & Wilkins***,** 107-8.

SUPEKAR, K., MENON, V., RUBIN, D., MUSEN, M. & GREICIUS, M. D. 2008. Network analysis of intrinsic functional brain connectivity in Alzheimer's disease. *PLoS Comput Biol,* 4**,** e1000100.

SWANK, R. L. 1949. Synchronization of spontaneous electrical activity of cerebrum by barbiturate narcosis. *J Neurophysiol,* 12**,** 161-72.

TEAM, R. D. C. 2008. R: A language and environment for statistical computing. *R Foundation for Statistical Computing, Vienna, Austria.*

TIAN, L., JIANG, T., WANG, Y., ZANG, Y., HE, Y., LIANG, M., SUI, M., CAO, Q., HU, S., PENG, M. & ZHUO, Y. 2006. Altered resting-state functional connectivity patterns of anterior cingulate cortex in adolescents with attention deficit hyperactivity disorder. *Neurosci Lett,* 400**,** 39-43.

TOPOLNIK, L., STERIADE, M. & TIMOFEEV, I. 2003. Partial cortical deafferentation promotes development of paroxysmal activity. *Cereb Cortex,* 13**,** 883-93.

VAN DEN HEUVEL, M. P. & HULSHOFF POL, H. E. 2009. Specific somatotopic organization of functional connections of the primary motor network during resting state. *Hum Brain Mapp,* 31**,** 631-44.

VARELA, F., LACHAUX, J. P., RODRIGUEZ, E. & MARTINERIE, J. 2001. The brainweb: phase synchronization and large-scale integration. *Nat Rev Neurosci,* 2**,** 229-39.

VINCENT, J. L., PATEL, G. H., FOX, M. D., SNYDER, A. Z., BAKER, J. T., VAN ESSEN, D. C., ZEMPEL, J. M., SNYDER, L. H., CORBETTA, M. & RAICHLE, M. E. 2007. Intrinsic functional architecture in the anaesthetized monkey brain. *Nature,* 447**,** 83-6.

WAITES, A. B., BRIELLMANN, R. S., SALING, M. M., ABBOTT, D. F. & JACKSON, G. D. 2006. Functional connectivity networks are disrupted in left temporal lobe epilepsy. *Ann Neurol,* 59**,** 335-43.

WANG, L., ZANG, Y., HE, Y., LIANG, M., ZHANG, X., TIAN, L., WU, T., JIANG, T. & LI, K. 2006. Changes in hippocampal connectivity in the early stages of Alzheimer's disease: evidence from resting state fMRI. *Neuroimage,* 31**,** 496-504.

WEISSKOFF, R. M., BAKER, J., BELLIVEAU, J., DAVIS, T. L. & KWONG, K. K. 1993. Power spectrum analysis of functionally-weighted MR data: what's in the noise? *The proceeding of 12th SMRM annual meeting, New York***,** 7.

WHITE, T., O'LEARY, D., MAGNOTTA, V., ARNDT, S., FLAUM, M. & ANDREASEN, N. C. 2001. Anatomic and functional variability: the effects of filter size in group fMRI data analysis. *Neuroimage,* 13**,** 577-88.

WHITFIELD-GABRIELI, S., THERMENOS, H. W., MILANOVIC, S., TSUANG, M. T., FARAONE, S. V., MCCARLEY, R. W., SHENTON, M. E., GREEN, A. I., NIETO-CASTANON, A., LAVIOLETTE, P., WOJCIK, J., GABRIELI, J. D. & SEIDMAN, L. J. 2009. Hyperactivity and hyperconnectivity of the default network in schizophrenia and in first-degree relatives of persons with schizophrenia. *Proc Natl Acad Sci U S A,* 106**,** 1279-84.

XU, G., XU, Y., WU, G., ANTUONO, P. G., HAMMEKE, T. A. & LI, S. J. 2006. Task-modulation of functional synchrony between spontaneous low-frequency oscillations in the human brain detected by fMRI. *Magn Reson Med,* 56**,** 41-50.

YANG, H., LONG, X. Y., YANG, Y., YAN, H., ZHU, C. Z., ZHOU, X. P., ZANG, Y. F. & GONG, Q. Y. 2007. Amplitude of low frequency fluctuation within visual areas revealed by resting-state functional MRI. *Neuroimage,* 36**,** 144-52.

ZHANG, D., SNYDER, A. Z., FOX, M. D., NOLAN, T. S., LARSON-PRIOR, L. J. & RAICHLE, M. E. 2007. Subject variability of spontaneous BOLD functional connectivity. *Soc. for Neuroscience,* Abstract viewer/planner, online.

ZHANG, D., SNYDER, A. Z., FOX, M. D., SANSBURY, M. W., SHIMONY, J. S. & RAICHLE, M. E. 2008. Intrinsic functional relations between human cerebral cortex and thalamus. *J Neurophysiol,* 100**,** 1740-8.

ZHANG, H. Y., WANG, S. J., XING, J., LIU, B., MA, Z. L., YANG, M., ZHANG, Z. J. & TENG, G. J. 2009. Detection of PCC functional connectivity characteristics in resting-state fMRI in mild Alzheimer's disease. *Behav Brain Res,* 197**,** 103-8.

ZHAO, F., ZHAO, T., ZHOU, L., WU, Q. & HU, X. 2008. BOLD study of stimulation-induced neural activity and resting-state connectivity in medetomidine-sedated rat. *Neuroimage,* 39**,** 248-60.

ZHONG, Y., WANG, H., LU, G., ZHANG, Z., JIAO, Q. & LIU, Y. 2009. Detecting functional connectivity in fMRI using PCA and regression analysis. *Brain Topogr,* 22**,** 134-44.